Unobtrusive Sensing Technologies for Supporting Remote Monitoring in the Home

Ke-Yu Chen

A dissertation
submitted in partial fulfillment of the
requirements for

Doctor of Philosophy

University of Washington

2016

Reading Committee:

Shwetak N. Patel, Chair

Linda Shapiro

James Fogarty

Program Authorized to Offer Degree:
Electrical Engineering

University of Washington

Abstract

Unobtrusive Sensing Technologies for Supporting Remote Monitoring in the Home

Ke-Yu Chen

Chair of the Supervisory Committee:
Associate Professor Shwetak N. Patel
Department of Electrical Engineering and Computer Sciencise Engineering

My thesis focuses on exploration and implementation of various sensing technologies that support in-home activity recognition. The technologies presented in this thesis include (1) a wearable device and a platform for studying the elders acceptance of carrying an attachment, (2) an IMS-based technique for capturing fine-grained characteristics of electrical events that can be attributed to human activities and (3) a technique to enable unmodified LCD monitors to sense human proximity and hand gestures. In particular, I have shown that human behaviors can cause time-varying EMI (electromagnetic interference), which can be sensed from a single set of sensing hardware installed anywhere in the home. These granular characteristics open a new feature space to explore insights of electrical events and can be used to enable various applications such as activity inference, energy disaggregation and motor failure detection. In addition, the IMS-based approach presented in this dissertation can potentially support continuous remote monitoring, acting as an automatic diary system, for helping the elderly increase their awareness of daily activities and in the meantime provides the rehabilitation researchers a low-cost method to track the patients activeness while the patients are in the home.

*To my dear wife **Shaoling** and beloved daughter **Aurelia** for your selfless support and companion, which infuse courage into me and make everything possible.*

TABLE OF CONTENTS

LIST OF FIGURES

LIST OF TABLES

GLOSSARY

AC: Alternating Current

ADL: Activity of Daily Life

ADC: Analog to Digital Converter

AR: Activity Recognition

CFL: Compact Fluorescent Lamp

CCFL: Cold Cathode Fluorescent Lamp

DC: Direct Current

DRM: Day Reconstruction Method

EADL: Enhanced Activity of Daily Life

EMI: Electromagnetic Interference

EMR: Electronic Medical Record

FFT: Fast Fourier Transform

IADL: Instrumental Activity of Daily Life

LCD: Liquid Crystal Display

LSD: Life Style Diary.

LSQ: Life Style Questionnaire

MS: Multiple Sclerosis

NALM: Non-intrusive Appliance Load Monitoring

PLI: Power Line Interface

RBF: Radial Basis Function

RPS: Revolutions Per Second

SCI: Spinal Cord Injuries

SMPS: Switched-Mode Power Supply

SVM: Support Vector Machine

SVR: Support Vector Regression

USRP: Universal Software Radio Peripheral

ACKNOWLEDGMENTS

I would like to thank everyone who have helped me in my PhD career. I can not have gone this far without your support.

First I would like to thank my family in Taiwan. You minimize my overhead and deal with all affairs for me on the other side of the earth. I am also loved by another family, the *UbiComp Lab* at University of Washington. **Eric** (Larson), you are the person to provide insightful opinions and boost me up to be a better researcher. **Sidhant**, thank you for your mentorship and encouragement whenever I need. What I learned from you is far behind the research; you are more like a family member than just a labmate. Thank you for still helping me even after you graduated. **Gabe**, you can always see those amazing details that I oversee; this is what I learned the most from you. My first CHI paper can never be done without your help. **Mayank**, I feel so blessed to have you with me in these past years. I know that if I need someone to talk, you will always be there and give me great opinions. **Tien**, you played an important role in the lab and take care of many things to support my research. You are always being helpful and willing to contribute to the whole lab. **Lilian**, you are a thoughtful person who is always sending me your regards in my tough times. You care about everyone in the lab and it is really great to have you in the lab. **Elliot**, you have no idea how happy I am when knowing about your joining to our lab. You are such a supportive person who tends to "yes" to all requests and provide immediate supports. My life would have become much harder without your significant help. **Ruth**, thank you for giving me the chance to deeply work with you. I definitely learned more from you than what you gained from me. You are so reliable and consistent and I never doubt you will be shining in your PhD. **Alex**, I really enjoy the happiness you brought to me and the lab. You are a considerate person and take good care of every tiniest heartbeat of the lab – I still remembered the food your brought for those who were staying late for the UIST

deadline. **Eric** (Whitmire) and **Josh**, I am happy for our lab to have both of you here. You are taking responsibility of running the lab, even it is in just your second year. I also learned a lot from both of you. **Edward**, you have been one of the important people in the lab. I also enjoy very much our conversations about the research. **Hanchuan**, thank you for bringing different aspects of your research to the lab and I learn a lot from it.

I would like to sincerely appreciate my advisor **Shwetak** from my deep heart. Thank you for giving me the opportunity to work with you in this awesome lab you built; thank you for always showing your support during my every tough moment; thank you for allowing me flexibly to schedule my time between the work and the family; thank you for leading me from a research apprentice to an independent researcher; thank you for never giving me up when I need time to learn and grow. Five years ago, I could barely write an article and knew very few about research; now I am confident and independent in doing my research and in the meantime able to help others. I would not be the person I am without your support, mentorship and encouragement. There are no words to describe my appreciation and how lucky I am to be your student. Thank you!

I would also like to thank other mentors outside the university. **Kent Lyons** and **David Nguyen**, thank you for taking me as your intern who has no track records. You have shown me how an awesome research can be. **Daniel Ashbrook**, you might be the nicest person I have ever met. You led me with your elegant pace in doing the research; you are always ready to listen and help. What I learned from you is definitely beyond the research. **Sean Keller**, I would like to thank you for pulling me to your group and hiring me as your intern. Your vision, leadership and knowledge in leading a research group is admirable; the experience of working with you is simply amazing. Thank you for always allowing me to work at my own pace and in the meantime being so supportive whenever I need your help.

Finally, I would like to thank my dear wife **Shaoling**. You always take care of everything for me and I have been so fortunate to have you by my side. Thank you for bring me a new family member, our baby daughter **Aurelia**, to my life. You both are the fuel to support me to explore the unknown as I know you will always be there for me.

Chapter

INTRODUCTION AND MOTIVATION

Understanding mobility patterns and daily activities of the elderly has been a research focus in rehabilitation studies. The changes in mobility patterns can relate to some conditions including, but not limited to fatigue, pain, sleep disorders, etc [21]. If left untreated, these secondary conditions can lead to worsening of symptoms or other complications, such as broken bones from falls or pressure ulcers from lack of movement. While there are many evidence-based strategies available to help reduce the onset, intensity and duration of secondary conditions, most of these are implemented after problems have already developed. If these problems were captured or anticipated earlier, complications and worsening of symptoms could be avoided [29, 75, 86]. The increase in symptoms and therefore secondary conditions highlights the importance of preventative care [5, 12, 93]. The use of continuous monitoring and self-management techniques are ways to encourage preventative care to reduce the incidence or impact of possible secondary conditions.

Traditionally, rehabilitation researchers use diary-style documents such as the Life-Style Diary (LSD) or Life-Style Questionnaire (LSQ) to study the mobility of subjects [60, 88]. This type of documents records the patient's room-to-room movements and helps researchers, using the bedroom as the center, to measure the subject's mobility [73]. Other researchers proposed Day Reconstruction Method (DRM) to gain more insights of the subject's daily life; it reports both how they move in home and what they do (e.g., eating, showering, reading etc.) [47]. These diaries, however, require self-reporting data from the subjects and causes huge burden for them. Especially for the people aging with disabilities, they usually suffer from memory loss and a couple of different issues such as spinal cord injuries (SCIs), muscular dystrophy or multiple sclerosis (MS). Logging the diaries every 30 minutes on a daily basis is extremely difficult for them and not practical as a tool for

long-term, continuous activity monitoring. Previous studies also revealed that these self-contained information may be subject to reporter bias and hence are not reliable [9, 22, 77].

Researchers have shown that in-home utility usage such as turning on a TV or using the microwave oven can be detected from a single sensing point [33, 34]. These approaches leverages infrastructure-mediated sensing (IMS) to capture electricity and water activities through a single sensing hardware installed in the home. Although low-cost and effective, this approach is lack of granularity; that is, they only detect *what* is being used without knowing neither *how* these appliances are used nor *how much* energy has been consumed. For example, the event of ''TV on'' does not necessarily mean the subject is actively watching TV; she could be fully asleep on the couch. Sensing fine-grained characteristics of electrical events (e.g., ''switching'' a TV channel or how energy being consumed by a laptop) provides many more clues on how a device is being used and could potentially provide more granular information for activity inferencing.

My thesis focuses on exploration and implementation of *various sensing technologies that support in-home activity recognition*. The technologies presented in this thesis includes (1) a wearable device and a platform for studying the elder's acceptance of carrying an attachment (Chapter 3), (2) an IMS-based technique for capturing fine-grained characteristics of electrical events that can be attributed to human activities (Chapter 4, Chapter 5 and Chapter6) and (3) a technique to enable unmodified LCD monitors to sense human proximity and hand gestures (Chapter 7). In particular, I have shown that human behaviors can cause time-varying EMI (electromagnetic interference), which can be sensed from a single sensing hardware installed anywhere in the home. These granular characteristics open a new feature space to explore insights of electrical events and can be used to enable various applications such as activity inference, energy disaggregation and motor failure detection. This IMS-based approach presented in this dissertation can potentially support continuous remote monitoring, acting as an *automatic diary system*, helping the elderly increase their awareness of daily activities and in the meantime, providing the rehabilitation researchers a low-cost method to track the patient's activeness while the patients are in the home.

1.1 Why Remote Monitoring and Challenges in Rehabilitation

Observing changes in daily routines can support early identification of a disease before it gets worse. Although early detection can cut costs in the long run, patients and physicians usually request a clinical diagnosis only when a problem rises and reaches considerable severity. Lack of immediate care and monitoring systems could lost the opportunity to identify a disease in its early stage. Among patients that requires continuous medical care and monitoring, nearly 20% in the US live in the rural areas, but only 9% physicians work in rural areas to provide immediate supports [38]. Access issues may get worse over time as many institutions predict an upcoming shortfall in primary care providers due to the growth of millions of new patients [3]. Insufficient sources of physicians can significantly reduce the number of visits and could cause a variety of problems in elder care. For example, clinicians will lack information about functioning and related behaviors of subjects between visits. In order to compensate this deficiency, clinicians typically collects self-reported data from the patients [60, 88]. Although straightforward, these activity logs (called *diaries*) have been demonstrated as unreliable [48]. Furthermore, writing these activity logs on a daily basis is a huge burden for the elder and therefore is not a long-term solution as a monitoring tool.

1.2 Ubiquitous Computing for Remote Monitoring and Rehabilitation

Ubiquitous computing plays a significant role in remote monitoring. Sensors and software systems embedded in the home and community, called *embedded assessment* [63], automate data capture, provide objective measurements of an individual's behavior and detect meaningful changes over time. Embedded assessment can serve several functions including three categories: (a) *monitoring*: to measure functional performance and positive and negative changes or to support early identification of disease and monitor disease progression, (b) *prevention*: to use data gathered to plan interventions that will promote health, and (c) *compensation*: to provide compensatory support for memory loss or to make caregiving more efficient and manageable. Examples of embedded assessment range from smart homes to consumer personal health technologies [7,30,43,61,70,91]. In clinical trials, these embedded

assessments have been proved as an efficient way to promote health for aging adults [23,24]. Intel-GE Care Innovations[1] is one example of commercial products that applies ubiquitous computing in remote monitoring. By combining data from distributed sensors, wearable devices, smart medical equipments and electronic medical records (EMC), the system can track patients' vital signs (e.g., heart rate and blood pressure) and identify their levels of activities (e.g., number of steps or mobility). This platform aims at building a bridge to connect the patients, family members and the clinic. Requiring key activities in the community through these sensing technologies, rather than only by clinic testing or self-report logs, can reduce the cost and burden of travel, improve recruitment and retention, and capture more reliable, valid, and responsive ratio-scaled outcome measures.

In this thesis, I will focus on part A (*i.e.,monitoring*). In particular, I will (1) first evaluate the elder's acceptance of using a wearable device that we designed for tracking their in-home movements through the field studies (Chapter 3) and (2) from my observations through these filed studies, show how infrastructure-mediated sensing technologies can be used to capture fine-grained, user-driven electrical events that can avail activity inference research (Chapter 4 to 7).

1.2.1 Wearable devices

Sensors worn on human body are intended to collect longitudinal and contextually sensitive data that can be processed to automatically detect important changes in behavior patterns caused by the onset of illness. Different types of sensing technologies have been used to measure a wide range of variables including location and movement, task completion, activities of daily living (e.g. brushing teeth or getting out of bed), physiologic measures (e.g. heart rate, galvanic skin response and pulse), sleep and falls and rehabilitation specific tasks such as back training and stroke rehabilitation [25, 70]. Although many new forms of wearable devices have been developed and tested in research environments, very few have been implemented in community settings of the elderly. The effectiveness of these technologies in

[1]Intel-GE Care Innovations: http://www.careinnovations.com

real home settings is still unknown. As a result, a couple of significant questions regarding the practicality of applying ubiquitous computing in remote monitoring arise:

- What is the elder's acceptance of a wearable device in daily usage?
- What is the elder's preference of a wearable device (e.g., size, weight, instrumentation, etc)?
- How ubiquitous computing can enable remote monitoring with minimal overhead to both the patients and rehabilitation researchers?

Answering many of the above questions motivate the first part of my thesis work which will be detailed in Chapter 3.

1.2.2 Infrastructure-mediated Sensing

Infrastructure-mediated sensing (IMS) has been proposed as one alternative method for low-cost and unobtrusive sensing of human activities [17, 33, 34, 67, 68, 69, 92]. This technique is based on the idea that human activities (e.g., vacuuming, using the microwave, or blending a drink) can be sensed by their manifestations in an environment's existing infrastructures (e.g., a home's water, electrical, and HVAC infrastructures), thereby reducing the need for installing sensors everywhere in an environment or on-body instrumentation. In one example of IMS, Patel *et al.* demonstrated the ability to detect the flicks of light switches using a single plug-in sensor by fingerprinting the transient electrical noise signatures on the power line [68]. Gupta *et al.* improved this method by utilizing the electromagnetic interference (EMI) produced by modern electronic devices in the home [34]. From a single sensing point, the presence of electronic devices can be inferred by training on the frequency domain EMI signatures of those devices in the home. Although useful, these techniques only detect *what* appliance is being used, that is, the on/off state of electronic devices. However, the continuous time-varying EMI has the potential to provide many more clues on how a

device is being used, what state the device might be in and how much power it consumes, yielding more granular information for activity recognition and energy disaggregation.

1.3 Thesis Contribution and Statement

In this dissertation, I present a technique that utilizes time-varying EMI to extract various, fine-grained information from electrical usage data. The first system, call **DOSE** (**D**etecting **O**perating **S**tates of **E**lectronic devices), leverages varying electrical noises for estimating the operating states of appliances. Electronic devices yield electromagnetic interference (EMI) when they are in operation [34]. I found that when an electronic device operates at different states (e.g., high vs. low CPU loads of a laptop) or under varying conditions (e.g., using vacuum cleaner on rug vs. hardwood floor), their EMI fluctuates distinctively based on the corresponding user behaviors. By analyzing time-varying EMI, the system is able to identify various operating states of an electronic appliance. In particular, I leverage domain knowledge of the device and semi-supervised clustering for state estimation, obviating the need of tedious labeling process on the data. This usage of domain knowledge as a prior for model training, instead of fingerprint-based approaches, makes DOSE easy for large-scale deployment as it does not require huge amount of labeled data. In contrast to ElectriSense [34] which focused on static, SMPS-based EMI for electrical event detection, this work investigated time-varying EMI induced by mechanically switching (e.g., vacuum cleaner), electronically switching (e.g., laptop), and the combination (e.g., hair dryer) circuits. I will detail the DOSE system in Chapter 4 and 5.

In addition, I discovered that the power consumption of appliances can be reliably estimated from the same time-varying EMI signals. The power consumed by electronic appliances varies with the voltage regulation mechanism inside its circuitry, which causes fluctuating EMI. By reverse-engineering the EMI signals, the power consumption of appliances can be robustly inferred in real time. This power inferencing system will be detailed in Chapter 6.

Throughout this dissertation, I provide support for my thesis statement:

Utility usage data with the observations of time-varying signals can be employed for estimating an appliance's state and real-time power to support in-home activity inference from a single sensing point.

In this thesis, although I focus on how time-varying EMI can be leveraged for sensing an appliance's states and power, these are just two applications that this varying signal can enable. I will further show that human proximity can cause EMI signal existing on LCD monitors to fluctuate. These varying EMIs can be leveraged to sense various hand gestures performed on unmodified LCD monitors. This system, called *uTouch*, will be detailed in Chapter 7.

Chapter

BACKGROUND AND RELATED WORK

Activity recognition (AR) is a well-studied, but still challenging problem [54]. Self-report data such as LSD (Life Style Diary), LSQ (Life Style Questionnaire) and DRM (Day Reconstruction Method) [47, 60, 88] had been traditionally used to collect activity-related information of the patients when they are in the home. From these self-report records, medical professionals believe that one of the best approaches to detect potential medical conditions in the early stage is to look at the changes in ADLs (activities of daily life), IADLs (instrumental ADLs) and EADLs(enhanced ADLs) [78]. As described in Chapter 1, these approaches require subjects to manually log their life events, which poses a significant burden when being used for long-term monitoring, especially for the elder or those aging with disabilities. These diary-based approaches could be inaccurate as the subjects may not fully describe a compound event (e.g., watching TV while preparing a meal) or sometimes even forget to do so. Processing these hand-written diaries is also difficult for the researchers; they need to manually input the logs, sometime scribbles, into digital formats before they can be used for behavioral analysis.

To alleviate this issue, researchers have explored various sensing techniques for automating data collection process [16]. These sensors were designed for retrieving different measurements, including movement sensors (e.g. accelerometers, pedometers, gyroscopes, motion sensors), physiological sensors (e.g. heart rate, blood pressure, breathing frequency) and contextual sensors (e.g. Global Position System (GPS), RFID, measures of ambient conditions such as light/sound). They have been used in various combinations to acquire an accurate view of physical activity in different settings. All of these technologies for sensing activities or acting as a remote monitoring tool can be categorized into four major categories: (1) computer-vision based approaches (2) distributed sensors on individual appliances (3)

wearable devices worn on the human body (4) infrastructure-mediated sensing (IMS). In this chapter, I will respectively introduce them and according prior arts.

2.1 Computer-vision based Approaches

Computer-vision based approaches provide a straightforward way to capture human activities. By analyzing the body postures in picture frames of video clips, the activities being performed can be extracted and interpreted to corresponding actions. Mihailidis *et al.* used 2D camera to capture activities of the older adults [61]. Zouba *et al.* identified different activities of the elderly by reconstructing 3D postures from the recorded 2D video frames [99]. These two systems first recognized the human silhouette by identifying the moving pixels in the frames and then reconstructed the 3D postures using a human posture reconstruction algorithm [10]. Romero *et al.* visualized aggregated motions over the observation space, behaving as a handy tool to discover possible daily activities [79]. Recently, commercial product such as Microsoft Kinect[1] has been very successful and used in human pose estimation. One example of applying Kinect in rehabilitation is ResponseWell[2]. This system employs the depth camera to capture and analyze the patient's body postures, and provide visual feedback for guiding rehabilitation activities (e.g., stretching the body). Although these vision-based approaches is capable of locating and identifying human behaviors, the potential privacy issues limits its applicability for whole-home activity recognition. For example, instrumenting the cameras in private space such as the bathroom or bedroom may not be appropriate in the home.

Recent work proposed by Hevesi *et al.* leverages low-resolution thermal sensor arrays to capture coarse-grained human activities such as using a coffee machine and taking a shower [40]. Instead of using pixel-level information, this approach uses indirect approach to infer activities and thereby minimize the risk of leaking private information from the sensing device. It however requires prior knowledge of appliances' locations for activity

[1]Microsoft Kinect: http://research.microsoft.com/en-us/projects/vrkinect

[2]ResponseWell: http://www.respondwell.com

inferencing and the sensing hardware installed in every rooms in home.

2.2 Distributed Sensors for the Smart Home Environment

To avoid possible privacy concerns that may be raised from cameras, researchers have used distributed sensors such as motion sensors or RFID tags deployed in a living environment to *indirectly* extract information of physical activities. Sensors are attached to home appliances (e.g., fridge, TV, washer and light switch), furnitures (e.g., chair and door handle), switches and doors to capture the subject's interaction with these items [64, 76]. As the sensor data do not directly relate to physical activities, it requires machine learning techniques to extract useful information from these sensor data. Fishkin *et al.* built a bayes estimator to extract human activities from RFID data [31]. Tapia *et al.* deployed 77 to 80 switch sensors in real-home settings for data collection and built a Bayesian Network classifier to analyze daily routines [91]. Using similar sensing approaches, Naeem *et al.* divided high-level activities (e.g., preparing a meal) into smaller components (e.g., using the fridge and toaster), creating a hierarchical structure for identifying an on-going activity even when part of sensor data were missing [66]. Buettner *et al.* attached battery-free RFID tags to home appliances and utensils, and applied Hidden Markov Model (HMM) to infer activities such as making a sandwich/coffee, reading a book or taking vitamins [11]. Similarly, Kasteren *et al.* utilized state-change sensors to collect data that were manually annotated and used for training a HMM classifier [94]. PlaceLab project is another example of using distributed sensors for sensing in-home activities [57]. In PlaceLab, researchers deployed a variety of sensors in a staged house including RFID tags, wired switches, cameras, electrical and water flow sensors, motion sensors, etc. Each activity was trained separately as a binary classifier rather than considering all activities in a single classifier. Recent works further combine distributed sensors deployed in the home with wearable devices or mobile phones to get more information of the subject's activities (e.g., the locations where the activity is performed) [20, 80].

In the above studies, researchers need to first manually label the data for supervised

learning. This labeling process, called Experience Sampling Method (ESM) [45,46], requires subjects to carry a portable device to input the activities they actually performed. When a possible event was detected, the device popped up a message asking the subject to input the activity they were performing (e.g., preparing a meal). Although accurate, the requirement of manually labeling procedure is not practical for long-term studies and difficult in the large-scale deployment. The alternative is to minimize subject's efforts by utilizing semi-supervised training methods. In SmartHouse project, Barger *et al.* deployed 8 motion sensors and on-off switch sensors in each room in a staged house for behavioral pattern inference by clustering triggered sensor events [7]. Features being used in clustering include start and end time of the first sensor event and total number of sensor firings while in the room. The assumption in this study was based upon the fact that the time of each activity is different; for example, the time spent in checking email is usually shorter than putting a book back to the shelf. After clustering the *unlabeled* activities, the system requires the subjects to map the identified activities to those they actually performed. Although it still requires user's involvement, this semi-supervised approach significantly reduces the user's efforts in generating the ground truth (*i.e.*, the actual activities they have performed) and training the classifier.

Other researchers interpreted the activities using language model, treating each activity as ''a sequence of discrete tokens (events)'' [35]. In this model, event sequences were represented as a suffix tree, where a path starting from the root to one of its leaves is one unique event sequence that maps a possible activity. The root node represented the first-fired sensor event and any root-to-leaf paths with in the same tree means an observed event sequence. In turn, the system discovered possible activity classes by finding the maximal clique in the tree. Using a different statistic model, Hu *et al.* utilized CRF (Conditional Random Field) to build a framework for recognizing multiple concurrent activities from sensor readings [36]. All these above methods do not require manual labels to get training data; on the contrary, the system first discovers possible activity classes and let users to label the activity actually being performed. Such method, called *Active Learning*, is a semi-supervised approach

that requires minimal involvements from the subjects. This model significantly reduces the efforts in collecting training data and increases scalability of the system deployment [84].

Using distributed sensors for activity recognition enables continuous data logging without leaking private (visual) information of subjects. However, the sensor-based approach has inherent noise from the inputs and becomes the bottle neck of such systems. For example, a motion event could be caused by a pet's movement instead of the actual human proximity; a subject sitting in front of a TV (e.g., detecting a motion event near TV) does not necessarily imply the event of ''watching TV''. Secondly, this approach needs a dense distributed sensor network to obtain acceptable accuracy (usually in a scale of instrumenting 50 to 80 sensors across the house). The high cost of installation and maintenance limits its scalability in real home settings.

2.3 Wearable Devices for health sensing

Wearable devices provide a mean to capture on-body, health-related measurements. They can monitor vital signs (e.g., heart rate and blood pressure), mobility (e.g., travel distance), the measure of life space and even the sleep quality [25]. Accelerometer has been shown an effective approach to obtain high-level activity data such as step counts or moving status (e.g., running, stand still, jump, walk, brush teeth) [6, 39, 44, 55]. Others combined accelerometer and RFID tags both worn on the wrist and hip for ADL recognition [4, 71, 89]. The idea behind these studies is to use accelerometer data for detecting activeness of gestures being performed and in the meantime employing RFID tags to capture the interaction between the subject and specific objects (e.g., a mug or the coffee machine). Instead of measuring on-body physical movements, researchers utilized fluctuations of GSM signal to track the subject's moving status [59, 87]. Using similar concepts, others use GPS to explore the interaction between a subject and the surroundings, and monitor changes in physical activity patterns over time [56, 58, 82]. In order to obtain granular information of physical activities, researchers combined multiple types of sensors, including accelerometer, barometer, humidity sensor, temperature sensor, microphone etc., to identify low-level activities of

individuals such as motion states, velocity and locations [90]. With proper interface designs, these sensors readings can be translated to meaningful information to further increase the subject's engagement in the physical activities [19]. In a recent work, Cohn *et al.* showed that human body can act as an antenna, called *humantenna*, and can be used for whole-body gesture sensing through a single wearable device [18].

Commercial products for monitoring high-level activities (e.g., step counts, running distance) such as Fitbit[3], Jawbone[4], Actigraph[5] and Nike+ are also quite successful. Live!y[6] is another example of commercial product that further combines a wrist watch and distributed sensors to provide a comprehensive platform for remote monitoring. The wrist watch leverages accelerometers to capture the subject's activeness (e.g., step counts or hand movements), and can also be used for fall detection. The distributed sensors can be attached to different home appliances (e.g., fridge, door) to infer the moving patterns, or to a pillbox to keep tracks of the patient's medication. This system is designed for independent elders based upon the architecture of Intel-GE Care Innovations (as described in Chapter 1).

While these wearable devices have shown a successful approach to infer physical activities, they have rarely been evaluated in the elder community, especially for those aging with various disabilities. To explore the elder's acceptance and preference of a wearable device, I have built the *uLocate* system for supporting mobility studies and have conducted field studies in 11 homes dwelling with people aging with disabilities. The system design and findings will be detailed in Chapter 3.

---

[3]Fitbit: http://www.fitbit.com/

[4]Jawbone: https://jawbone.com/

[5]Actigraph: http://www.actigraphcorp.com/

[6]Live!y: http://www.mylively.com

2.4 Infrastructure-mediated Sensing

Infrastructure-mediated sensing (IMS) has emerged as one alternative approach for activity inferencing. [17, 33, 34, 67, 68, 69, 92]. This technique is based on the idea that human activities (e.g., vacuuming or using the microwave) can be sensed by their manifestations in an environment's existing infrastructures (e.g., a home's water, electrical, and HVAC infrastructures), thereby reducing the need for installing sensors everywhere in an environment or on-body instrumentation. Utility data, such as electricity and water usage, can often reveal the nature of human activities in home. According to the research in 1980s by Raaij *et al.*, energy used by individuals in their homes is influenced by various factors such as building characteristics, personality of the residents, socio-demographic factor, etc [95]. This research further suggested that routines can become predictors of electricity consumption. Therefore, the way a resident uses her home appliances can significantly change the signal patterns of home power and water consumption, which could therefore conversely infer the corresponding habitual behaviors [2].

Researchers have shown that aggregated power consumption data can be used for sensing occupancy [51] or automatic HVAC (heating, ventilating, and air conditioning) control [83]. These studies estimated the occupancy by identifying daily usage patterns from fluctuations in energy usage. Taking a step further, Molina-Markham *et al.* demonstrated that without any prior knowledge or training, the power consumption data can reveal a range of information such as the number of residents in home, sleep routine, eating routine etc. [62]. Likewise, Beckel *et al.* identified various properties of a household (e.g., size, number of bedrooms, family or single resident, employed or retired) from the power consumption [8]. By analyzing the patterns of current flows, Perez *et al.* also showed that power usage can be further disaggregated into loads attributed to diverse appliances (e.g., kettle, oven or TV) and could be potentially used for kitchen activities recognition [74]. The above studies are grouped in the realm of *NALM* (Non-intrusive Appliance Load Monitoring), where a single energy detective hardware (TED) is typically instrumented in the breaker panel of a household to collect aggregated real current or power consumption [37].

NALM is an effective tool to infer high-level activities from the utility data, obviating the need of distributed sensor network (Section 2.2). This method, however, requires a step change in energy data and usually needs high-frequency consumption measurements [49] and intensive training process [96]. Another major limitation of NALM is that this method mainly focuses on high power consuming appliances such as oven, washer and dryers. For those relatively low power consuming appliances (e.g., laptop, lamps or chargers) which can usually reveal more fine-grained human activities, NALM is incapable of being applied and capturing those events as the system complexity increases exponentially with the number of appliances. To overcome this issue, Patel *et al.* has shown transients by mechnical switches can be used for electrical event detection [68]. Taking a step further, Gupta *et al.* leveraged EMI (Electromagnetic Interference) sensing to capture the electronic activations [34]. Most recent electronic devices employ switched-mode power supply (SMPS), which is highly efficient and compact in size, but unavoidably causes loud EMI noise. These noises can be regarded as the fingerprints of distinct devices and repurposed for electrical event detection. By instrumenting a single high-pass filter and analog-to-digital converter (ADC) to the wall outlet in a house, these EMI can be easily captured. Similar EMI sensing technique was also shown in the industrial applications for detecting motor failures [85].

As a counterpart of ElectriSense [34], Jon *et al.* proposed a single-sensing-point solution to disaggregate in-home water usage [33]. The system leverages the fact that individual water fixtures from different activities (e.g., using a kitchen faucet vs. flushing a toilet) can cause discernible pressure changes in the water pipe. By installing a pressure sensor at any position in thethe house's water pipe network (e.g., faucet, toilet pipe), the system is able to identify different water activities in a home. Using the similar sensing method, Thomaz *et al.* used the pressure fluctuations in the water pipe network to recognize high-level, water-based activities in the kitchen and bathroom (e.g., shave, brush teeth and clean dishes) [92].

The above infrastructure-mediated sensing techniques [33, 34, 92] provide low-cost, easy-to-install solutions for activity recognition. In this thesis, I claimed that by exploring

fine-grained characteristics of IMS-based signals, the system can afford more granular information for supporting activity recognition. In particular, I have found that when an electronic device operates at different states (e.g., high vs. low CPU loads) or under varying conditions (e.g., using vacuum cleaner on rug vs. hardwood floor), their EMI fluctuates distinctively based on the corresponding user behaviors. By analyzing time-varying EMI, the system is able to identify various user-driven operating states of an electronic appliance. The core algorithm and implementation details will be detailed in Chapter 4 and 5. From the same varying EMI signals, I will further show that the power consumption of home electronic appliances can be robustly inferred in real time. The algorithm of inferring real-time power will be detailed in Chapter 6.

Chapter

USING WEARABLE DEVICES IN REMOTE MONITORING

Location is a good measure of life space mobility, that is, the extent to which individuals venture out into their community and the assistance they require to do so [60, 73, 88]. *uLocate* is a ubiquitous location tracking system for people aging with disabilities [15]. The indoor/outdoor nature of our system facilitates measurement of the full range of an individual's life space. Such an monitoring system can log the room-to-room movement patterns of subjects, observers changes in mobility and provides real-time data to the rehabilitation researchers so they can identify possible diseases in early stages. Through this study, I plan to answer the following research questions:

- How feasible is it to implement the system in the home and community settings of people aging with disabilities?
- How acceptable is it for participants to have the system installed in their home and how easy is it for them to use the system on a daily basis?
- How accurate are the location data collected by the system?

This chapter details the system design, user studies, challenges in system deployment, results and analysis.

3.1 System Design

Figure 3.1 shows the system architecture of uLocate, including indoor and outdoor tracking. For the indoor positioning, we[1] adopted the network-based location system manufactured

[1]This is the universal "we" to represent a collaborative work and applies throughout this thesis. I am the leading researcher in these projects and accomplished most components of them.

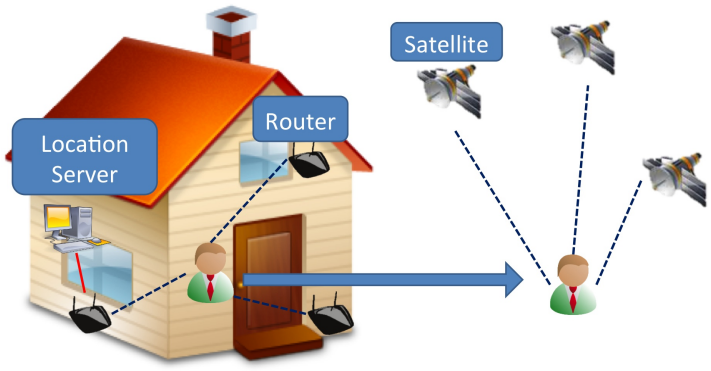

Figure 3.1: System Architecture of uLocate. The indoor subsystem exploited existing WiFi network for location tracking. When the subject moves outdoors, the system adapts to keep track of the subject by GPS.

by Ekahau[2]. We installed wireless access points (WAPs) in the participants' house and used them to localize the tag by triangulation. In particular, the tag searches nearby WAPs and sends the collected RSSI (received signal strength indication) as the fingerprinting to the location server for reasoning its position. For the outdoor location sensing, we used GPS to collect data of the subjects' outdoor activities due to its simplicity.

In the section, I will respectively detail three key components of uLocate: a portable sensor tag, the visualization software and the middleware.

3.1.1 Hardware

The sensing tag includes two parts, a WiFi tag for indoor tracking and a GPS logger for outdoor tracking (see Figure 3.2). One side of the tag (black) is part of the Ekahau T301A WiFi tag[3] while the other side (white) is the GPS logger. In order to ease the burden on our participants to carry the tag, one side of the cap of T301A tag was removed and assembled

[2]http://www.ekahau.com

[3]Ekahau T301A: http:// www.ekahau.com/products/wi-fi-tags.html

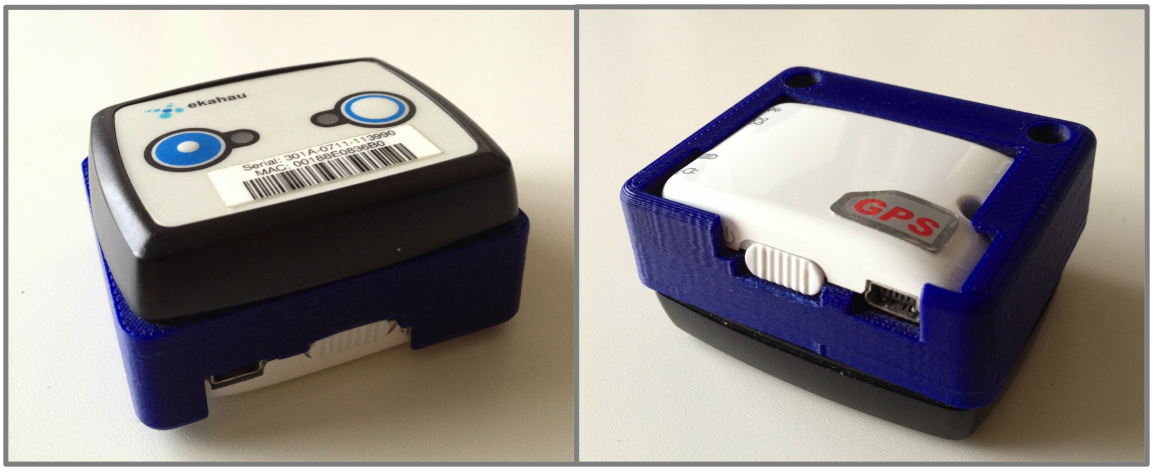

Figure 3.2: A single sensing tag of uLocate with dimension of 54mm x 45mm x 26mm. **(Left)** WiFi tag for the indoor tracking. **(Right)** GPS logger with a customized cap for the outdoor tracking.

with the GPS logger by a customized 3D-printing cap. We chose iBlue 860E[4] as our GPS data logger because of its compactness. It is the smallest GPS data logger we can find in the market. The integrated tag is only 70 grams with compact dimensions (54 mm x 45 mm x 26 mm). The Ekahau on the tag did not require to be charged during the 6 weeks of study; however, the GPS on the tag has a battery life of 11 to 14 hours when continuously logging the data. Therefore, participants were asked to charge the GPS logger each day before they went to the bed.

We also set up a laptop as the location server in each participant's home for data collection. To collect the data, the WiFi tag sends RSSIs (Received Signal Strength Indication) to the laptop every 2 minutes. The sampling rate of GPS logger varied with the moving speed (*i.e.*, per sample / 1 second for driving, 15 seconds for running, 30 seconds for walking). Although the memory of GPS logger is large enough to store up to weeks of data, we requested our participants to download the GPS data to laptop every night before they

[4]iBlue 860E: http://gpsdatalogger.thebestpricegps.com

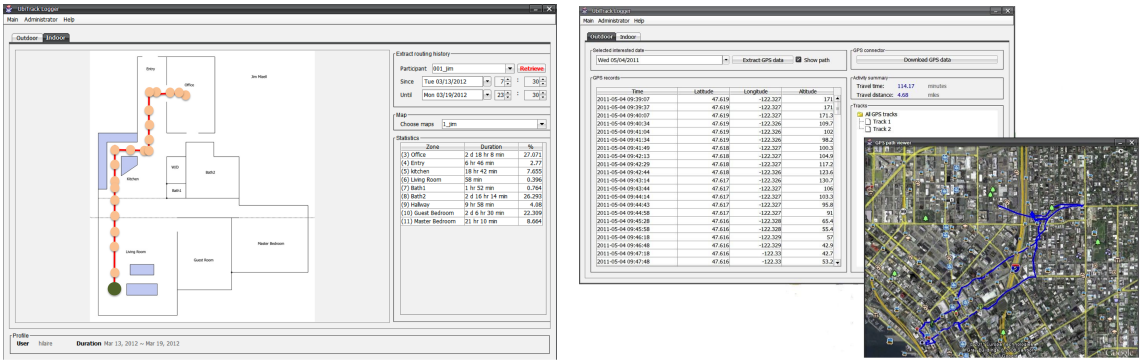

(a) Indoor view (b) Outdoor view

Figure 3.3: uLocate Software Platform. **(a)** Indoor view shows the route and profile of the subject. **(b)** Outdoor views includes an interactive map, trip routes, time and distance.

are ready to sleep so the database can be up to date. To reduce the participant's burden, I developed an automatic downloading software running as a background process (called ''watchdog'') on the laptop. When the participant plugged in the GPS logger, the watchdog process detected the appearance of the device and automatically downloaded the GPS data. After the data was fully downloaded, watchdog clear the contents on GPS memory for the next day usage.

3.1.2 Software

In addition to the hardware design, we also developed a software platform for participants to review their visualized and statistical location data including moving routes in their house, total time spent in each room, total travel distance of an outdoor trip, thus allowing them to review their real-time and history activity status (see Figure 3.3a). The software extracts the raw data (*i.e.* location positions) from the server database through Ekahau APIs and visualizes them as meaningful information. Users can specify the period of interest and explore the route of their indoor movements and the total time spent in different rooms

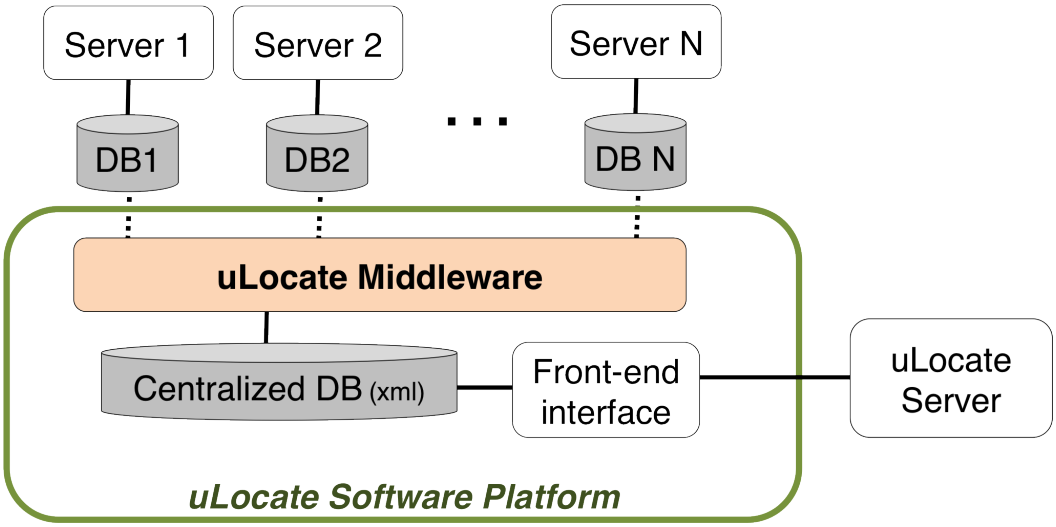

Figure 3.4: Middleware in uLocate Software Platform. The middleware accesses the Ekahau database and converted the location data to XML format, which are then stored in a centralized DB. It allows rehabilitation researchers to access data of multiple subjects from a single portal.

during this period. For outdoor activities, as show in Figure 3.3b, the platform displayed participants' routes and, the total travel time and distance of each route. We embedded Google Earth[5] into our platform and provided an interactive map view that allowed users to easily view the route from different angles. We chose Google Earth instead of Google Maps because it can operate without the Internet at a lower resolution. Many of our participants did not have Internet connections in their home and thereby Google Earth is the way to work around that.

3.1.3 Middleware

As we described, the uLocate software platform utilized Ekahau APIs to provide a handy channel to review their location tracking data. However, Ekahau APIs do not allow multiple

[5]Google Earth: http://www.google.com/earth/index.html

location servers running on the same computer. It means that if the researcher want to retrieve data from multiple subjects, he or she needs to switches different servers. In order to overcome this limitation, I developed a middleware [14] in uLocate software platform (see Figure 3.4). The middleware accessed the Ekahau database and converted the location data into our customized XML format. All converted data were collected and stored in a centralized DB so that the researchers can access all participants' data from a single portal.

3.2 User Study and System Deployment

In this section, I will detail demography of participants, the study design, and challenges I faced in the system deployment.

3.2.1 Participants

uLocate was evaluated in the home environments of 11 participants with disabilities who were 45 years of age or older. The participants were recruited from a pool of individuals who had completed a large-scale survey project funded by RRTC (Rehabilitation Research and Training Center) on Aging with Physical Disabilities. We did not apply exclusion criteria or screen participants based on their home setting or the nature or severity of their disability. Rather, we wanted to investigate feasibility within the context of the ''real-world'', naturally occurring challenges that might be found in a large-scale implementation.

Table 3.1 shows demographic data about participants. Participants ranged in age from 46 to 80 years (five males and six females), including individuals with spinal cord injury, multiple sclerosis, late effects of polio, and muscular dystrophy. Some participants used wheelchairs (motor and manual), while others were ambulatory.

3.2.2 Study Design and System Deployment

We first conducted a long-term study (home 1 - 5) with the study period of three to six weeks and a follow-up short-term study (home 6 - 11) for one-week long. In our first visit to a participant's house, we collected informed consent and measured the floor plan of the

Home	**Mobility Aids Used**	**Size (ft2)**	**Style / # of Rooms**	**Weeks of Study**	**# of Routers**	**Room Accuracy (%)**
1	Walk	1350	House/8	6	5	61.6
2	Powered wheelchair / Grabber	520	1BedApt/4	6	4	63.4
3	Manual wheelchairs	700	House/5	3	4	*
4	Powered wheelchair	1390	House/13	3	6	87.2
5	Walk	185	House/9	3	7	79.3
6	Powered wheelchair	816	1BedApt/4	1	4	81.2
7	Powered wheelchair	737	1BedApt/4	1	4	79.8
8	Walk	2000	House/8	1	5	82.6
9	Walk	2230	House/9	1	5	85.1
10	Powered wheelchair	890	1BedApt/4	1	4	83.9
11	Walk	1220	1BedApt/6	1	5	85.2

Table 3.1: Information and indoor tracking accuracy for each household of the participants

house. In our second visit, we deployed the system and provided training to our participants. In each home, we installed WiFi APs (WAPs) for the indoor location tracking and then performed the site survey of the whole house to build the fingerprints from the collected data. Figure 3.5 shows some examples of the WAP installations. We tried to install the WAPs behind or below the furniture to minimize the intrusion caused by the deployment. We tested different topologies and number of WAPs in our participants' house to test the effect on accuracy of the indoor tracking system. We also set up a laptop that functioned

as a local server for collecting location data.

Participants were then trained in how to use the system, including (1) how and when to carry the tag, how to download data, (2) how to review data using the visualization software and (3) how to charge the GPS logger. Participants either carried the tag or attached it to their wheelchair. During the study, self-reported diaries were collected and include their location (*i.e.*, where they are) and activities (*i.e.*, what they are doing) every 30 minutes during the day. The study period cover both weekdays and weekend. At the beginning of each study, researchers wrote qualitative field notes about interactions with participants during the deployment process. In particular, we conducted interviews regarding (1) daily routines (e.g. What does a typical day look like? How far do you normally travel?) and (2) perceptions about use of technology (e.g. What is your experience level with computers and technology? How comfortable are you with new devices?). At the end of the study, we interviewed participants about the acceptability and ease of use of uLocate and asked them a series of open-ended questions in the following categories:

- Acceptability and challenges in use of the system
  - Did you experience any difficulties when carrying the tag?
  - Any challenges with managing the tag (charging, turning on GPS)?

Figure 3.5: Example of WAP Installation. Red circles mark the location of installed WAPs.

- Did the installation of the uLocate system in your home cause any problems?

- Data use

  - Did you use the visualization software and if so, did you have any problems?
  - Now that you can see the information that was collected, for what purposes do you think it would be useful to collect this information?
  - Would you be comfortable sharing your data with others (e.g. family, caregivers, doctors)? Did you have concerns about loss of privacy?

3.3 Results and Findings

In this section, I will report the analytic results including the statistic motility data, accuracy of the indoor tracking system and the user feedback.

3.3.1 Accuracy Evaluation

We reported the accuracy of indoor location tracking in Table 3.1. We used the diaries reported by the participants as the ground truth and compared them with uLocate system. As listed in Table 3.1, the room-level accuracy ranged from 61.6% up to 87.2%. The low accuracy in Home 1 and 2 was due to the limitation of the Ekahau system. Home 2 is a small 1-bedroom unit in an apartment, in which the kitchen and bedroom are both small and tightly connected to each other. Since the accuracy of the Ekahau system is 3 - 5 meters, this ''small room'' problem deteriorated the room accuracy. Similarly in Home 1, the low accuracy (61.6%) was due to the fact that three connected rooms (kitchen, office and dining area) are small and close to each other. Home 3 is a resource limited and environmentally dynamic house. During our study in home 3, the location server was unplugged and turned off due to the power outage. Therefore, we did not present any results from home 3.

In Home 4 and 5, we respectively installed 6 and 7 routers, and performed more site surveys to get better accurate models. The accuracy increased tremendously to 87.2% (Home 4) and 79.3% (Home 5). Home 4 is a big house with spacious rooms, which relieved

the system error tolerance (*i.e.*, 3 - 5 meters). Home 5 has a small dining area tightly close to the kitchen, which slightly degraded the location accuracy. However, comparing home 5 with home 1, we can see the significantly incremental accuracy (from 61.59% to 79.27%) when we use more routers (from 5 to 7). The short-term study (*i.e.*, home 6 - 11) is to confirm reproducibility of our findings in Home 4 and 5. As shown in Table 3, the accuracy of the indoor tracking is encouraging (79.8% to 85.2%), showing the stability and reliability of the uLocate system.

For home 1 - 5, we calculated weekly average time spent in each room (indoors) and total travel distance (outdoors) as shown in Table 3.2 and 3.3. We found that participants who have fewer rooms in the home spent more time in a single room (*i.e.*, their living rooms or offices) and about a quarter of their time in the bedroom sleeping. Participants differed in the amount of time they spent outside and the distance traveled. One participant prefers to stay outside and has volunteer activities to keep him active. One participant (Home 4) worked from home and had relatively few hours outside.

3.3.2 Participant Feedback

Acceptability and challenges in use of the system

In general, participants reported that the system was easy to use, did not require significant effort on their part and did not interfere with their daily lives. Participants felt that the installation of WAPs in their home was not intrusive. Only one participant noted that when his children and grandchildren visited for a holiday, it was difficult to find an available power outlet in part because of the WAPs.

Participants felt that the tag was light and easy to carry or attach to their wheelchair, and only required very few effort to download GPS data. As noted earlier, we designed a simple, automatic GPS reader program for extracting participants' data from the GPS logger to the laptop and asked them to charge the GPS sensor and download data on a daily basis. However, **participants noted that remembering to charge the device was a challenge**. Most participants were able to remember to charge the device consistently by

building it into their daily night time routine. One participant (Home 3) had consistent difficulty remembering to charge the device, which resulted in missing data for several days.

Home	**Indoor (Weekly Average)**								
1	Kitchen 20.7%	Living Room 26.3%	Master Bdr 11.9%	Master Bath 0.9%	Office 19.5%	Dining Room 0.6%	Guest Bdr 9.4%	2nd Bdr 9.3%	Hallway 1.4%
2	Kitchen 12.3%	Living Room 41.1%	Master Bdr 46.6%						
3	*								
4	Kitchen 1.1%	Living Room 6.0%	Master Bdr 25.4%	Master Bath 2.0%	Office 59.1%	Dining Room 0.0%	Laundry 0.9%	Activity Room 4.0%	Hallway 1.5%
5	Kitchen 1.7%	Living Room 47.0%	Master Bdr 24.0%	Master Bath 3.6%	Office 19.5%	Dining Room 0.6%	Guest Bdr 2.0%	2nd Bath 1.6%	

Table 3.2: Statistics of location tracking data (home 1 - 5). Indoor tracking data shows the percentage of the participants staying durations over the period of studies.

Home	**Outdoor (Weekly Average)**
1	79.9 miles, 34.2 hours
2	64.7 miles, 22.7 hours
3	*
4	42.5 miles, 14.3 hours
5	32.1 miles, 16.4 hours

Table 3.3: Outdoor tracking data demonstrated weekly (average) travel distance and time.

Participants were also asked to turn on the GPS unit when going outside and turn it off when returning indoors. All participants forgot to perform this task occasionally and reported that there were a few gaps in their outdoor data. Our participant in Home 3 consistently forgot to turn the GPS on and off when going outside. Several participants noted that **it would be better if there were a way for the system to sense when they crossed the boundary between indoors and outdoors automatically**. Finally, in order to make the tag as compact as possible and reduce participants' burden, we chose the smallest GPS logger in the market. Since the GPS device itself is small, the switch on the device was also tiny. We found that **several participants had some problems using this tiny switch to turn the GPS on and off**. Although most of them figured out a method for powering on the device (e.g. with a fingernail) within a few days, the size of the switch was an impediment.

Data Use

We demonstrated the visualization software for participants and taught them how to use it, but did not require them to do so. In our interview, we asked participants whether they used the software and whether it was difficult to use. **The majority of participants reviewed their data occasionally out of curiosity, but not frequently**. None of the participants had difficulty using the software. When we asked the participants regarding what they learned from looking at their data, several participants noted that it showed them that **they are not as active as they thought and were not getting outside as much as they should**. However, in contrast, our participant with LEP expressed surprise about how much he moved around in a half-hour period and noted that it made him consider ways to be more efficient because he was trying to preserve muscles in his polio-affected leg.

We also asked participants for what purposes the data could be used. In general, participants thought the system gave a general sense for physical effort or activity. They thought **their physicians might find it useful to know the level of activeness they were engaged in**. They did not believe that their caregivers, spouses or children would be

interested in that level of detail about their movement.

We asked whether participants would be comfortable sharing their data with other individuals and whether they had any concerns about privacy. Surprisingly, most participants in our small sample had no concern about the privacy of their location data. Only one younger and computer-savvy participant expressed concern. She noted that she would not mind sharing her data, but would want control over it. In particular, she noted that she would want to provide data to someone else only after she had an opportunity to review. **She would not want it to be reviewed in real time and noted that one major concern would be that if they system was hacked**; it could allow someone to identify her patterns of travel and times when she was typically not home. If someone knew these patterns, they could burglarize her home or perhaps put her at risk of assault. She thought that summaries of data might make more sense when sharing with others.

3.4 Discussion

Although we did not specifically ask participants for recommendations for improvements or additions to the system, they offered several. Recommendations fell into three categories:

1. *Goal setting*

   Participants felt that a system like uLocate that collected data automatically on a behavior would be very useful to them in managing health issues related to their disability, although in order to do so, the system would need to track more than just location. Exercise and physical activity was one common theme for which participants would like automated measurement. Participants identified several types of activities including (1) doing sit-ups and spending time on a rebounder trampoline for our participant with LEP and, (2) weighting bearing activities like standing in front of her pinball machine for a period of time for our participant with MD. Another area participants identified as important were health behaviors related to their disability such as reclining their wheelchair to raise their feet and reduce pressure, spending time on an incline table or transitions from sit to stand. Finally, participants were

interested in more general health information such as blood pressure, lung capacity and frequency of bathroom use (related to bladder infections). Across all these types of health-related behaviors, participants were interested in measurements over time showing show incremental changes that might be hard to identify without data.

2. *Prompting*

   If more relevant variables could be measured by the system, then several participants noted that they would want it to be able to prompt them to engage in positive health behavior (e.g. exercise, sit/stand, pressure relief). One participant noted that such prompting would ideally be contextual so that she was prompted at the time and place when she should do something.

3. *Hardware*

   A few of the participants noted that they would like it if the system were integrated into a smart phone so they would not have to carry multiple devices and/or connect to a computer to access data.

4. *Limitation*

   First the device usually obtains high-level activities or motion status. These coarse-grained data are not sufficient to reconstruct the daily life events that usually includes complex activities. For example, data from a wrist-attached accelerometer may appear very similar in ''washing dishes'' and ''cleaning the tub''. For those with multiple sensors that can identify more low-level activities, they demand more power as more sensors being exercised and therefore requires users to charge frequently. Furthermore, users needs to attach the device on body and sometimes need to relocate it (e.g., moving the device to another jacket when leaving home). All these issues might become problematic when devices being applied to the elder; they could forget to charge the battery or even forget where they put the sensor.

In this chapter, I demonstrated the accuracy, feasibility and acceptability of using the uLocate system in the elder-care related study. Based on the evaluation of this system, we have confirmed that the tag is compact and easy-to-carry and the uLocate platform provided a friendly, easy-to-use interface and useful visualized information for our participants. However, we have also begun to identify the challenges faced in our implementation of embedded assessment in real world contexts with diverse range of community-dwelling individuals. Key challenges includes the overhead of using a wearable device and the coarse-level recognized activities that this system enables. To address these issues, I will show that how time-varying electrical noise can be leveraged to extract fine-grained information of user-driven electrical events (Chapter 4 and 5) and real-time power estimation (Chapter 6). I will also illustrate that similar varying EMI can be used to convert unmodified LCD monitors into touch sensitive surfaces for human proximity detection (Chapter 7).

Chapter

DETECTING USER-DRIVEN OPERATING STATES OF ELECTRONIC DEVICES USING A SINGLE SENSING POINT

The ability to sense, model, and infer human activity in the physical world remains an important challenge in pervasive computing. Electricity and appliance usage information can often reveal the nature of human activities in a home. For instance, sensing the use of vacuum cleaner, a microwave oven, and kitchen appliances can give insights into a person's current activities. Instead of putting a sensor on each appliance, the technique presented in this chapter is based on the idea that appliance usage can be sensed by their manifestations in an environment's existing electrical infrastructure thereby reducing the need for installing sensors everywhere in an environment. Prior approaches using this technique could only detect an appliance's on-off states; that is, they only sense *what* is being used, but not *how* it is used.

This chapter presents **DOSE** (**D**etecting **O**perating **S**tates of **E**lectronic devices), a significant advancement for inferring operating states of electronic devices from a single sensing point in a home (see Figure 4.1). When an electronic device is in operation, it generates time-varying EMI (Electromagnetic Interference) based upon its operating states (e.g., vacuuming on a rug vs. hardwood floor). This EMI noise is coupled to the powerline and can be picked up from a single sensing hardware attached to the wall outlet in a house. Unlike prior data-driven approaches, I employ *domain knowledge* of the device's circuitry for semi-supervised model training to avoid tedious labeling process. In this chapter, I will describe three different types of appliances, their circuit model and how they produce time-varying EMI signals when functioning at different states or under different physical uses. Specifically, these three types are motor-based appliances, SMPS-based appliances and mixed-mode appliances; the corresponding theory of operations will be respectively

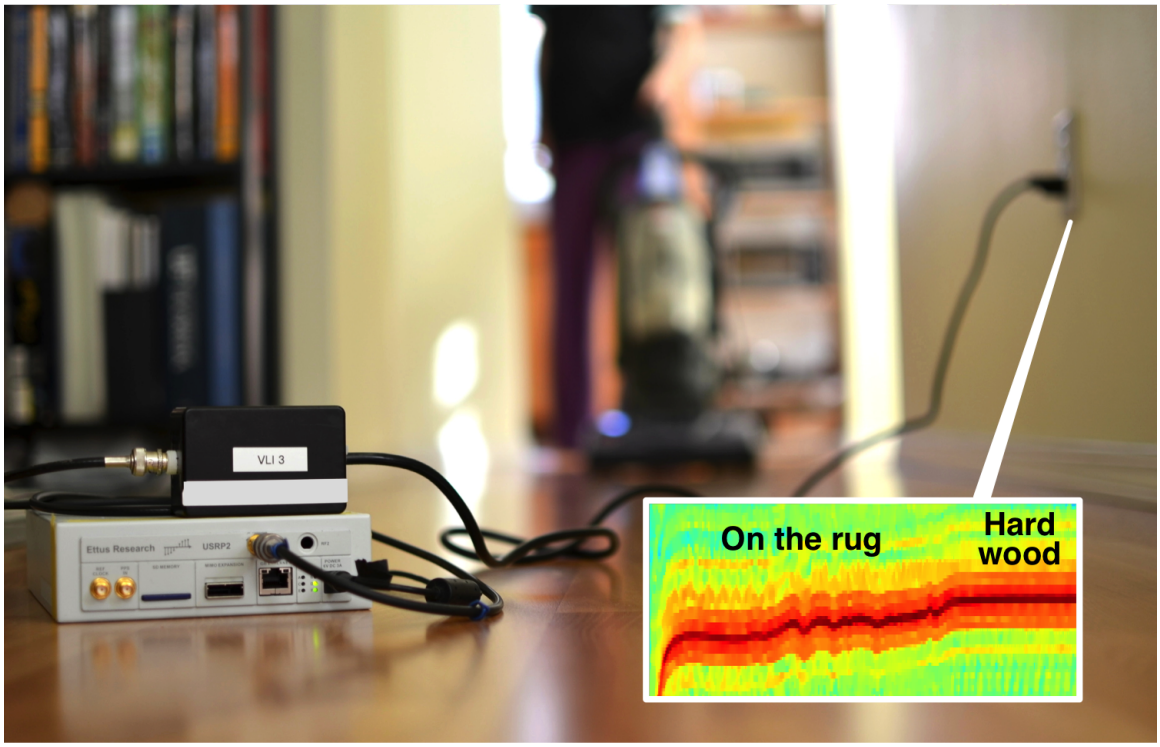

Figure 4.1: DOSE detects user-driven operating states of electronic appliances through a single sensing point installed to the wall outlet in the house.

detailed in Section 4.1, 4.2 and 4.3.

4.1 Motor-based EMI

Motors exist in a variety of home appliances such as vacuum cleaners, blenders, and food mixers. Commutator motors are energy efficient because they yield high rotational speed with relatively low power consumption. However, due to mechanical switching mechanism between the brushes and commutator, it inevitably generates strong EMI.

Figure 4.2 illustrates the schematic view of a three-slot, two-pole brushed motor. This motor consists of three commutator slots (''arcs'' in Fig 4.2) and three electromagnets, each of which has two poles (north and south). Two brushes (marked as ''red'' and ''green'' in

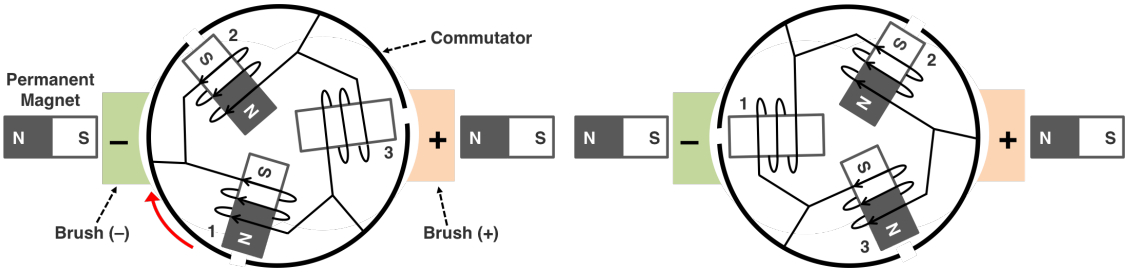

(a) Start-up (b) Poles switch

Figure 4.2: The schematic view of a three-slot, two-pole brushed motor. **(a)** When the motor is on, electronic currents through commutators (arcs) turn iron bars into electromagnets, generating a clockwise force. **(b)** Breaking and making contacts between commutators and brushes switches poles of conducted electromagnets, making the motor consistently rotate clockwise and generating EMI.

Fig 4.2) are used to supply electric currents to the circuitry. When the motor is in operation (Fig 4.2a), electric currents from commutators induce magnetic fields on iron bars, turning them into electromagnets (the ''bars'' insides the commutators in Fig 4.2). It is noted that the third iron bar does not form any magnetic field as there is no current flowing through it. There are two permanent magnets on both sides to generate rotation forces. In this example, the first iron bar is attracted by the left permanent magnet while the second is repelled, generating a clockwise force to the motor. The breaking and making of contacts between the commutator and brushes causes poles of the conducted electromagnets to switch, forcing the motor to consistently rotate clockwise (Fig 4.2b). High-efficiency motors usually have more slots (usually 21 to 25) and even more brushes in order to yield a stronger torque.

4.1.1 Commutating EMI due to mechanical switching

The motor EMI is caused by the mechanical switching phenomena. As the motor rotates, the action of breaking and making contacts between the commutator and brushes yields periodic

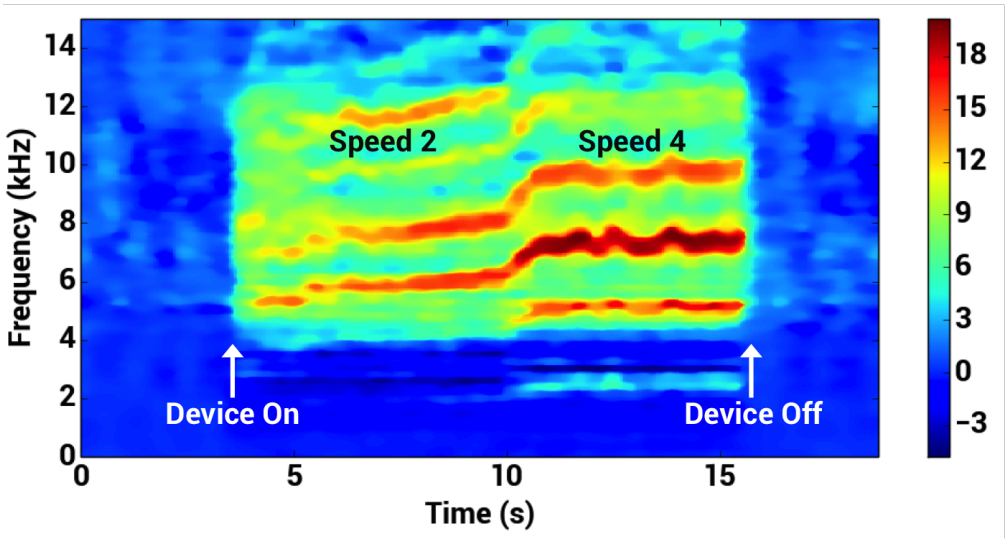

Figure 4.3: Time-varying EMI of a blender operating at different speeds. Higher rotation speed (from 10s to 15s) produces EMI at a higher frequency of 7.1 kHz.

current spikes at the motor's rotation rate multiplied by the number of commutator slots. That is, the EMI appears at the harmonics of the motor's rotation speed. For example, a motor with 21 slots and a rotation rate of 460 RPS (revolutions per second) yields current spikes at 21*460 = 9660 Hz, which manifests itself as EMI of the same frequency. This type of EMI, called *commutating EMI*, propagates mainly through conduction over the powerline network and also yields a small amount of radiated emissions.

Besides the motor's fundamental EMI, there are two other factors affecting the induced time-varying signals. First when the motor is turned on, it takes one to two seconds to reach the specified operating speed. This speed-up duration appears as a ''ramp-up'' EMI (see Fig 4.4). In addition, there exists electrical resistance between each brush-commutator terminals. These impedances affect motor rotations, causing relatively weaker EMI near the fundamental frequency. We leverage these various EMIs as features for estimating motor operating states. We will detail our state detection algorithm in a later section.

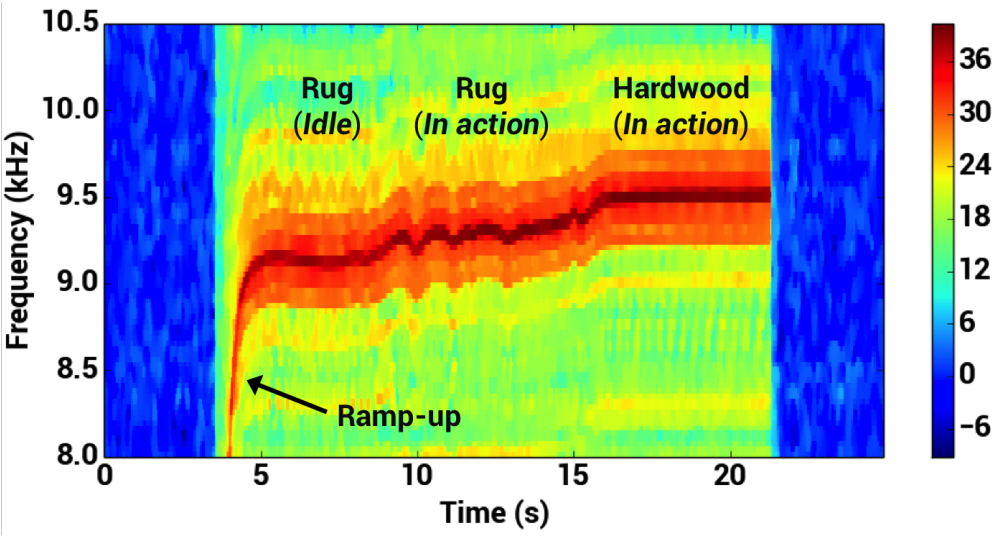

Figure 4.4: Time-varying EMI of a vacuum. When being used on a rug (from 5s to 15s), the motor rotates at lower speed and yields fluctuating EMI due to uneven airflows.

4.1.2 Time-varying EMI at different rotation speeds

Commutating EMI appears at the harmonics of the motor's rotation rate. When the motor operates at different speeds, the EMI in turn appears at distinct frequencies. Figure 4.3 shows fluctuating EMI when a blender (Cuisinart PowerBlend600) operates at different speeds. In the first duration (5s to 10s in Fig 4.3), the blender was running at a relatively low speed, yielding EMI at roughly 6 kHz. When it switches to a higher speed (10s to 15s in Fig 4.3), EMI frequency ramps up to 7.1 kHz as the motor's rotation speed increases.

Time-varying EMI in response to different physical uses

It is noted that when the blender motor spins at a higher speed, water within the blender container is vigorously stirred, causing air pockets and liquid to collide randomly with the blades. This uneven air/liquid resistance causes the blender speed to fluctuate, thus causing the irregular fluctuating EMI (as visible in Speed 4 section of Figure 4.3). We also discovered

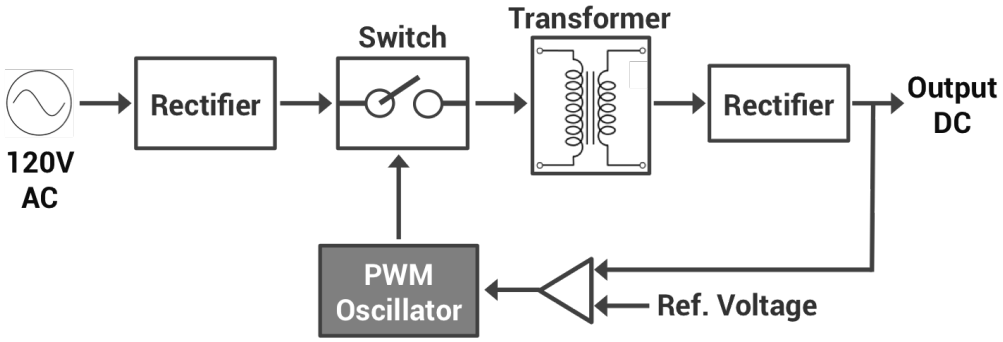

Figure 4.5: Block diagram of an AC-to-DC SMPS. Voltage regulation is accomplished by adjusting the ratio of on-off durations of PWM oscillator, which causes time-varying EMI in different operating states.

time-varying EMIs when a vacuum is used on different surfaces. Figure 4.4 illustrates the fluctuating EMI when a vacuum cleaner (Bissel 6584) was used on the rug and hardwood floor. In a vacuum cleaner, the motor spins to exhaust the air from the machine, making the dust collection container a temporary vacuum. To balance the pressure, the air outside the cleaner flows into the container and then releases from the motor vent. This air circulation sucks the dusts into the machine and releases the air from the machine. When being used on the rug, the motor rotates at a lower, uneven speed due to the uneven airflows disturbed by the rug. The reduction and distrubance in motor rotations therefore yield an EMI that fluctuates at a relatively low frequency (5s to 15s in Fig 4.4). Once the vacuum cleaner moves to a hardwood floor, the air intake becomes largely unhindered yielding a static EMI at a higher frequency (16s to 21s in Fig 4.4).

4.2 SMPS-based EMI

SMPS (switched-mode power supply) has been extensively used in modern electronic appliances due to its small size and high efficiency. Unlike traditional linear power supply, SMPS manages power by switching the supply between complete-on, complete-off and low

dissipation. Because the power supply operates at high dissipation only for a very short period, it minimizes unnecessary power wastage. Figure 4.5 shows the block diagram of an AC-to-DC SMPS. The key component of SMPS is a pass-transistor, which controls the frequency of oscillator that switches the stored energy from the inductors to the load that an electronic device requests. To reduce the size of the supply, SMPS usually operate from tens to hundreds of kilohertz. This switching action inherently generates strong EMI near the frequency where SMPS switches between different modes. We will refer this frequency as *switching frequency*. Gupta *et al.* leveraged SMPS-based EMI for electrical event detection and have shown the stability of signal patterns across different homes [34]. Here I further found that EMI signals can temporally vary with the operating states of devices.

4.2.1 Time-varying EMI at different CPU loads

In SMPS, the voltage regulation is accomplished by adjusting the ratio of on-off durations. As shown in Fig 4.5, the output DC is compared with the reference voltage to adjust switching frequency of the PWM (pulse-width modulation) oscillator. Electronic appliances with varying loads such as laptops can cause EMI fluctuations near its switching frequency. Figure 4.6 illustrates one example of the time-varying EMI when a laptop (Acer Aspire

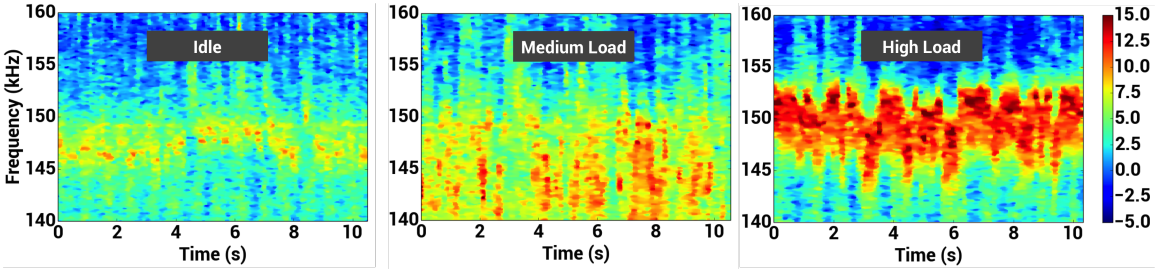

Figure 4.6: Time-varying EMI of a laptop (Acer Aspire, 15-inch) with CPU at **(left)** idle, **(middle)** medium load and **(right)** high load. When the CPU is running at high load, the dropping output voltage causes the oscillator to operate at a higher frequency to draw more power, yielding the EMI at higher frequency and magnitude.

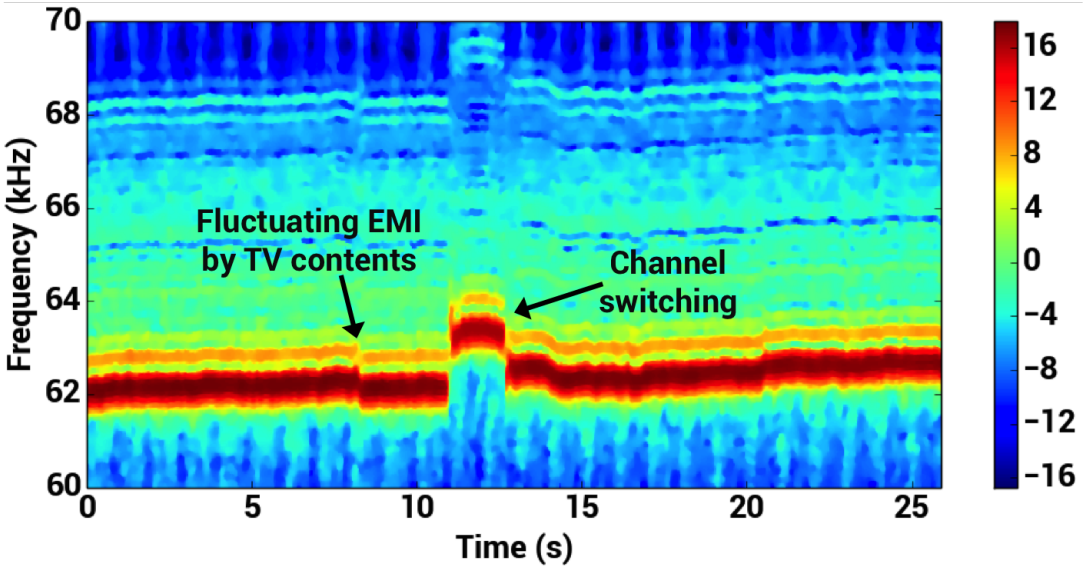

Figure 4.7: Time-varying EMI of a TV. When a TV is switched to another channel, the TV turner resets the center frequency, resulting in a transient glitch (11s to 13s) in its EMI signal.

5736Z) operates its CPUs at idle, medium and high load. When the CPU is running at a high load (*i.e.*, 90 to 100%), the dropping output voltage causes the oscillator to operate at a higher frequency to draw more energy, yielding the EMI at a higher frequency and magnitude (Fig 4.6, right). In other two modes, idle and medium load, we observed relatively weaker but still discernible EMI (Fig 4.6, left and middle). We note that the signal patterns are distinct on different laptops and PCs that can be attributed to manufacturer differences in power regulation circuitry. These unique fingerprints between different computers could be used for manufacturer identification or abnormal detection, such as detecting large power draws that may indicate an impending device failure (e.g., a malfunctioning video card).

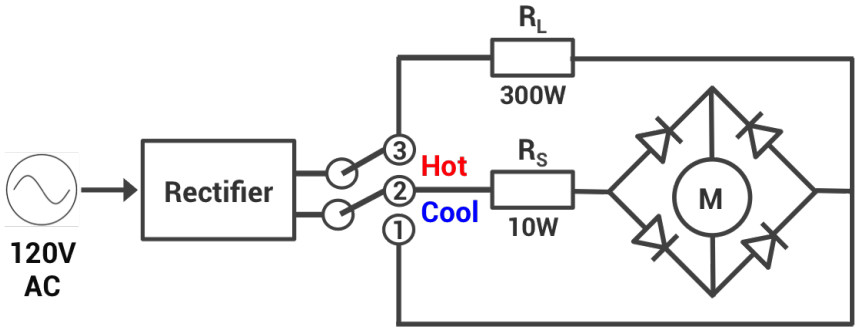

Figure 4.8: The simplified schematic view of a dual-mode hair dryer. While the device was switched to ''hot'' mode (*i.e.*, terminal 2 and 3), a large, parallel resistance (R_L) increases total current loads to the circuitry and affects rotation speed of the motor-driven fan (marked as ''M''), causing time-varying EMI.

4.2.2 Time-varying EMI caused by transient actions

Another type of time-varying EMI that we discovered is caused by transient actions such as switching a TV channel. Figure 4.7 shows the EMI signal of a TV (Sharp 42-inch) when it is switched from one channel to another. As shown in Figure 4.7, we observed a glitch, or sudden change in EMI, between 11s to 13s when the action was performed. On further investigation of the TV tuner's circuitry and operation, we found that when a TV switches to a new channel, the TV tuner resets the center frequency, causing the oscillator to operate at a different frequency for a short period. Prior research by Enev *et al.* has shown that TVs produce varying EMI signals that correlate to the screen content being displayed [27]. The EMI change from a channel switch is distinct from EMI change as a result of screen content; we have found that due to its large transient nature, it can be robustly detected and extracted.

4.3 Mixed-mode EMI

In addition to a motor, certain appliances such as hair dryers and fan heaters employ large resistive components to generate a stream of hot air. When the device is running in different modes (e.g., warm vs. hot), changes in resistive loads affects the motor operation and result in discernible EMI patterns for state estimation. Of course, this finding extends to other appliances where any other component affects motor operation as well, such as a torque screwdriver.

Figure 4.8 illustrates a simplified schematic view of a dual-mode hair dryer (*i.e.*, hot and cool air). The AC source is first rectified to DC current. When the hair dryer operates at cool mode (i.e., making contacts at terminal 1 and 2 in Fig 4.8), only the low resistive load (R_S) and the motor-driven fan are actuated. When it switches to hot mode (*i.e.*, terminal 2 and 3 in Fig 4.8), the large resistive load (R_L) is in parallel with R_S, which increases the total current load to the circuitry and changes the fan's rotation speed. These behavior changes induce distinct EMI patterns at respective operating states. Figure 4.9 shows an example of this time-varying EMI when a hair dryer switches from the cool to hot mode.

In the next chapter, I will introduce the process pipeline of my state estimation algorithm. The key insight of the state estimation algorithm is incorporating human knowledge into the model training process, which avoids the requirement of collecting labeled data as requested in a traditional supervised training approaches. The obviation of labeled training data allows DOSE for the large scale deployment.

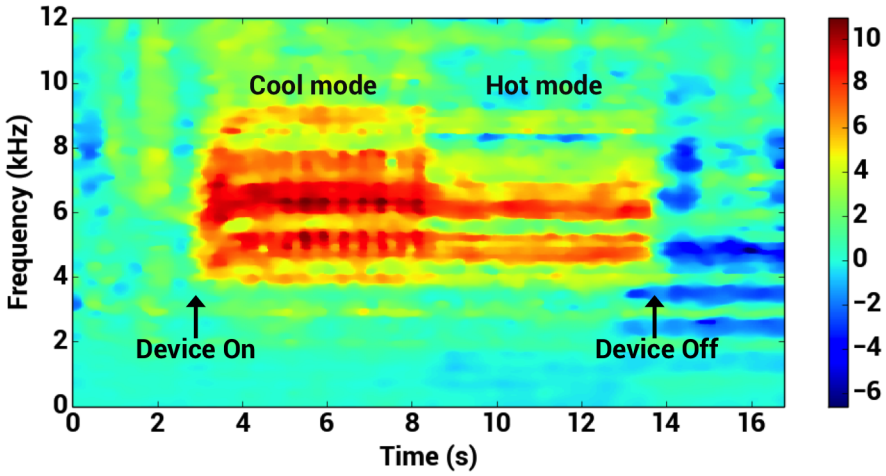

Figure 4.9: Time-varying EMI of a hair dryer in two different operating temperatures.

Chapter

SEMI-SUPERVISED TRAINING FOR APPLIANCE STATE ESTIMATION

This chapter describes the process pipeline of state estimation algorithm (Section 5.1), study design, evaluation and results (Section 5.2). I will also discuss some potential applications from the DOSE system and the possibility of combining power consumption data to estimate states of appliances that do not produce observable EMI signals (Section 5.3).

5.1 State Estimation Algorithm

Fig 5.1 shows the processing pipeline for operating state detection and classification. The key insight is the use of domain knowledge in model training; specifically, I leverage semi-supervised training for state estimation that only requires the number of states as the prior in the training process. It avoids the tedious labeling process in the data collection and makes the system easy for the large-scale deployment. Each components in the process pipeline will be detailed in this section.

5.1.1 Data Acquisition

The first step is to retrieve the electrical noise data from the power line infrastructure. To record EMI signals, we follow the experimental setup in [34] with minor adjustments. A power line interface (PLI) is plugged in the wall outlet to obtain the analog signal (see Figure 4.1). The PLI was modified from [34] and has a high-pass filter with a cut-off frequency at 5.3 kHz. This corner frequency was chosen to strongly reject 60 Hz and harmonics, avoiding possible damages to the sensing hardware while being low enough to capture low RPS motor EMI (usually between 5 to 15 kHz). The filtered signal is fed into a USRP (Universal Software Radio Peripheral) N210, which functions as an ADC (analog-to-digital)

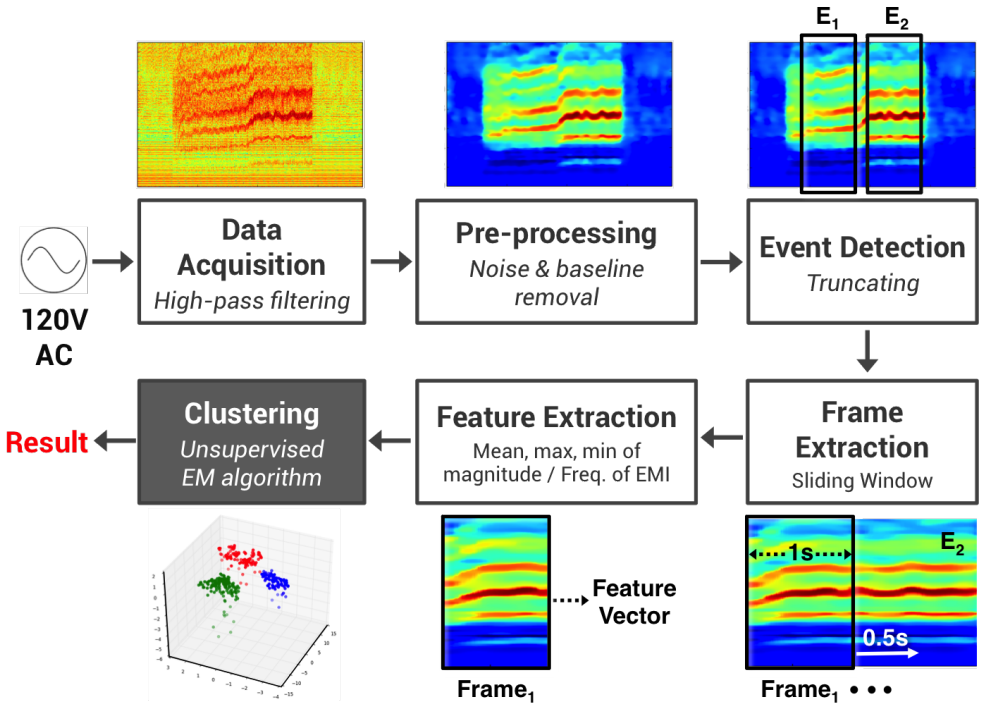

Figure 5.1: Processing pipeline of operating state detection and classification.

converter sampling at 500 kHz. We next compute Fast Fourier Transform (FFT) over these time-domain data, yielding 16384-point FFT vectors with 30.52 Hz bins. This resolution of bin size allows us to observe small EMI fluctuations in different operating states. The FFT vectors are streamed to our processing pipeline for the state detection and classification.

5.1.2 Pre-processing

We first remove the baseline signal from recorded data. To do so, we average the first 100 FFT vectors in each recorded data file as the baseline vector, and subtract it from the remaining FFT vectors. The differential vectors represent EMI produced by a later-actuated electronic device. Next we perform filtering to remove noises resulting from the sensing hardware and powerline network. In particular, we apply a median filter with a

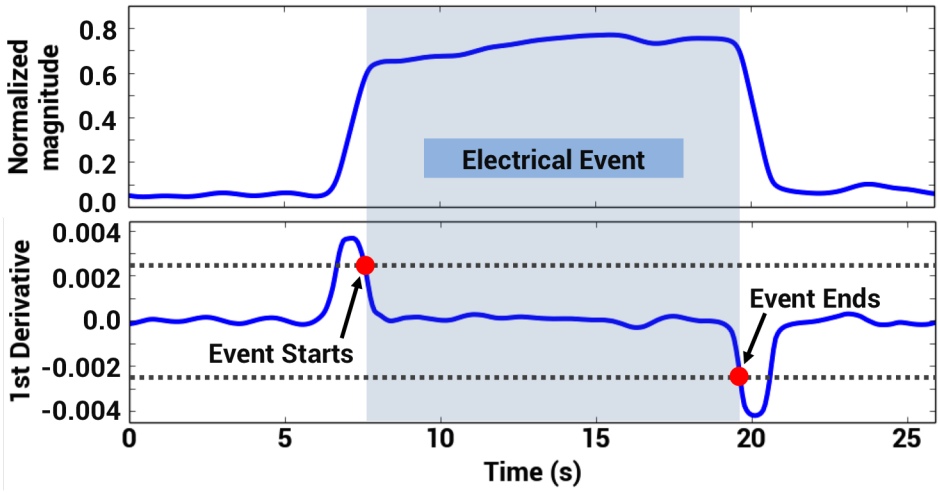

Figure 5.2: Event detection procedure. **(Top)** Rising and falling edges represent on/off of an electrical event. **(Bottom)** The intersection of the threshold lines (dotted) and 1st derivative curve of the top curve represents the start and end of an electrical event (red circles).

window size of 10 to removed sparse noise. To further smooth the data, we use TVD (Total Variation Denoising) with regularization parameter of 20 [52, 81]. TVD was designed to remove noise from images with high total variation while preserving important details such as corners and edges. Since EMI signals inherently have excessive, sparse noises, TVD can efficiently remove the noise without damaging most signal characteristics.

5.1.3 Event Detection

After the noise and baseline removal, we truncate the recorded data to extract the event segments. To this end, we sum up each FFT vectors and plotted the total magnitude fluctuation over time (Fig 5.2, top). Any significant variation in this curve represents a possible electrical event and can be easily segmented by a threshold-based approach. Figure 5.2 demonstrates this event detection procedure. The top figure in Fig 5.2 shows

the normalized magnitude of the EMI data, where the rising and falling edge respectively correspond to on and off of an electrical event. To identify the event, we take the 1st derivative of this magnitude curve (Fig 5.2, bottom). The intersection of the threshold lines (dotted lines) and the 1st derivative curve denotes the start and end of an event (red circles). In this study, we empirically decided the threshold value of 0.0025 using the data collected from our study. This threshold is able to robustly detect all electrical events while inducing only two false alarms.

After extracting the event segment, we further truncate the FFT vectors to a specified frequency range that covers all operating states of a device. This 2nd truncating procedure is critical for the feature extraction. As we will only extract features within the specified spectrum, the truncated FFT vectors can more precisely represent the signal characteristics. Previous research [34] has shown that the target EMI frequency can be easily located by switching a device on and off, and therefore, we assume such information already exists. In this study, we manually turn on and off for each operating state of a device to retrieve the target frequency range of each device.

5.1.4 Frame Extraction

For the truncated event segment, we further chunk into smaller units (called frames) by a sliding window of 1 second with 0.5s overlapping. According to our observations, the EMI shows stable signal characteristics within the same operating state. This short-term analysis therefore servers two purposes in this study: (1) to confirm the stability of EMI characteristics within the same operating states, and (2) if EMI fluctuates dramatically in the same states, to analyze the variation.

5.1.5 Feature Extraction

We extract aggregated features from each frame based on signatures of different time-varying EMI. The first six features are *mean*, *maximal* and *minimal* magnitude and frequency of the peak EMI; they describe the characteristics of the fundamental EMI. For motor-based

devices, there usually exist multiple peak EMIs due to uneven rotations caused by the fractions and electric resistance. To capture this, we extract the *gap* between two dominant frequency peaks as the 7th feature. Some EMI has distinct total magnitude variation such as laptops (under different CPU loads) or hair dryers (under different temperature modes). Therefore we choose *average magnitude* of the frame as the 8th feature. In the end, the system extracts an 8-tuple feature vector for each frame.

5.1.6 Clustering

For classification of operating states, we choose EM (expectation maximization) clustering algorithm due to some key advantages. One advantage of the EM algorithm is its adaption to uneven cluster sizes. As we expect a resident may use each device in different states unevenly in daily life, thus the cluster sizes corresponding to different appliances may vary a lot. EM typically outperforms other similar algorithms such as k-means which is more sensitive to the cluster size. In addition, EM allows clusters to overlap. If an appliance has two similar operating states (e.g., similar rotation speed in 2 modes of a food mixer), their respective clusters will unavoidably overlap in the feature space.

Perhaps more importantly, EM only requires the number of clusters as the input parameter. From the user perspective, we perceive the states of an appliance either from its outlook (e.g., 6 buttons of a blender), physical use (e.g., vacuuming on different surfaces) or its circuit model (Figure 4.2, Figure 4.5, Figure 4.8)). Whenever we get a new device, these human observations can be employed as the prior knowledge to train the model, obviating the need to label each individual state during calibration. In this prototype, we applied EM clustering on individual appliances and trained their models separately. For implementation, we used Scikit-learn package, a machine learning library for python.

5.2 Evaluation, Results and Analysis

In this section, we will detail the study design, data collection process, experimental results and analysis.

EMI type	Device	Make / Model	Operating states	Actual clusters	Predicted clusters	Accuracy
Motor-based	Vacuum Cleaner	Bissel 6584	Rug / Hardwood / Hose	3	3	**100%**
		Hoover Elite II		3	3	**100%**
		Eureca 1432A	Rug / Hardwood	2	2	**98.5%**
	Blender / Food mixer	Hamilton Beach 62560	6 Rotation Speed	6	5	**87.4%**
		Cuisinart PowerBlend 600		6	6	**89.9%**
		Oster Listed 654A		6	6	**84.0%**
SMPS-based	Laptop / Computer	Acer Aspire 15"	Idle / Medium / High Load	3	3	**99.7%**
		Dell Inspiron 15"		3	3	**98.8%**
		Toshiba Portege 13"		3	3	**92.1%**
		PC (300W)		3	3	**100%**
	Television	Vizio 32"	Channel switching (hit rate)	*	*	**100%**
		Sharp 42"		*	*	**90%**
Mixed	Hair Dryer	Remington Speed2Dry	Cold / Warm / Hot	3	3	**81.5%**
		Tashin Powerslit TS-318A		3	3	**81.8%**
		Tashin TS-3000		3	3	**96.7%**
		Gibson GSN-760		3	3	**100%**

Table 5.1: The list of devices in our study and classification accuracy.

5.2.1 Study Design

We set up our experiments in a real home environment. This residential house is a triplex, 1100 sq. ft. townhouse of two residents (one male, one female). To explore the temporal stability of the signal, the data collection process was conducted across 2 months, including multiple sessions at different time (morning, afternoon and night) on both weekdays and weekend. During each session, we asked one resident to turn on a device to a specified operating state for a random time (5s to 10s) and then turned it off. When one resident was executing the requested action, the other resident remained performing her daily routines such as cooking, using computers or watching TV. Each electrical event was manually labeled. It is noted that these labeling data are only used for evaluation, not for the model training. Throughout the study, 580 electrical events were collected in total.

To collect the data, we installed the sensing hardware (*i.e.*, a PLI and USPR N210) and a laptop in the participant's house. The laptop is a local server for recording EMI data and the follow-up processing pipeline. For each type of time-varying EMI, we respectively chose four to six different appliances and in total, 16 electronic devices were evaluated in

our study. Table I shows the model, brand and target operating states of these devices. As ElectriSense [34] has shown the stability of EMI signals across different homes, we believe findings in this study can apply to other households.

5.2.2 Defining Operating States

Different appliances of the same type usually have minor difference in operating states. For example, one blender has 6 speed modes while the other may have 7. In this study, we chose the same number of states for devices within the same categories in order to get a baseline to compare between them (see Operating states Table I).

Operating states of motor-based devices

For vacuum cleaners, we defined two states based on the surface where it is used (*i.e.*, on a rug or hardwood floor). Most vacuum cleaners have a hose, which can be detached from the machine and used separately. Here we defined ''using the hose'' as the 3rd state. One of our vacuum cleaner (Eureca 1432A) does not equip a hose so we only evaluated it on two defined surfaces. For other motor-based appliances (*i.e.*, blenders and food mixer), the states are defined as their operating speeds.

Operating states of SMPS-based devices

For laptops, we defined three different states based on the CPU usage. In the **idle** mode, we turned off all applications and keeps the CPU load below 10% usage. In **medium load**, we run our testing script that periodically calculates a specified math equation and meanwhile open a couple webpage and youtube videos, maintaining CPU loads fluctuating between 30% to 60%. To simulate a **high load**, we run an on-line benchmark called SilverBench[1], forcing the CPU usage above 90%. For TV, we define the state as the action of switching a channel.

[1]SilverBench: http://silver.urih.com

Operating states of mixed-mode devices

We defined states of a hair dryer by the operating temperatures – cold, warm and hot. Some modern hair dryers have various temperatures modes combining with different speeds. As the factor of speed has been evaluated in motor-based appliances (*i.e.*, vacuum cleaner, blender and food mixer), in this category, we focus on temperature variation, that is, how a large resistive load affects the time-varying EMI.

5.2.3 System Performance and Analysis

As EM is semi-supervised learning, the output of our processing pipeline are unlabeled classes, each of which represents an unknown operating state. For analysis purposes, we assigned each predicted class to its actual label based on the majority vote. Classes with the same label are merged and assigned to the label with the highest vote. Table 5.1 shows the classification results of individual appliances.

Overall our system presents the average accuracy of 93.8% across 16 appliances, showing the system stability in state estimation. All vacuum cleaners report high classification accuracy. We noted that the 3rd state (*i.e.*, using the hose) shows a highly discernible cluster in our trained EM model. In the study, we asked the participant to use hose to clean the corner of a wall. Compared to the machine used on a rug, the hose moves unevenly above the surface and causes an irregular EMI fluctuation. In addition, the detachment of a hose affects the airflows through the container due to the changes in air pressure. These two factors causes time-varying EMI distinct from the other two modes (*i.e.*, rug and hardwood floor), yielding high classification accuracy.

Similarly, almost all laptops/PC and TV report high accuracy. Toshiba laptop (13-inch) reports a slightly lower accuracy (92.1%). As this model produces a relatively weaker EMI than other computers, it induces less discernible EMI between different CPU loads; the confusion occurs between the ''idle'' mode (recall=81.7%) and ''medium load''. The EMI of Sharp TV (42-inch) is sensitive to the contents being displayed and produced some dramatically fluctuating EMI. In such case, the EMI caused by channel switching becomes

unrecognizable and thereby slightly downgrades the event detection rate (hit rate of 90%). To further explore the system robustness, we recorded 40-min EMI data from both TVs without any actions of channel switching. We only detected two false alarms, showing the robustness of our algorithm against this fluctuation.

Blenders and food mixers show a relatively low accuracy (84% to 89.9%). The Hamilton food mixer has confusions between speed mode 2 and 3, which are merged into the same class with low accuracy (recall=54.7%). Similarly, the Cuisinart blender has confusions between speed mode 3 and 4 (recall=64.4%), while the Oster blender has confusions among speed mode 1 (recall=76.5%), 2 (recall=65.9%) and 3. These confusions resulted from the similar characteristics between operating states. When we examined the data, we found the frequency and magnitude of those confusing states are quite similar. After filtering (Fig 5.1, 2nd step), these minor differences between states are smoothed out and become hard to differentiate. It implies that fundamentally the device may not have as many discernible operating speeds as it claims.

Finally, we saw high variations of the accuracy in different hair dryers (81.5% to 100%). For two hair dryers with relatively low accuracy (81.5% and 81.8%), the confusion occurs between the ''cold'' and ''warm'' mode; we observed similar EMIs in these two modes. Our inference is that in the warm mode, the parallel resistive load is small in these devices. That is, it does not cause discernible changes in the total current loads compared to that in cold mode, yielding similar EMI patterns. As described earlier, the difference in the circuit design between hair dryers is attributed to different manufacturers.

5.3 Discussion

In this section, we discuss various applications that DOSE could potentially enable, including (1) energy disaggregation (2) activity recognition (3) machine failure detection. We also explor appliances that does not generate observable EMI and show their states could possibly be inferred from the current loads.

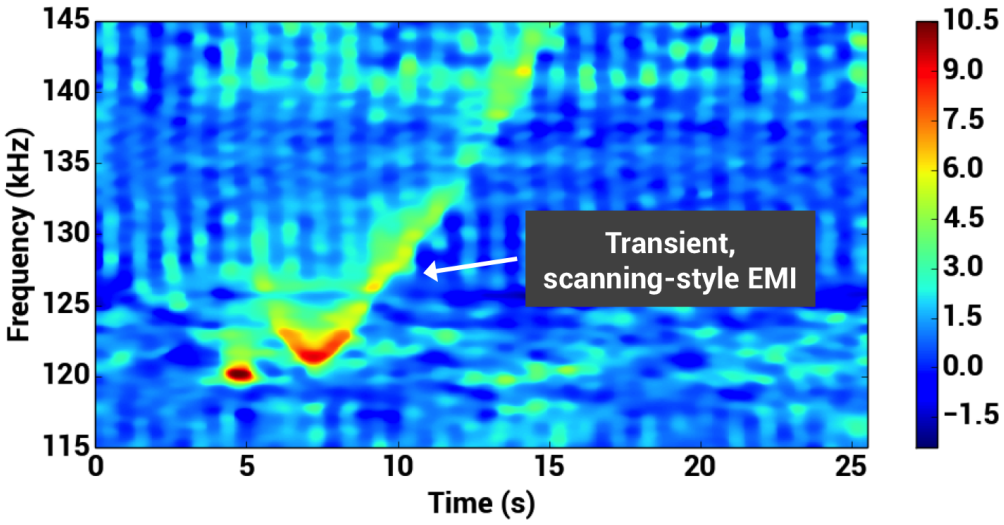

Figure 5.3: Time-varying EMI of a TV. This TV produced a scanning-style EMI when it switches the channel.

5.3.1 Energy Disaggregation

In this work, we showed distinct signal characteristics when a device operates at different operating states. For the same type of devices, we further found that there also exists minor differences in their EMI. For example in the Oster blender (Listed 564A), we observed a strong EMI between its fundamental and 1st harmonic, while we did not see similar pattern in other blender or food mixer. Gibson hair dryer (GSN-760), instead of a continuous EMI, produces a switching-style EMI when operating at cold mode. Similarly in Vizio 32 TV, when switching to a new channel, the TV produces an transient, scanning-style EMI between 115 and 145 kHz (see Fig 5.3). This transient signal in spectrum is away from its fundamental frequency and was not found on the other TV. These small but significant differences between devices could provide granular information for manufacturer identification and energy disaggregation. Especially for the same type of devices, their EMI usually overlap within the similar frequency range (e.g., motor-based devices below 20 kHz). These nuance in the time-vary EMI can be employed to differentiate them.

5.3.2 Activity Recognition

Understanding fine-grained electricity data could be beneficial to activity-inference researches. For example, different behaviors of using a hair dryer (e.g., cold vs. hot) could imply different residents within a household. The duration of using the vacuum cleaner in different areas (e.g., rug vs. hardwood floor) could possibly infer active areas in home. In addition, the fluctuating EMI of a blender could attribute to what food is being processed; for example, the action of ''ice crush'' shows time-varying EMI during the process. Finally, the action of switching a TV channel can be strongly indicative of a ''watching TV'' activity. This interaction between a resident and an appliance might be difficult to capture through a motion sensor [12] as a sensor event does not directly related to the actual activity; it can be fired by other possible activities such as ''reading'', ''using a computer'' or a pet passing through. We believe the finding in this work is an important step to support the whole-home activity recognition.

5.3.3 Detecting Machine Failure

The system could also be used for machine failure detection by observing changes in known states or the presence of a new, abnormal operating state. For example, a blender may show abnormal EMI caused by malfunction in its motor (e.g., observing low frequency EMI when the blender runs at a relatively higher speed). A computer that yields a high magnitude EMI in its idle mode may relate to a flawed hardware (e.g., a video card). A vacuum with a decreased frequency EMI could correspond to a plugged vent filter or even the motor failure.

5.3.4 Combining Other Sensing Approaches

While we leverage time-varying EMI for operating states estimation, some home appliances such as old washer or fridge do not produce observable EMI signals. From an earlier survey by Froehlich *et al.*, the on/off states of these devices could possibly be extracted from their current or consumption data [5]. To explore the possibility of inferring operating states from the aggregated energy usage, we installed the experimental current sensor provided by

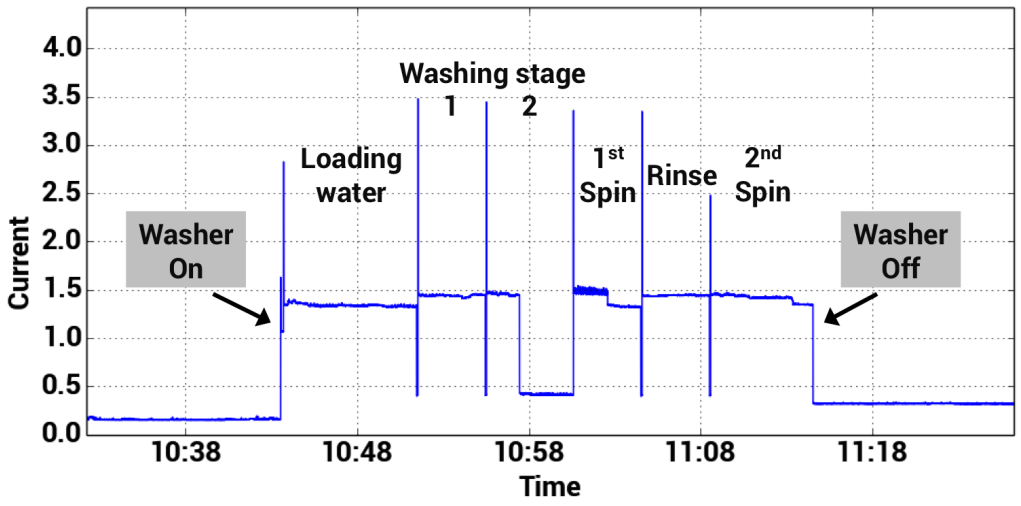

Figure 5.4: Current loads of a stacked washer, showing discernible patterns that represent different stages.

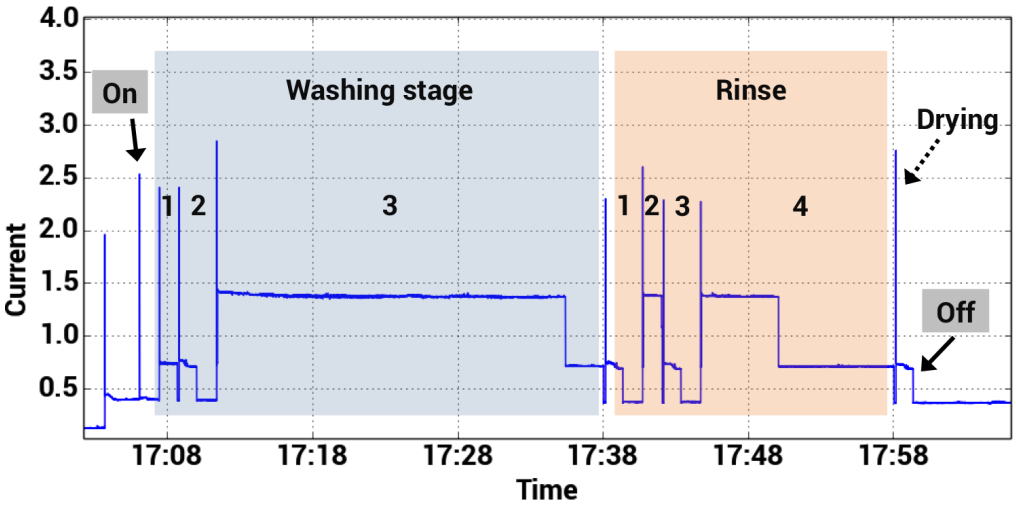

Figure 5.5: Current loads of a dishwasher. The dishwasher was manually turned off after the drying stage began.

Belkin in the participant's house. Figure 5.4 shows the current loads of a stacked washer (General Electric, WSM-2420) in a complete high-load washing cycle. The current loads show discernible signal patterns representing different operating states of a complete washing cycle. Similar phenomenon can be observed on a dishwasher (Whirlpool DU810SWP), as shown in Figure 5.5. To truly support the whole home activity inference, we believe it requires leveraging both time-vary EMI and disaggregated current/power data as we reported in this work. As described earlier, disaggregating current or power usage from the total consumption relies on step changes in its signal. It requires further signal processing and machine learning techniques to detect these step changes that attribute to different operating states.

In this chapter, I demonstrated the algorithm and techniques to extract user-driven operating states from time-varying EMI and how we could use these fine-grained information for a couple of potential applications. In the next chapter, I will further show that these varying EMI, using the same sensing device, also highly correlates the power consumption of appliances. By reverse-engineering the EMI signals, the power consumption of an appliance can be reliably inferred using a training-free model.

Chapter

INFERRING REAL-TIME POWER CONSUMPTION OF APPLIANCES FROM ITS EMI

In this chapter, I introduce another application that makes use of the time-varying EMI to estimate the apparent power usage of appliances. Instead of putting an in-line sensor at each appliance, the system uses the same single sensing device (as presented in presented in Chapter 4 and 5) which can be placed anywhere in the home and can track power consumption of multiple appliances in real time. This technique is based on the observation that most modern appliances rely on voltage regulation in their power supply to efficiently cope with varying loads of an appliance. The EMI emanated by such appliances highly correlates to its power consumption. By reverse engineering EMI signals, power consumed by an appliance can be reliably inferred. I will first illuminate the physical phenomenon that causes the fluctuating EMI by an appliance's voltage regulation process, followed by the process pipeline of power inference. Finally, I will show the evaluation and present the results.

6.1 Overview of Power Estimation Mechanism in the Home

An essential prerequisite for home energy conservation is to understand how much and where electricity is being consumed in order to develop effective eco-feedback interfaces [32]. One common approach to retrieving such information is to install power sensors on individual appliances or near each of them [50]. Although straightforward, this approach assumes periodic sensor maintenance, has an associated installation burden, and sometimes installing an in-line power sensor is not convenient (e.g., built-in or hardwired appliances). Another approach is to use the NILM (Non-Intrusive Load Monitoring) technique, which uses a single-point sensor to acquire total power usage in the home and applies machine learning

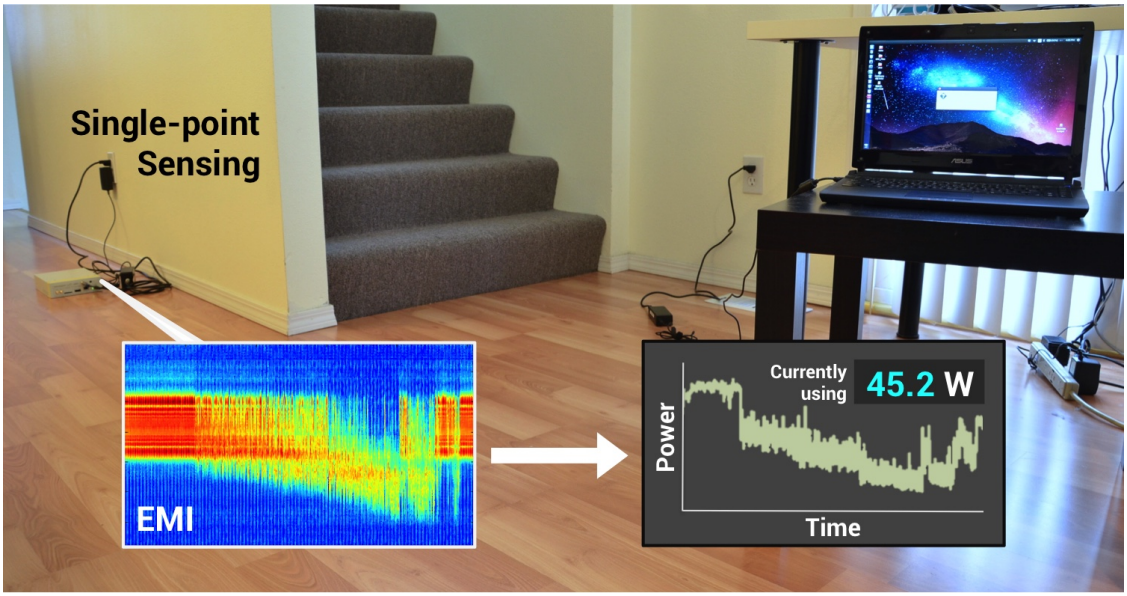

Figure 6.1: This technique leverages EMI signals to infer real-time power usage of appliances using a single sensing device that does not need to be placed in-line with any appliance.

techniques to extract power usage for individual appliances [28, 37, 49, 96, 98]. This method is limited to identifying easily distinguishable higher consuming appliances and does not perform well when applied to multiple time-varying devices running simultaneously (e.g., a laptop and a television) [98]. In addition, though the installation is easier than deploying multiple sensors, it poses installation problems for users who have limited access to their breaker panel or power meter (such as in apartment complexes or accessory dwelling units).

I present an alternative approach to tracking real-time power usage of multiple appliances using a single sensing device in the home (see Figure 6.1). This technique leverages existing EMI (Electromagnetic Inference) emanated by appliances for power estimation. Modern electronic devices regulate their power by adjusting the operating frequency of oscillator within its power supply (e.g., laptop, TV) or controlling its motor spin rates (e.g., a vacuum cleaner). This regulation mechanism generates varying EMI, which indirectly but highly correlates to corresponding power consumption. This strong EMI-power correlation allows

us to infer power usage of a particular device given its EMI. These EMI signals are coupled onto the power lines and can be sensed using a single set device plugged anywhere in the home. Our approach therefore does not require the user to have access to a breaker panel or install a 2nd device to monitor whole-home, per-appliance power usage. Thus, the same device can infer both how much [this chapter] and where [34] electricity is being used. In particular, we explore the most common appliances and focus on those appliance classes that have previously been ignored – those time-varying appliances whose power usage typically fall below the threshold used in most NILM techniques (see Table 6.1). These appliances fall in two categories: SMPS-based (Switched-Mode Power Supply) and motor-based appliances. Although they affect EMI in very different ways, they both exhibit a strong EMI-power relationship. Using only the power consumption profiles (*i.e.*, min, max, and average power) from the Energy Star[1] website, our training-free models present promising results at an average accuracy of 90.2% across all appliances when compared to an in-line power monitor. I will detail this EMI-based power estimation algorithm, study design, evaluation and analysis in the following sections.

6.2 Theory of Operation

The varying EMI signals originate from the switching mechanism in the appliances - either electronic (for SMPS) or mechanical (for motors). We will describe their difference next and how they affect EMI.

6.2.1 Switched-Mode Power Supply (SMPS)

In Chapter 4, we have seen the block diagram of an AC-to-DC SMPS (in Figure 4.5). As stated earlier, the key component of SMPS is a pass-transistor; it controls the PWM (pulse-width modulation) oscillator that switches the stored energy from the inductors to the load that an appliance requires. This switching action generates strong EMI near the frequency that the oscillator switches the energy (*i.e.*, the *switching frequency*) when SMPS switches

[1]Energy Star: http://www.energystar.gov

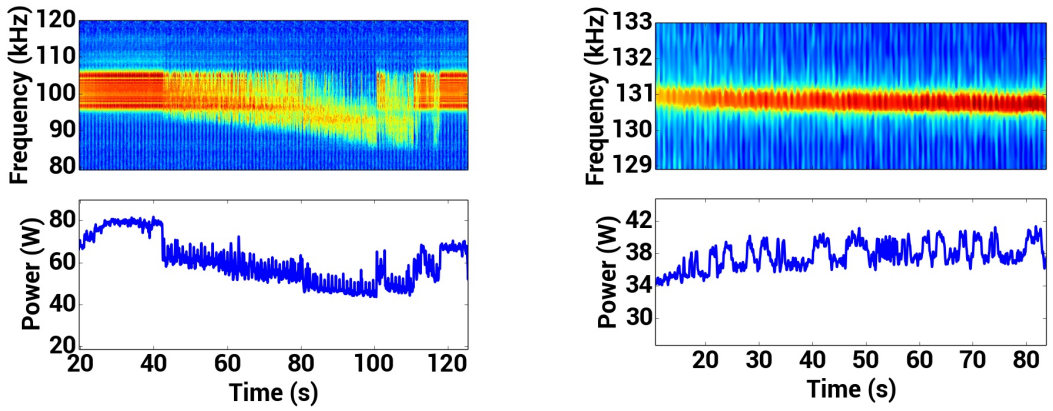

(a) Frequency-based Regulation

(b) Magnitude-based Regulation

Figure 6.2: EMI and power consumption of two appliances with different voltage regulation mechanisms. An appliance can regulate its power by **(a)** changing the switching frequency, or **(b)** adjusting the PWM duration.

between different modes. In a SMPS, output voltage regulation is achieved by adjusting the ratio of on-off durations of the switch. To this end, the output DC is first compared with the reference voltage. When the power supply detects a voltage drop – in the situation where a laptop is executing intensive jobs and demands more power from the SMPS, it either adjusts switching frequency or duration of the PWM oscillator which makes the switch to stay ''on'' for a longer duration in order to generate more power for the appliance. Appliances with varying loads such as laptops and TV can hence cause EMI variations near its switching frequency.

Figure 6.2 illustrates an example of these two different regulation mechanisms. When a laptop (Figure 6.2a, left) executes CPU intensive jobs, the dropping of the output voltage causes the oscillator to operate at a higher frequency to draw more power, yielding EMI at a higher frequency and magnitude. On the other hand, a LCD display (Figure 6.2b) regulates its power by adjusting the pulse duration while the switching frequency remains the same.

In such devices, the EMI frequency is almost constant near its switching frequency, but the magnitude of EMI varies with its power consumption. It should be noted that modern appliances that claim high energy efficiency by design have adaptive power supplies and varying load profiles to save power. For instance, starting late 2000s, LCD TVs became more efficient by dynamically controlling backlight based on the screen content.

6.2.2 Motors

Besides SMPS-based devices, motor-based appliances such as hair dryer or vacuum cleaners also produce loud EMI noise (see Figure 4.2). The electrical noise results from the breaking and making of contacts between its brushes and commutators [72]. This type of EMI, called *commutating EMI*, is caused by the mechanical switching inside the motor and its EMI frequency appears at the harmonics of the motor's rotation rates. Under different physical uses (e.g., moving a vacuum from hardwood floor to a rug), the motor spins at different rates to maintain sufficient suction force. This causes its EMI and power consumption to vary accordingly. This strong EMI-Power relationship can be leveraged for inferring the devices power consumption.

6.3 System Design and Implementation

Figure 6.3 shows the processing pipeline of our power inference algorithm. This pipeline, although designed for power estimation and utilizes fundamentally different feature extraction and selection process, still share similar process for operating state estimation (Figure 5.1). That is, from the same EMI signals, this process pipeline (in Chapter 5 and this chapter) can infer both *how* (*i.e.*, operating states) an appliance is being used and *how much* energy this appliance consumes. Besides activity recognition, these fine-grained information could potentially inform new machine learning features for energy disaggregation and more insights to model appliance usage in the residential houses. I detail each components of this process pipeline in this section.

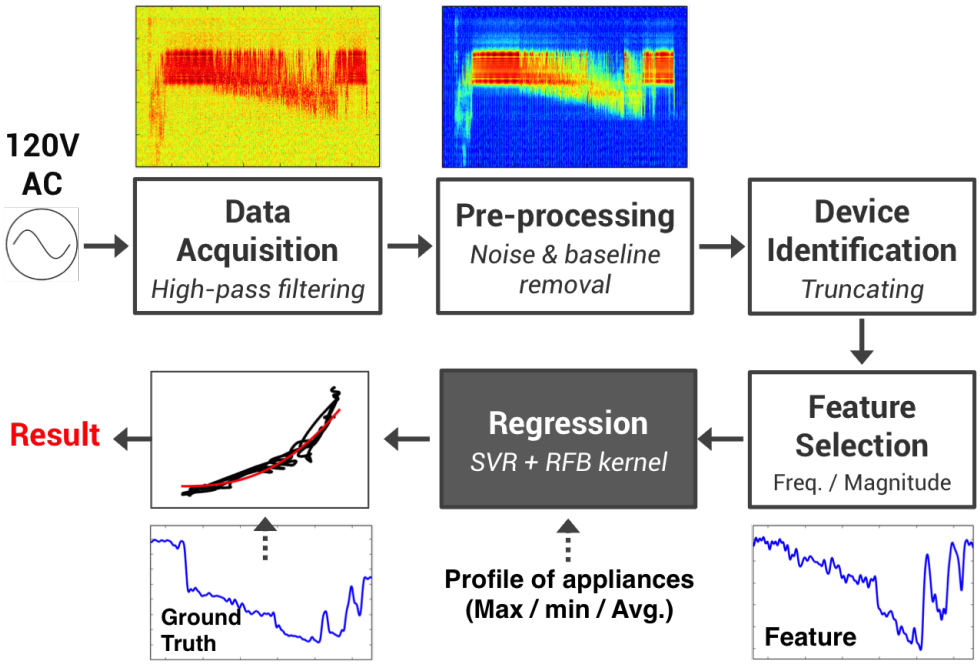

Figure 6.3: Process pipeline for our power inference algorithm. The regression model only requires the min, max and averages power from the appliance profiles.

6.3.1 Data Acquisition

To record the EMI signals, we replicated the hardware set-up in [34] with minor adjustments. A power line interface (PLI) is plugged in a home to obtain the analog signal. We modify the PLI to include a high-pass filter with cut-off frequency at 5.3 kHz. This corner frequency was chosen to strongly reject 60 Hz and harmonics, avoiding possible damages to the sensing hardware but be low enough to cover maximum frequency range. The filtered signal is fed into a USRP (Universal Software Radio Peripheral) N210, which functions as an ADC (analog-to-digital) converter sampling at 500 kHz. We next compute Fast Fourier Transform (FFT) over the data, yielding 16384-point FFT vectors with 30.52 Hz bins. This resolution of bin size allows us to capture small but possibly significant details in EMI. The FFT vectors are streamed to a laptop for power estimation.

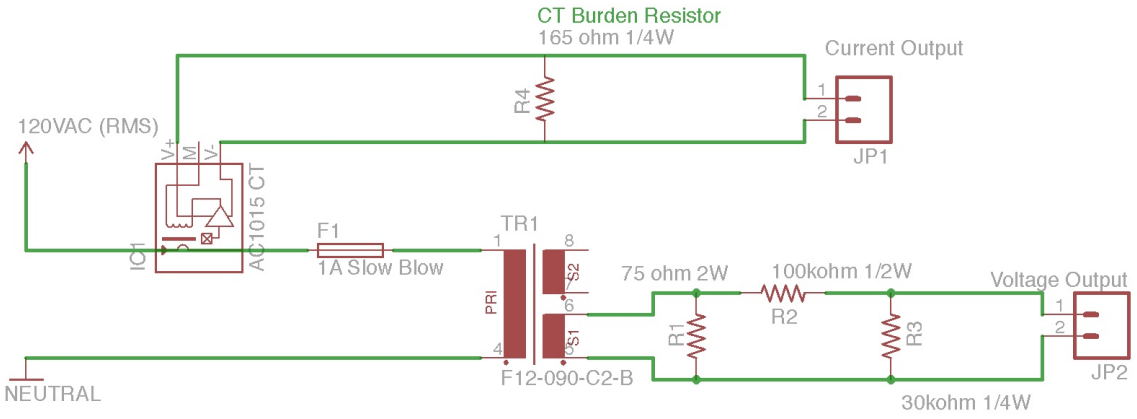

Figure 6.4: The schematic of our data acquisition hardware for the ground truth collection.

To collect energy usage ground truth, we built a data acquisition unit (DAQ) that enables us to measure the power consumption of individual devices (see Figure 6.4). The ground truth data is streamed through an Arduino to the same laptop where the USRP2 connects. This ensures that EMI and power data share the same wall clock and minimizes possible skews in time alignment. For the purpose of this study, we configure the sampling rate of our DAQ at 1 kHz.

6.3.2 Pre-processing

To detect EMI changes, we first remove the baseline signal from observed EMI. In particular, we average the first 50 FFT vectors in each recorded data file as the baseline vector, and subtract it from the remaining vectors. The differential represents EMI produced by a later-actuated appliance. For each FFT vector, we next remove noises by a low-pass filter using a Blackman window with a cut-off frequency of 100 Hz. In our real-time system, we simply use a sliding window of 100 FFT vectors where the 1st half is used for the baseline vector calculation.

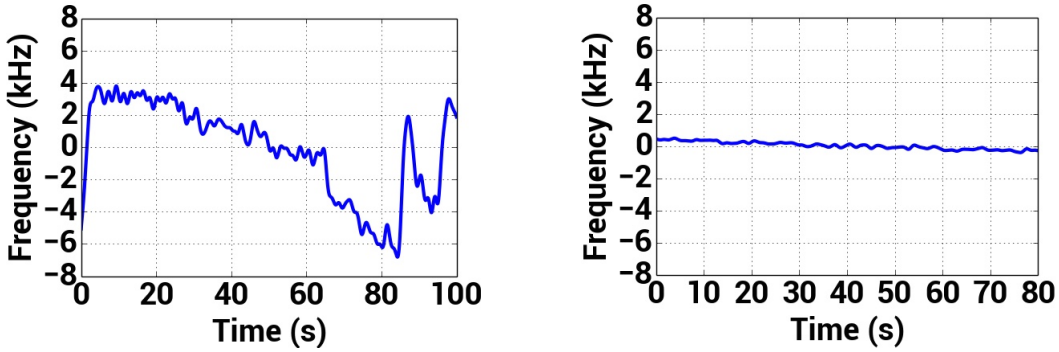

(a) Frequency-based Regulation

(b) Magnitude-based Regulation

Figure 6.5: Variations in EMI frequency of two appliances (corresponding to Figure 6.2a and 6.2b). The variance in EMI frequency is used to select the best feature.

6.3.3 Device Identification

The next step is to identify where each individual appliance is on the frequency spectrum. Previous research [34] has shown that the target EMI frequency can be located by switching a device on and off, and therefore, we assume such information already exists. In this study, we turn each devices on and off a few times to retrieve this information.

6.3.4 Feature Selection and Extraction

As indicated earlier, different types of voltage regulation impact how EMI correlates to its actual power consumption. To capture this, we calculate two features from each FFT vector: (1) the *fundamental frequency* and (2) *average magnitude*. They respectively describe the switching frequency and the noise magnitude of EMI. Specifically, we calculate the fundamental frequency by finding the frequency with peak magnitude in a FFT vector, while the average magnitude is the L-2 norm of a FFT vector. As the EMI patterns uniquely relate to the voltage regulation mechanism, we design an automatic feature selection procedure to decide which feature to use for individual appliances. Intuitively, we leverage variations

in EMIs fundamental frequency to make such a decision. In particular, we first find the fundamental frequency in each FFT vector. For each training data, it yields a curve that tracks a device's EMI fundamental frequency overtime. We next subtract the mean from this curve and calculate the standard deviation. Figure 6.5a and 6.5b shows the frequency variation of two different appliances (corresponding to Figure 6.2a and 6.2b). From our observations, devices that regulate its power by adjusting PWM durations always yield a low standard deviation (between 0.001 to 0.5 kHz based upon its EMI bandwidth). We hence set up our threshold at 1 kHz. That is, for appliances with frequency variation above this threshold, we use fundamental frequency as the feature; for the rest we use the average magnitude. We should note that this feature selection process only needs to execute once in the training process and the decision is applied to all testing data. Figure 6.6 illustrates one example (LP1 in Table 6.1) of the selected feature and corresponding power consumption ground truth. We can see the feature curve (Figure 6.6, top) is highly correlated to the power curve (Figure 6.6, bottom).

6.3.5 Regression

To infer the power consumption, we build a regression model using two different approaches, as described below.

First Approach: Using Minimal Training Data

The first approach involves both EMI and the power data for model training. We plugged in the appliances in-line with our DAQ device to collect their power usage for 2 minutes. In order to cover the actual dynamic range of power consumption of an appliance, we design a protocol to collect the training data:

- **Laptops**: we (1) first boot up the device, (2) stay idle for 20 sec after logging into the system (3) run a testing script to boost CPUs up to 100% for 20 sec, (4) let it idle for another 20 sec and then (5) turn it off.

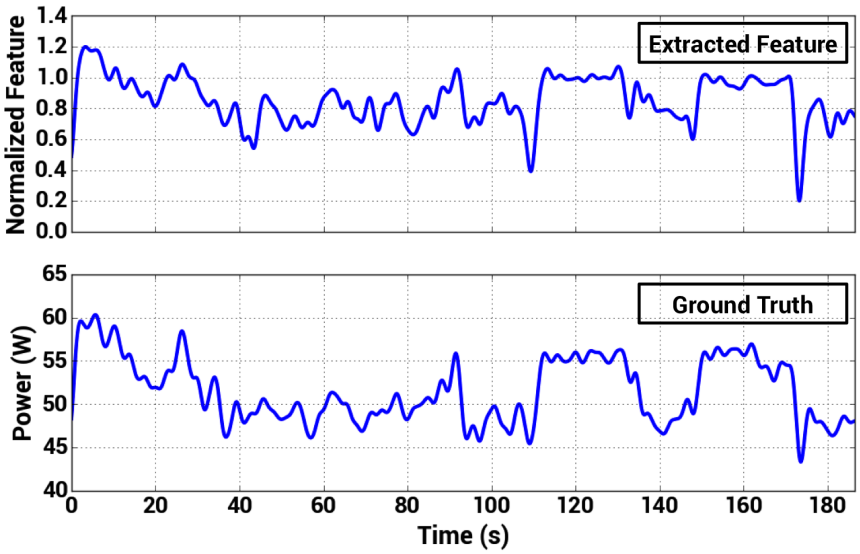

Figure 6.6: One example of the power consumption ground truth (bottom) and normalized feature (top) of LP1 in Table 6.1. Our system automatically chooses the feature that best correlates to power consumption.

- **TV/LCD**: As power consumed by a display relates to its brightness, we run a script that randomly switches the panels background color between white and black.

- **Motor-based appliances**: We moved the vacuum cleaner between a hardwood floor and a rug to capture spin rate variations caused by uneven surfaces. For the hair dryers, we switch the device between different temperatures.

Using this 2-minute training data, we train a regression model for individual appliances using SVR (Support Vector Regression) with a RBF kernel (Radial Basis Function). To avoid possible scaling issues, all features and target vectors are zero mean with a unit variance. We implement this model using a machine learning library (scikit-learn) in Python.

Second Approach: No Training and Using Publicly-available Appliances Profiles

While we believe that collecting only 2-minute of training data is a low overhead for end users or researchers deploying this in field for a small number of targeted appliances, the power data of some appliances might be still hard to get (e.g., a wall-mounted TV). In our second approach, we use only a device's *min*, *max* and *average* power to build a training-free regression model. The Energy Star website hosts a database that lists the profiles of many home electronic appliances and hence these numbers can be easily retrieved. This is an ever-growing database. Thus, for our regression we only assumed the min, max and average power values.

From the first approach, we found that the regression model, although non-linear, is close to linear. We therefore assume a linear model built from the profile. Specifically, we first map the min and max feature values (extracted from EMI data) to the min and max power, and then interpolate between them. In order to compensate possible bias, we subtract this linear line by the residual between its mean and the average power.

6.4 Evaluation and Results

6.4.1 Study Design

We set up our experiments in a residential townhouse (triplex, 1100 sq. ft.) of there residents. Table 6.1 lists the devices tested in our study. To explore the temporal stability of the signal, we collect the testing data on five different days, including multiple sessions in the daytime (8am – 6pm) and at night (6pm – 10pm) on both weekdays and weekend. Each session lasted 2 to 3 minutes. In each session, we asked one resident to perform activities on different appliances:

- **Laptop**: randomly performing 4 tasks: playing a movie (hard drive) and youtube videos (network), running a CPU benchmark and do nothing (idle); this covers basic daily activities on a laptop.

- **TV/LCD**: playing a video chosen randomly from 3 different movies.

ID	Model	Accuracy (2-min)	Accuracy (Profile)	Feature Selection	Device Type
LP1	Acer 5736Z	95.6%	91.2%	Fundamental Frequency	SMPS
LP2	Asus U36J	98.8%	90.5%	Average Magnitude	SMPS
LP3	Dell 1545	97.4%	95.6%	Fundamental Frequency	SMPS
LP4	Toshiba Portege-R700	90.4%	86.5%	Fundamental Frequency	SMPS
T1	Benq GL2760H	99.4%	99.3%	Fundamental Frequency	SMPS
T2	HP S2231	99.1%	94.7%	Average Magnitude	SMPS
T3	Panasonic 53-inch TV	92.1%	82.4%	Average Magnitude	SMPS
T4	ViewSonic VA903b	99.2%	93.1%	Average Magnitude	SMPS
M1	Bissel 6584	99.6%	96.0%	Fundamental Frequency	Motor
M2	Tashin PowerSlit	90.1%	80.6%	Average Magnitude	Motor with resistive load
M3	Remington Speed2Dry	87.7%	81.9%	Average Magnitude	Motor with resistive load
	Average Accuracy	**95.4%**	**90.2%**		

Table 6.1: List of devices in our study (LP=Laptop, T=TV/LCD, M=Motor-based appliances) and the evaluation results using 2-min training data (marked as 2-min) and only the appliance power profiles (marked as Profile). The feature selection is device dependent and our system is capable of automatically choosing the best feature by examining the variance of EMI frequency.

- **Hair Dryer**: randomly switching between different temperatures.
- **Vacuum Cleaner**: moving it on both hardwood floor and a rug.

When one resident was executing requested actions, the other remained performing her daily routines such as cooking, laundry or using a computer. In total, 450 minutes of testing data were collected.

6.4.2 Results and Analysis

Feature Selection Results

The result of feature selection is listed in Table 6.1. We can see that this selection for the best feature is appliance dependent; we need to choose the feature for individual appliance:

- SMPS with varying EMI frequency (LP1, LP3, LP4, T1).

- SMPS with varying EMI magnitude (LP2, T2, T3, T4).
- Motor only (M1).
- Motor with large resistive load (M2, M3).

This selection process in our design is automatic and only needs to perform once in the training process. The decision is applied to all testing data. We should note that most motor-based appliances such as vacuum cleaners and blenders generate EMI with varying frequency as they regulate the motor spin rate, and hence the best feature is the fundamental frequency (M1 in Table 6.1). Some motor-based appliances use extra large resistive components to control the operating temperatures (M2, M3 in Table 6.1). In such case, the system picks the average magnitude as the best feature because the resistive load affects the EMI in magnitude instead of frequency.

Accuracy Results I: Regression Using Minimal Training Sets

Table 6.1 lists the performance of 11 appliances. Overall, our system presents promising results at an average accuracy of 95.4% across appliances. One laptop (LP4) shows a relatively low accuracy of 90.4% (σ=9.2%). This is due to the fact that LP4 yields a weaker EMI and hence the feature vectors contain more noise. One TV (T3) reports a slightly low accuracy of 92.1% (σ=8.4%). When we exam the data, we found a strong noise interference from another appliance near its fundamental frequency at around 28 kHz, which deteriorates the observed EMI signals.

We noted that hair dryers (M2 and M3) also report a relatively low accuracy of 90.1% (σ=10.1%) and 87.7% (σ=13.7%). This is due to the indirect relationship between observed EMI and its actual power consumption. Such device (e.g., fan heaters) leverages a motor-driven fan and a large resistive load to control the temperature of blasts. That is, the actual power consumption is the synergy of these two components. The resistive component can be indirectly observed in the slowing of the motor due to the increased current for the heating

element in the hair dryer. While the observed EMI is yielded from the motor, using only the EMI data for inferring power is not completely sufficient as it does not describe the whole circuitry that attributed to its entire power usage. On the other hand, the vacuum cleaner (M1) generates EMI mainly from the motor, which manifests itself to a stronger correlation to the power it consumes and shows a high accuracy of 99.6% (σ=0.3%).

Accuracy Results II: Regression Using Publicly-available Appliances Profiles

The second experiment explores a training-free model using only min, max and average power from the profile. As we expected, the accuracy of all devices declines with the simplified model. The accuracy downgrades with the model nonlinearity in individual appliances. For instance, the power consumption of the hair dryer keeps constant when it operates at the same temperature. When it switches between different temperatures, the feature curve appears as a step function instead linear; using a linear model is insufficient for power predictions. Overall our system still reports a promising result of 90.2% accuracy across devices.

6.5 Discussion

In this chapter, we have seen a new technique to track real-time power consumption from an appliance's EMI using a single sensing device. This approach leverages time-varying nature in EMI emanated from the appliance as it regulates the varying power. By reverse engineering EMI signals, the training-free model can reliably infer power usage using only the appliance power profiles. We have shown the feasibility of using this approach on 11 appliances in a real home and implemented a real-time system. This technique can provide more information of in-home activities (e.g., the activeness of using a computer) and could enable whole-home power monitor to build a low-cost eco-feedback interface for sustainability-related research. Although we have shown encouraging results from this study, there exist some limitations and challenges from the current prototype. We discuss these limitations in this section and plan some future works.

6.5.1 Signal Fading and Interference

Our approach uses the fingerprint of EMI signals for power estimation. Due to the effect of signal fading caused by the powerline impedance between appliances and the sensing devices, our system relies on the static position of sensing device relatively to the appliances to retain the EMI-power relationship. In our case, we targeted the home environment where residents usually keep their appliances at the same spots and hence this issue could be minimized. However within a dynamic environment, it would require frequent re-calibrations (*i.e.*, re-mapping the power profiles to new EMI baselines) to rebuild EMI-power models. A previous study by Kong *et al.* reveals that the location of electronic appliances can be inferred by measuring the signal attenuation caused by power lines impedance [53]. Combining this location information, it is possible to build an adaptive model that auto-calibrates the system to compensate the environmental dynamics.

6.5.2 Appliances with Low EMI Variations

While our power estimation algorithm was evaluated on appliances with EMI variations in frequency or magnitude, the system could easily adapt to those appliances with low power variation and therefore low EMI variation. One LCD (T4) in our study is a relatively small display. This display does not consume considerable power and hence we did not observe high power consumption or EMI variation from this device. The evaluation still shows robust results on such devices (99.2% using 2-min training data and 93.1% using training-free model).

6.5.3 Combining Prior Knowledge of the Appliance Circuitry

As indicated earlier, we found that some appliances (e.g., hair dryer or fan heater) leverage both motor and resistive components to control its operating temperature. The outcome of this synergy is a step function in its EMI-Power relationship. Given this prior knowledge, we could build the training-free model, instead of a naive linear interpolation, as a step function. The number of steps is equal to the number of buttons (or temperature modes) on the

devices. By combining these human observations as the prior knowledge, the training-free models could better describe the EMI-power relationship. As we expect the power profiles database to be more thorough in the future, these steps will become accessible directly from on the Energy Star website.

6.5.4 Combining NILM

We believed that the EMI-based power estimation approach overcomes major limitations in NILM and can be applied to a significant number of home appliances. Our technique however relies on the existence of EMI emanated from appliances for power inference. That is, this system is not able to catch electrical events from appliances without generating EMI (e.g., fridge, oven or old washer/dryer). Those appliances with no observable EMI are usually relatively high power consuming appliances and can be easily disaggregated from NILM. As indicated earlier, one major limitation of NILM is scalability; the model complexity increases as the number of appliances being tested raises. By combining the EMI-based power estimation, the computation overhead of NILM could be significantly reduced as we could estimate power for most appliances through their EMI signals while leaving only a small portion of appliances for NILM.

In this chapter, I demonstrated the algorithm and techniques to track the real power of multiple appliances using the same time-varying EMI that we have seen in Chapter 4 and 5. In the next chapter, I will further show that similar varying EMI caused by human proximity can be observed from the crystal panel of unmodified LCDs. By leveraving the EMI signals, any number of LCDs can be converted to touch sensitive surfaces from a single set of sensing device.

Chapter

BEYOND SENSING APPLIANCE STATES: DETECTING HUMAN PROXIMITY AND TOUCH GESTURES ON UNMODIFIED LCD MONITORS

Existing solutions for sensing human proximity or enabling touch interaction on LCD screens require modifying the display or adding additional sensors to the interaction surface. In this chapter, I present a new sensing approach, called *uTouch* [13], which detects and classifies touches and hovers without any modification to the display and without adding any additional sensors to either the interaction surface or the user (see Figure 7.1). This approach utilizes existing signals in the LCD display which are amplified when a user brings their hand near or touches the LCD front panel. These signals are coupled onto the power lines, where they appear as time-varying EMI which can be sensed using a single set of devices as introduced in previous chapters.

To enable touch interaction on LCD monitors, researchers have used optical sensors and cameras [1, 42, 65, 97] in addition to infrared sensors [26, 41, 42, 65]. Although these systems typically provide finger-level accuracy for multiple touch points, they require instrumenting or modifying the LCD in order to sense the user's touches. Additionally, most of these systems can only detect a gesture when the user is touching the surface, and are unable to sense when a hand is approaching the surface or hovering above it. Capacitive sensing has been used to allow interfaces to detect hands that are either approaching or hovering above the surface [34]. This work also leverages capacitive coupling, but does so *indirectly*, without instrumenting the interaction device.

In the following sections, I will first describe the theory of operation which enables our system and present a feasibility study to demonstrate the detection and classification of 5 different gestures across 11 users and 8 LCD displays of various types (for both PCs

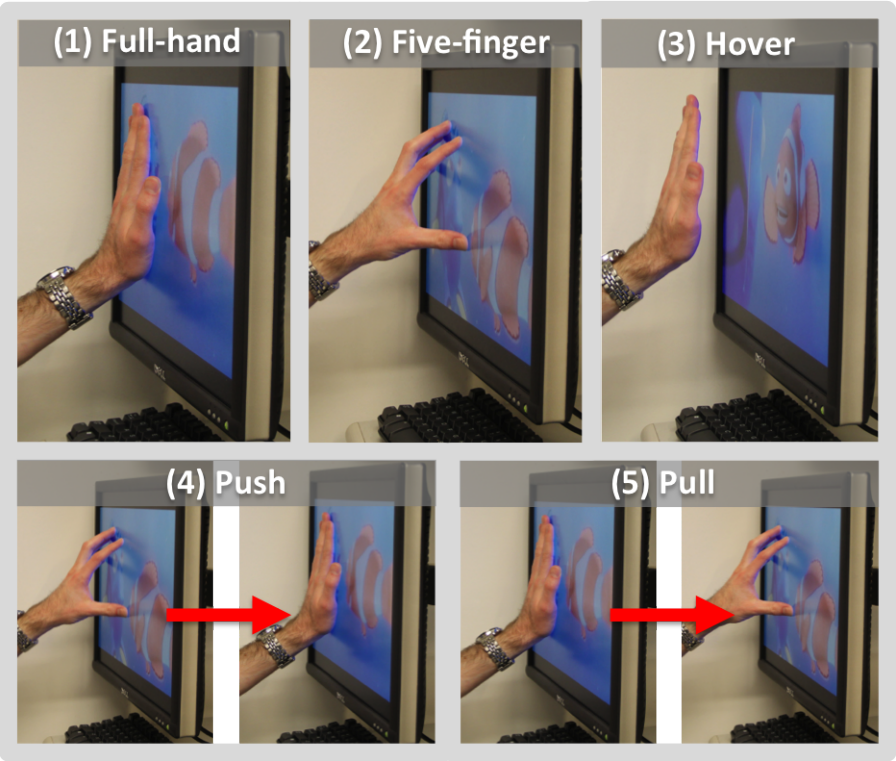

Figure 7.1: uTouch detecting hand gestures on unmodified LCD monitors.

and laptops). I describe the signal processing and machine learning needed to implement the uTouch system, and present a real-time implementation of uTouch along with some prototype applications.

7.1 Theory of Operation

As described above, uTouch leverages existing signals in the LCD panel which are strongly coupled onto the power line when the users hand touches or hovers above the surface of the panel. This section describes the mechanism behind this phenomenon.

7.1.1 LCD Fundamentals

First, it is important to understand the basic operation of the active-matrix LCD panel. A backlight produces uniform white light using either a cold cathode fluorescent lamp (CCFL) or light emitting diodes (LED). Regardless of the type of backlight, the white light passes through a polarizer, a liquid crystal (LC), a color filter, and a second polarizer before being emitted at the front of the display. The intensity of the light (*i.e.*, gray level) is controlled by the strength of the electric field applied to the LC. Pixels are made by closely grouping red, green, and blue colored filters and controlling the intensity of the light through each filter to produce the desired color.

Although the panel is made up of a large array of pixels, only a single row of pixels is enabled at a time, and therefore small thin-film transistors (TFT) are used to enable each electrode. Figure 7.2 shows a small section of an LCD panel array. The column or source drivers charge the column data lines with the appropriate voltage to apply to each pixel in the active row. Although this data voltage is applied to the source of every transistor in the column, only a single row is enabled by the row or gate drivers. With the gate voltage applied only to the active row, a field is created on all of the electrodes in that row. Each row is selected once per frame, and enabled periodically at the refresh rate. I will refer to the rate at which the display switches active rows as the *row rate*. The row rate is dictated by the refresh rate of the display (commonly 60 Hz) and the number of rows. Note that the row rate is closely related to the horizontal sync rate (hsync) at the monitor's native resolution; however, unlike hsync the row rate will not change when the driving resolution is changed.

7.1.2 Row Rate EMI

As explained above, the row select lines and column data lines are changed every row, at the row rate. As a result of this, the row and column drivers consume power in bursts at the row rate. In the same way that current spikes from a digital clock couple EMI onto the power line, the current spikes from the row and column drivers result in EMI on the power

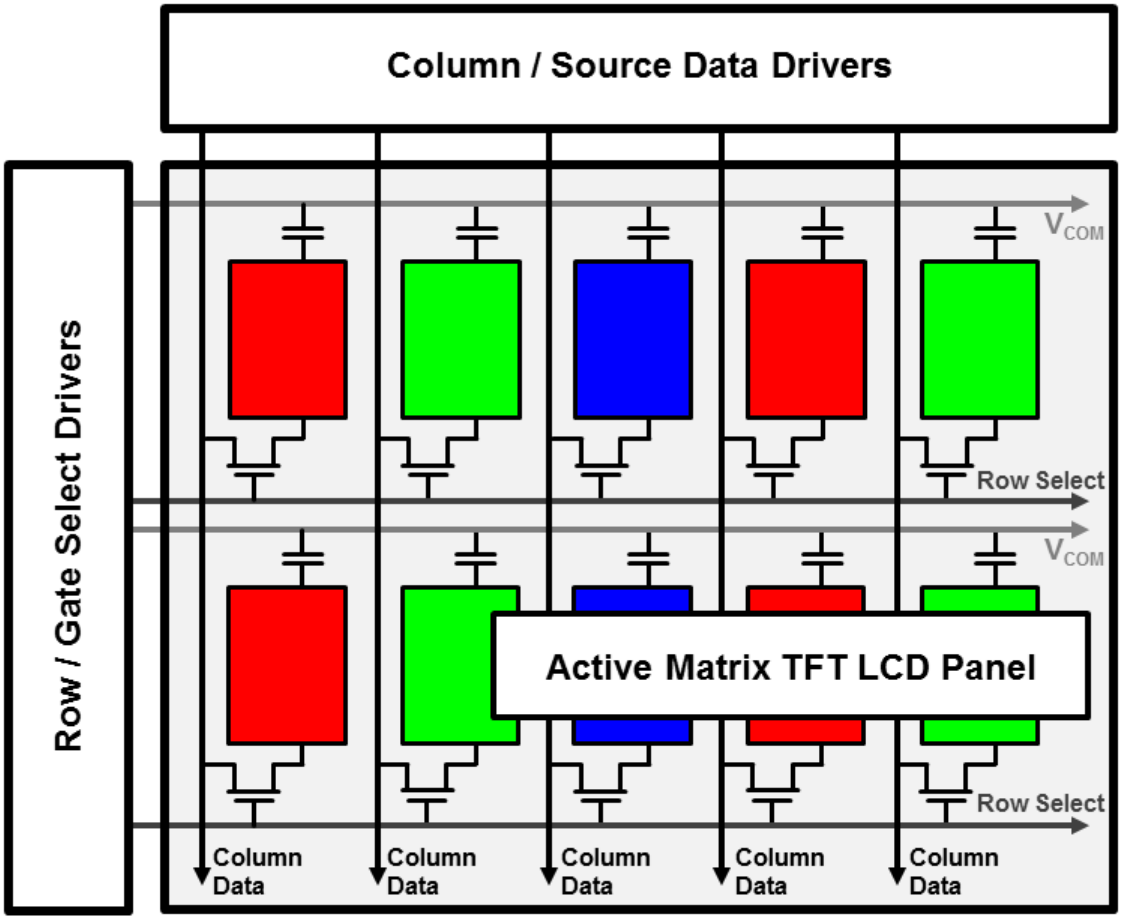

Figure 7.2: Simplified schematic of a small section of the LCD panel and the row and column drivers.

line at harmonics of the row rate. Although the row and column consume more power than any other part of the LCD with the exception of the backlight, internal filtering to limit EMI typically keeps these signals be-low the noise level on the power lines. In addition to harmonics of the row rate, EMI is also observed on some monitors at harmonics of half of the row rate. This is due to the method used for panel polarity inversion. To prolong the life the liquid crystal, the polarity of the electric field is inverted each frame, and to prevent

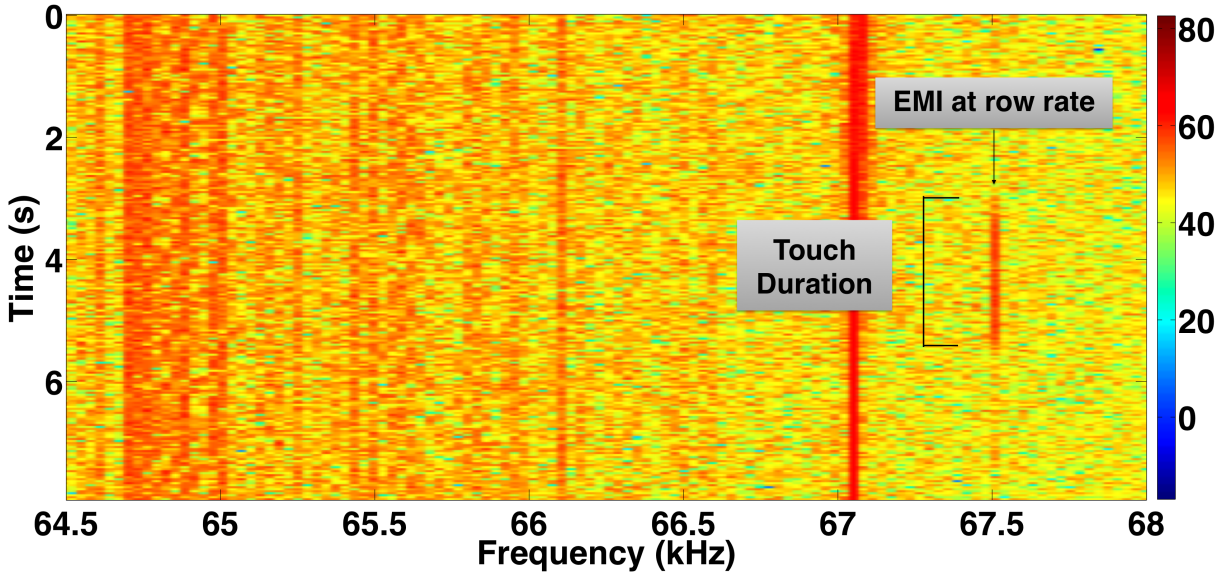

Figure 7.3: EMI seen at the row rate of 67.5 kHz is observed to be well above the noise level during the user's 2 second touch of the LCD panel.

visible flicker the polarity of adjacent rows and columns is commonly opposite. However, many LCDs group adjacent rows in what is called line-paired inversion. In this case, if we assume that the colors of nearby pixels are typically similar, then the voltages on the column data lines only change significantly every other row. This will therefore cause EMI at half of the row rate.

7.1.3 Sensing Panel Touches and Human Proximity

Although the row rate EMI on the power lines is typically below the noise level, when a user's hand hovers over or touches the panel, a very large capacitance to ground is added in parallel with the row select lines and column data lines. This added capacitance results in significantly higher power consumption by the row and column drivers, which causes higher levels of EMI at harmonics of the row rate (and half of the row rate in LCDs that use line-paired inversion). This EMI is both conduced onto the power line through power supply of

ID	Model	Size / Resolution	Panel / Backlight	Interface	Refresh Rate (Hz)	Row Rate (kHz)
M1	Asus VW246H	24 in / 1920x1080	TN / CCFL	HDMI (to PC)	60.0	67.5
M2	ViewSonic VX2035wm	20.1 in / 1680x1050	TN / CCFL	DVI (to PC)	60.0	65.3
M3	Samsung 226BW	22 in / 1680x1050	TN / CCFL	DVI (to PC)	59.9	64.7
M4	Dell 2007WFP	20 in / 1680x1050	S-IPS / CCFL	DVI (to PC)	60.0	64.7
M5	Dell 1703FPs	17 in / 1280x1024	TN / CCFL	VGA (to Laptop)	60.0	64.0
M6	HP S2231	21.5 in / 1920x1080	TN / CCFL	DVI (to PC)	60.0	67.5
L1	Acer ASPIRE5736Z	15.6 in / 1366x768	TN / LED	N/A	60.0	47.1
L2	Dell INSPIRON1545	15.6 in / 1366x768	TN / CCFL	N/A	60.0	49.4

Table 7.1: Six monitors (M1-M6) and two laptops (L1, L2) used in the core experiment.

the LCD and radiated onto the power lines by the panel and user, whose body acts as a re-radiating antenna of this noise. The resulting EMI on the power line at the harmonics of the row rate can be seen well above the noise level as shown in Figure 3. Further-more, the amplitude change of this EMI is a function of the strength of the capacitive coupling between the panel and the body. This noise is therefore a robust signal for sensing different kinds of touches and hovers on the panel.

7.2 Experimental Procedure

In order to explore the ability to use this phenomenon to sense touch gestures, we set up an experiment in a real home environment and conducted a user study of 11 participants (3 female) on 6 LCD monitors and 2 laptops of various types. Table 7.1 shows the variety of monitors used in the study. Data collected in this study was analyzed offline; however, I also demonstrate a real-time implementation of uTouch in a later section.

To measure the EMI on the power line, I used similar hardware as described in Chapter 5. An analog high-pass filter (HPF) in with a corner frequency of 5.3 kHz is used to reject the strong 60 Hz component. The output of the HPF is sampled through a 12-bit analog-to-digital converter in the USRP (Universal Software Radio Peripheral). The digitizer in USRP was configured at 1 MS/s and performed a 32768-point fast Fourier transform (FFT), producing the frequency resolution (or bin size) of 30.5 Hz.

In our study, I used 5 different touch gestures shown in Figure 7.1, including full-hand

touch (FH), five-finger touch (FF), hover, push and pull. In a push gesture, the user was asked to first perform a five-finger touch, followed by a full-hand touch (*i.e.*, the hand is ''pushed'' toward the pan-el), and the pull was exactly the opposite. Each participant performed 6 repetitions of each these 5 touch gestures on the six monitors, M1 - M6, listed in Table 7.1. Five of the 11 participants were asked to perform an additional study on the 2 laptops (L1 and L2). To help participants and to en-sure consistency, I built a data collection program that indicated when to begin and end each gesture. This program randomized the order of gestures to decrease the temporal bias. Furthermore, I turned on all monitors for at least 1 hour before each experiment to avoid possible EMI variations due to the LCD warm-up. Two participants repeated the experiment in multiple sessions on different days to explore the temporal stability of the signal; the other 9 participants performed one session on different days in the two-week duration. For consistency, all monitors used the same background image; although our real-time system demonstrates the ability for uTouch to operate with dynamic backgrounds. All experiments were conducted in a residential apartment with the monitors plugged-in away from the plug-in power line sensor.

7.3 Analysis

The data analysis described in this section is divided into three sections, signal pre-processing, touch gesture event detection, and gesture classification.

7.3.1 Signal Pre-processing

Although the touch EMI is produced at many harmonics of the row rate as well as the harmonics of half of the row rate (i.e., on monitors which use line-paired inversion); we only need to use one harmonic for all of our processing. For our uTouch prototype, we manually selected the harmonic with the highest power individually for each monitor; however, this process can be easily automated in the future. To automate the selection of the EMI peak, a one-time calibration process can be performed in which the user performs a touch gesture

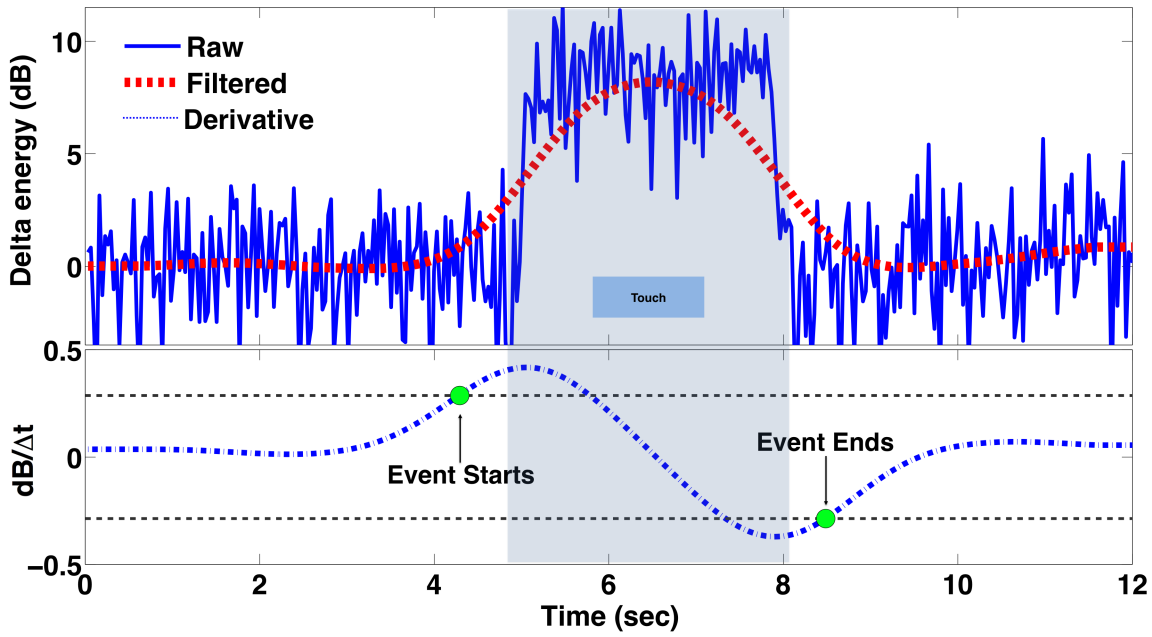

Figure 7.4: The amplitude (top) of the EMI frequency is plotted during a touch event, indicated by the gray area. The filtered amplitude (top) and derivative (bottom) are shown along with the threshold used to determine the start and end of the event.

two or three times on each LCD. Using this training data, we can algorithmically choose the best harmonic to use.

After selecting the EMI peak, I sum the energy of the magnitude of the FFT in the selected frequency bin with the 2 adjacent bins, and then filter the result. I apply three passes of the Savitzky-Golay smoothing filter with a degree of 1 and frame length of 39. Figure 7.4 (top) shows the summed energy as well as the filter output. Although this filter produces a very smooth output, the filter delay is quite long; however, I will discuss how this can be shortened in the implementation of our real-time system in a later section.

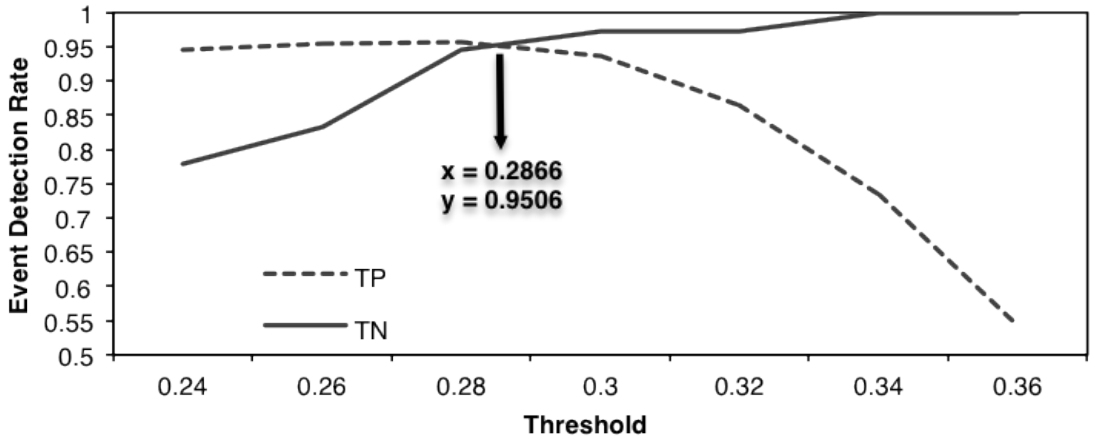

Figure 7.5: Likelihood ratio plot showing the tradeoff between the true positive (TP) and true negative (TN) rate as a function of the global threshold.

7.3.2 Touch Event Detection

To identify the start and end point of the performed touch gesture, I took the first-order derivative (*i.e.*, sample-to-sample difference) of the smoothed summed energy curve, and then further filtered the signal with another 2 passes of the Savitzky-Golay filter. The end points are chosen to be the positions when the derivative curve exceeds a globally defined threshold, as shown in Figure 7.4 (bottom).

The global threshold for event detection was selected to be at the equal error rate using all of the data from our user study. The equal error rate is represented by the intersection of the true positive (TP) and true negative (TN) curves on the likelihood rate plot shown in Figure 7.5. Using the select-ed global threshold, I obtain a false positive (FP) rate of 4.94%.

7.3.3 Touch Gesture Classification

After an event is detected, features are extracted from the smoothed energy curve for gesture classification. The feature selection was based on our observations of the data, and

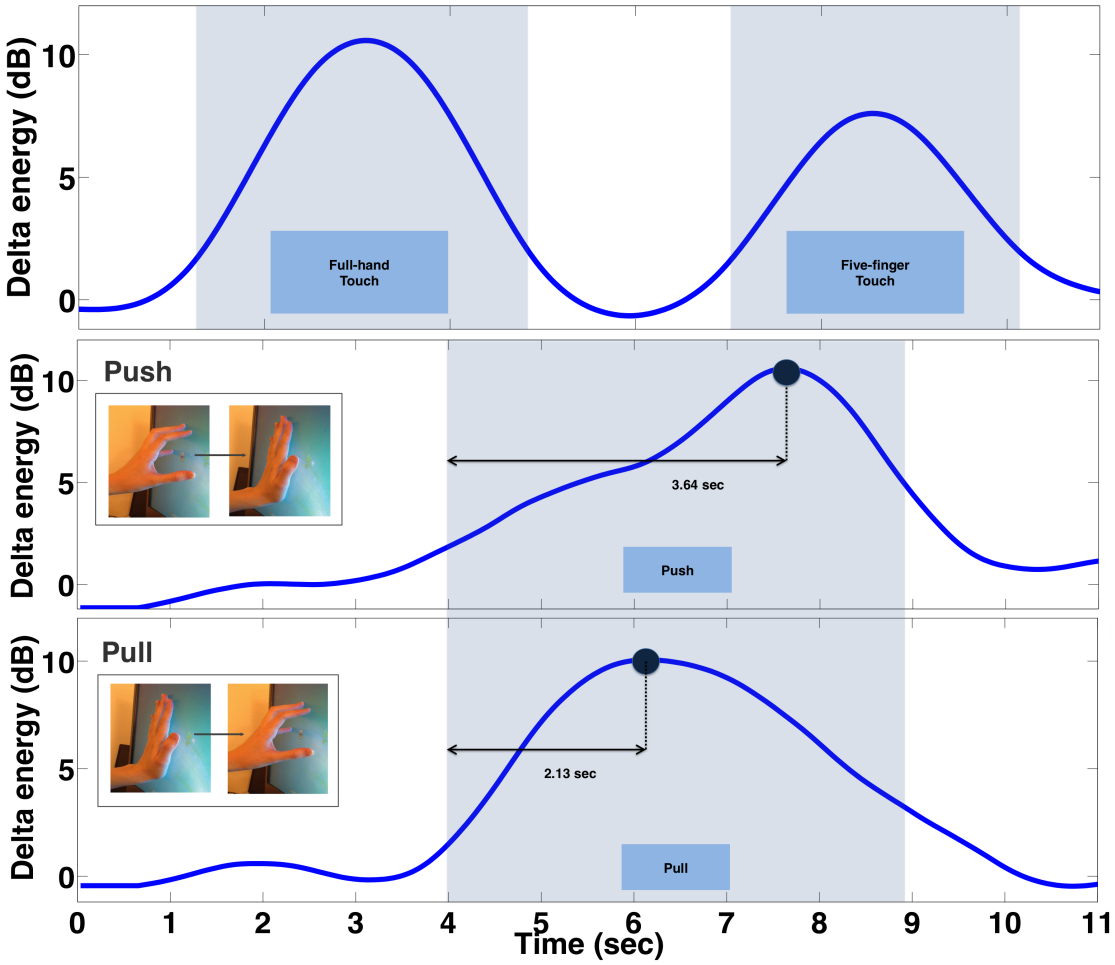

Figure 7.6: Summed energy curves representing full-hand and five-finger touches (top) as well as the push and pull gestures (bottom). The gray shaded area indicates the touch duration.

the differences between touch gestures. Figure 7.6 shows the summed energy over time for a full-hand touch, five-finger touch, push gesture, and pull gesture. The gray shaded region indicates the time period of each touch event.

From Figure 7.6 (top), it is clear that the amplitude change is much greater for a full-hand touch compared to a five-finger touch. This is because the full-hand couples more

strongly to the LCD panel, causing more power consumption at the row-rate, and therefore more EMI is coupled onto the power line. To capture these amplitude differences I use the following three features: (1) *maximum amplitude*, (2) *average amplitude*, and (3) *change in amplitude*. The maximum amplitude feature is simply the maximum value of the smoothed energy during the touch duration. The average amplitude is computed by summing the amplitude during the segmented touch duration and dividing by the duration. The change in amplitude is computed by subtracting the average amplitude during the touch duration from the average energy in the 3 seconds prior to the touch.

The push gesture starts with the five-finger touch and then transitions to the full-hand touch, while the pull gesture does the opposite. These gestures can therefore be distinguished using the asymmetry in the capacitive coupling between the hand and the LCD panel. The push gesture begins with weaker coupling (*i.e.*, less EMI), and then transition to more coupling (*i.e.*, more EMI), and the opposite is true for the pull gesture. This asymmetry in the EMI strength can clearly be seen in summed energy curves shown in Figure 7.6 (bottom). To capture these differences, two additional features are used: (4) *peak amplitude position*, and (5) *amplitude asymmetry*. The peak amplitude position is the relative position of the maximum amplitude in relation to the segmented touch duration. The amplitude asymmetry is computed by taking the difference between the average amplitude in the first half and second half of the segmented touch duration.

For each segmented event, these 5 features are used in a support vector machine (SVM) classifier to determine the most likely touch gesture. The classification was performed using the SMO implementation of the SVM included in the WEKA machine learning toolkit.

7.4 Results and Analysis

7.4.1 Touch Event Detection

Using a global threshold and the touch event detection algorithm described earlier, I obtain an average detection rate of 96.4% (σ=9.5%). As shown in Figure 7.7, the detection rate is above 97% for all touch gestures, with the exception of the hover and push gestures. The

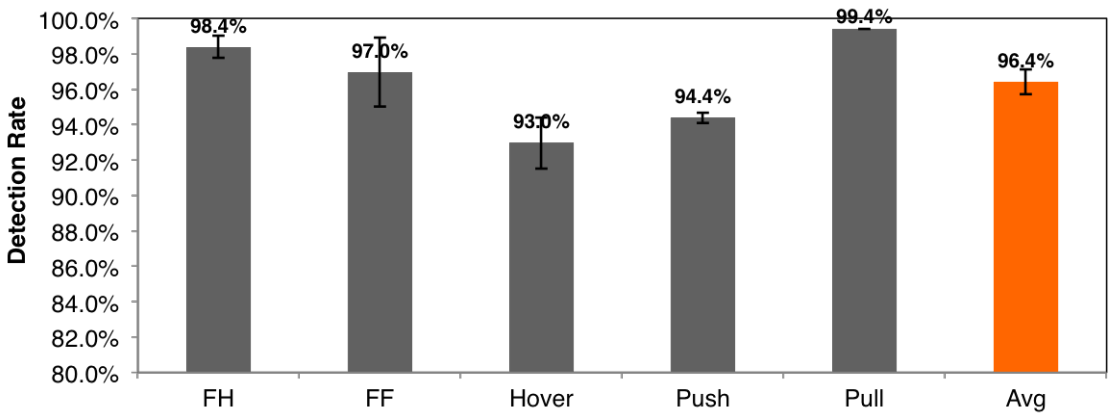

Figure 7.7: Event detection rate for all gestures.

detection rate is lower for the hover, because the hand is farther from the panel, resulting in less capacitive coupling, and thus less EMI. The lower detection rate for the push gesture is likely due to the way that most users performed the gesture. I observed that users tended to approach the screen more slowly when performing the push gesture when compared to the other gestures. Since our detection algorithm is based on the derivative of the EMI, this slow approach results in fewer detections.

7.4.2 Touch Gesture Classification

In order to explore the feasibility of using uTouch to classify user gestures, I treat the analysis as a machine learning problem. In order to determine whether uTouch has the ability to classify different gestures for a variety of LCD screens and users, I trained a 5-class (*i.e.*, representing the 5 touch gestures) SVM classifier for each monitor and user. In order to model a realistic use case, I trained the model using only the first two examples of each touch gesture, and then tested the model on all remaining examples. This represents the use case in which a user performs each gesture twice, and can then use the system without the need for retraining. I obtained an average classification accuracy of 68.3% (σ=22.5%). At random chance, the classification would be 20%, and thus this result shows

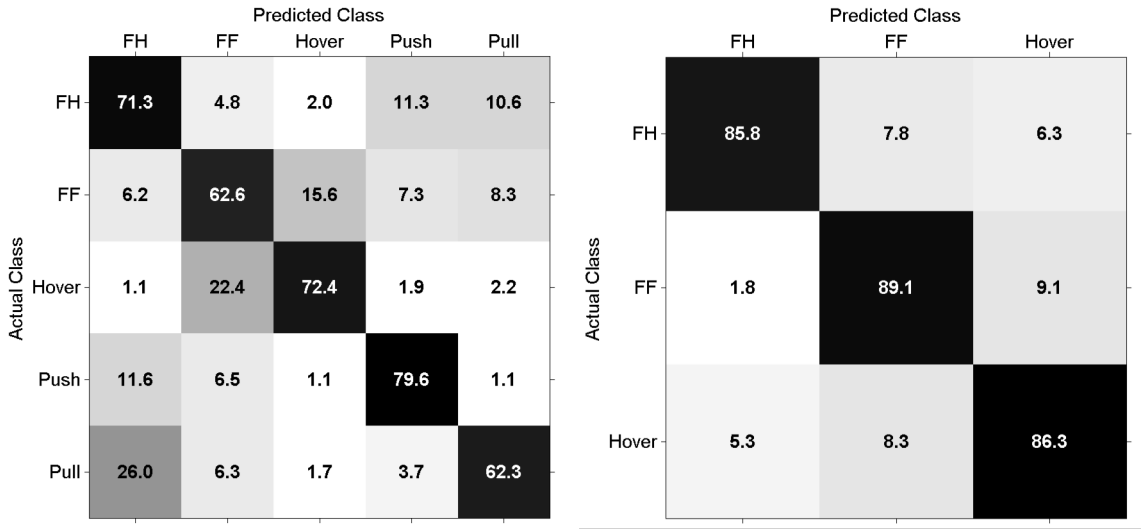

Figure 7.8: Confusion matrix of the 5-gesture (left) and 3-gesture (right) classification.

that there is in-fact a signal on the power line which can enable indirect sensing of touches on uninstrumented LCD panels.

From the 5-class confusion matrix in Figure 7.8 (left), it can be seen that there is significant confusion between the five-finger touch and hover. During these actions, the palm, which represents the largest area of the hand, is at about the same distance from the LCD panel, and therefore has nearly the same capacitive coupling. These similarities cause the amplitude of the EMI to be nearly the same, which results in the observed confusion. In addition, there exists confusion between the full-hand and five-finger touches and the push and pull gestures. This is due to the fact that the push and pull gestures are comprised of full-hand and five-finger touches. I believe that a larger training set would allow more robust classification of these 5 gestures. As shown earlier, using only two training examples we are able to classify all 5 gestures with 68.3% accuracy; however, using a reduced gesture set of 3 gestures (hover, push, and pull) yields 86.3% (chance=33%) with a standard deviation of 17.3%. Figure 7.8 (right) shows the 3-class confusion matrix, which shows considerably fewer misclassification. Note that due to imperfect event detection, there are a different

number of test examples in each classification run (although the training set is always the same size), and thus the accuracies reported in the confusion matrices do not average to the aggregate accuracies reported above.

Two of the users in the study returned to repeat the experiments on separate days in order to explore the temporal stability of the signal. One user performed the experiment on 6 separate days and the other on 3. I trained a model using only the data from the first day, and then ran the classifier on the data from the remaining days. In this analysis, I am able to classify the 3 gestures used above with 83.8% accuracy (σ=11.8%). Since the performance was not degraded substantially over the case in which I used only data from one session, we can conclude that our signal is temporally stable over many days, even when the noise level and load on the power line changes.

It should also be noted that although the standard deviation of the classification accuracy for the 5-class problem is high, this variation is almost entirely due to differences in the monitors. The standard deviation of the classification accuracy across all 11 users in our dataset is only 5.5%, while it is 20.3% over the 8 LCD screens used. This low variation across users indicates that it may be possible to build a generic model, and thus require no per-user training. To test this hypothesis, I trained a 3-gesture classifier (*i.e.*, using the same 3 gestures used above) on the data from 10 of our 11 users, and then ran the classifier on the data from the remaining user. We folded across all 11 users, and achieved an average accuracy of 88.8% (σ=13.6%). This high level of accuracy indicates that it is possible to build a generic model using a large database of users, and then a new user can operate the system robustly without any training.

7.5 Real-time Implementation

The offline analysis described above is useful for showing the feasibility of using uTouch to detect and classify touch gestures; however, it is also important to demonstrate the ability for uTouch to work in real-time. I therefore implemented a real-time version of our system and designed some prototype applications. In order for uTouch to run in real-time with

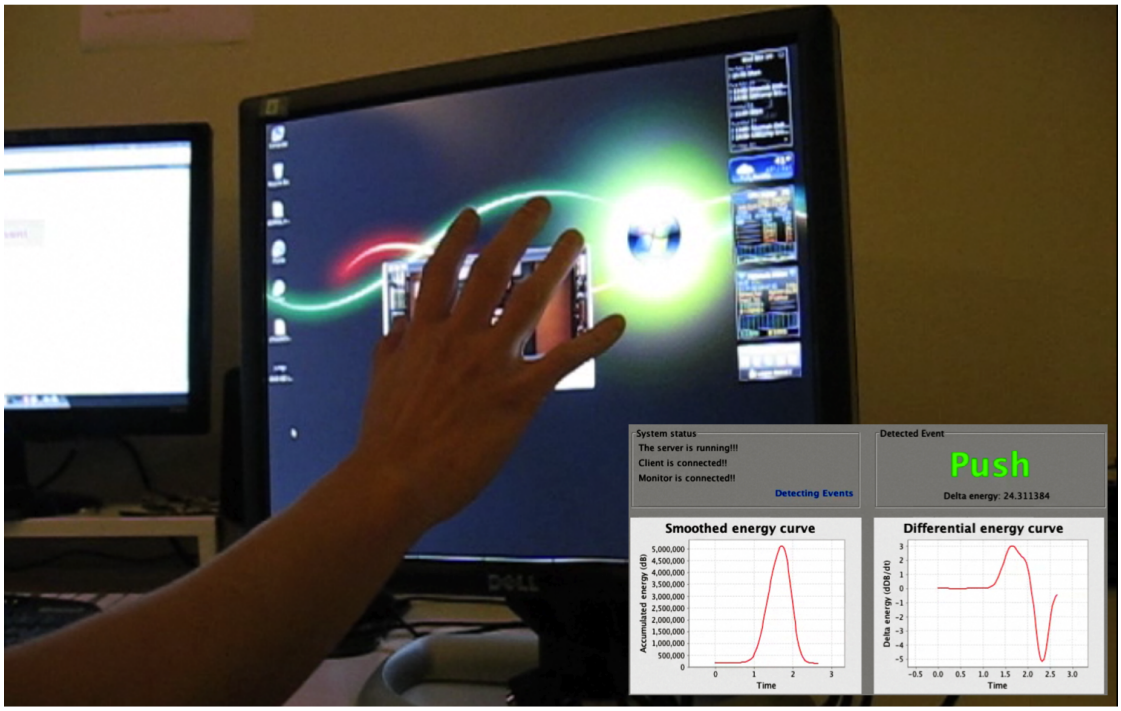

Figure 7.9: Using uTouch in video control. The user is performing a push gesture for a full-screen view.

low latency, I simplified much of the processing and machine learning. The summed energy signal is only filtered once using a SavitzkyGolay filter with a degree of 1 and a frame length of 3. In addition, a moving average filter of length 3 was used to further smooth the signal. I used a simplified decision-tree classifier using only two of our original features (*i.e.*, maximum amplitude and peak amplitude position). This implementation has little perceivable latency and shows high event detection and classification rates when used on our best performing monitor (*i.e.*, M5). Figure 7.9 shows this real-time system as well a gaming interface and video playback controller.

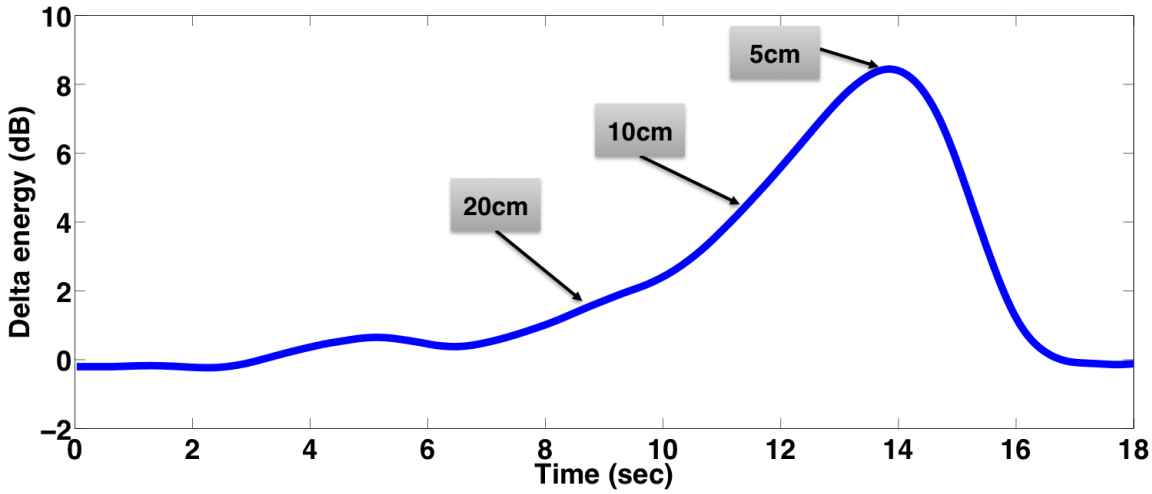

Figure 7.10: Observed EMI amplitude as a hand is slowly approaching the panel from a distance of 20 cm to 5 cm.

7.6 Discussion

Since our sensing technology works using the capacitive coupling between the body and the LCD panel, it is conceivable that we can also detect hand waves and other similar gestures which happen in the space in front of the panel. The hover gesture is an example of a gesture which can be detected without touching the LCD panel. Figure 7.10 shows the amplitude of the EMI produced as a hand is slowly brought near the LCD panel. This demonstrates that it may be possible to determine the proximity of a user's hand from the monitor.

Our sensing approach also enables us to detect the gray level of the image on the display. This is because the EMI signal coupled onto the power line is a function of the power consumption of the row and column drivers in the display. The column drivers change the voltage that they drive onto the column data lines as a function of the intensity of the light (*i.e.*, gray level). Therefore, the amount of EMI coupled onto the power line when the user touches the display is related to the gray level of the pixels. Figure 7.11 shows an experiment in which a user performs gestures on a display and varies the gray level of the

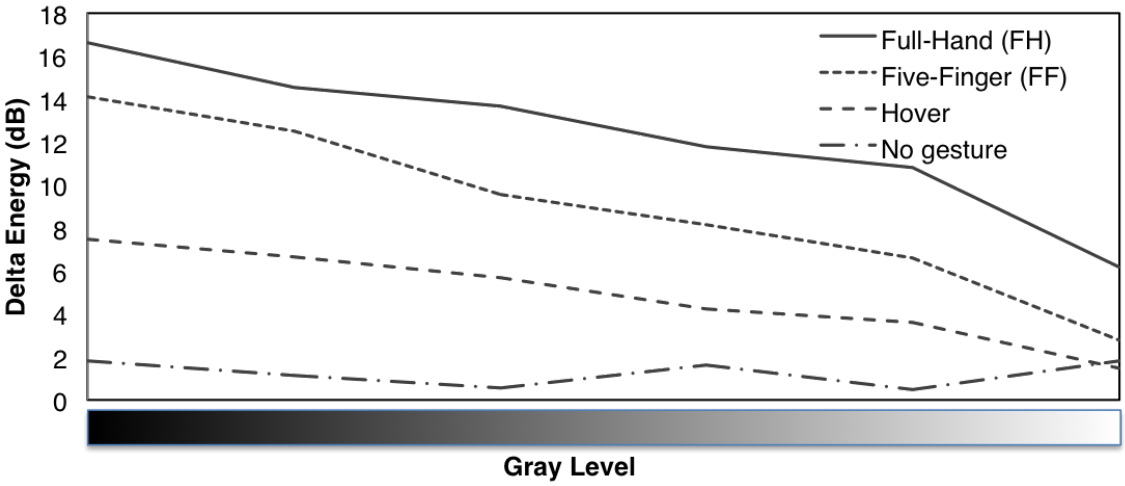

Figure 7.11: Observed EMI changes as a function of the LCD screen's gray level.

display's background. For the normally white TN panel used, higher volt-ages are used to produce black and then strong EMI is ob-served when the display is black.

In this chapter, I demonstrate an approach for passively detecting and classifying a user's touches and hand hovers over an uninstrumented LCD panel. Our approach utilizes existing signals in the LCD display which are amplified when a user brings their hand near or touches the LCDs front panel. These signals are coupled onto the power lines, where they appear as electromagnetic interference which can be sensed using a single device connected elsewhere on the power line infrastructure. uTouch can be used in a variety of applications such as multimedia controls, gaming interfaces and home automation control.

Chapter

CONCLUSION AND FUTURE DIRECTIONS

In this dissertation, I presented a sensing technique that can extract fine-grained information of electrical appliance usage in the home. The main contribution is the observation of leveraging time-vary EMI to infer appliance operating states and its power consumption. I have shown that from the same EMI signals, the system can infer not just *what* appliance is being used [34], but also *how* these appliances are being used and *how much* power each individual appliance consumes. These fine-grained information could give many more clues to infer the residents' activities in the house, which will be discussed later in this chapter.

Besides EMI sensing, I also presented a wearable device that could facilitate remote monitor for the elderly. In the field studies where we evaluated this wearable device (*i.e.*, the location tag in Chapter 3) within 11 homes, I have shown that the subjects enjoyed using the wearable device as its compact design, although the studies revealed two potential bottlenecks of using such a wearable device: it requires the subject to remember where they attach the tag and to charge the device regularly.

8.1 Applications and Implications

The applications from these fine-grained electrical usage are tremendous. In this section, I will discuss some examples of how to apply this sensing technique in different fields of research.

8.1.1 Activity Recognition

As my studies indicate in Chap 3, rehabilitation researchers still suffer from inefficient tools to help them record the subjects' mobility and/or activities in the house. Although identifying appliance-level usage based on EMI sensing technique [34] has shown an effective

approach to extract such information, it is still insufficient to infer the activity a subject actually performs. For example, by sensing the bedroom lights off followed by the TV turned on, it is possible to infer their movement from the bedroom to the living room, but it is uncertain to conclude whether the subject is watching TV or not – he/she might be reading or sleep while keeping the TV being turned on. Combining the detailed information revealed in this dissertation could help the rehab researchers better understand the subjects' fine-grained activities in the home. For example, knowing the action of *switching a TV channel* is a much stronger indication of the *watching TV* activity because it means that the subject is actively interacting with the device. We also found there exists some active elders who spend significant amount of time in using a computer. By comparing the varying EMI from their laptops/PC, the system could infer their activeness when they are using those devices.

8.1.2 Occupancy Identification

The other information that fine-grained electricity usage can reveal is the usage pattern. As two residents dwelling in the same house may use an appliance very differently, these varying EMI could be potentially used for occupancy *identification*. For instance, by examining the varying EMI patterns of a hair dryer, the system could identify the number of residents in the house (e.g., one may prefer hot blast while the other tends to use cold/warm blasts).

8.1.3 Energy Disaggregation

Besides the applications in activity inference, the findings in this thesis could also avail the energy disaggregation research. A fundamental limitation of EMI sensing, as indicated in [34], is the requirement of supervised learning – it requires the fingerprint of electrical noise to train the classifier. The observations of time-varying EMI create a new space to explore many more features which could reduce the training effort. As indicated in Chap 5, human knowledge could play a significant role in training the classifier for state estimation. Here are some examples:

- Motor-based devices (e.g., a blender) with 7 buttons implies 7 operating states.

- EMI from motor-based appliances shows EMI at a step function (as its EMI frequency jumps at a function of the motor's rotation rate), while SMPS-based devices only shows continuous changes in its EMI due to the voltage regulation in its circuitry.

- Motor-based devices usually shows wide EMI bandwidth (up to 40 kHz) but SMPS-devices tends to has much narrower bandwidth (2 to 10 kHz).

- Among all motor-based appliances, the vacuum cleaner usually consumes highest power as its motor spin rate is the highest, which manifest itself at a relatively high EMI frequency (e.g., 10 to 15 kHz) compared to others (e.g., blender between 6 to 8 kHz and food mixer between 4 - 6 kHz).

- Among all SMPS-based appliances, the TV usually shows the most narrow bandwidth with largest EMI frequency variation as it usually regulate its power by changing the *frequency*, while the laptops tends to have wider EMI bandwidth.

Using these human knowledges as *prior*, the researchers in the related field can explore more interesting features for disaggregating the electricity usage or to the very least identifying different categories of appliances (e.g., computers vs. CFL bulbs vs. vacuum cleaner) in a unsupervised manner.

8.2 Future Direction

My thesis summaries a portion of my research on wearable devices and EMI sensing that I have accomplished throughout my PhD career. As the extended work from the previous work ElectriSense [34], I showed further deep understanding and applications from EMI sensing. In particular, from the same EMI signals, ElectriSense answered *what* appliance is being used while this dissertation explores *how* and *how much*. I believe this is a significant advancement in EMI-based sensing research, but meantime I would like to enlighten several future directions that this work can be further extended and applied to.

8.2.1 Combining other sensing approaches

A critical insight from this dissertation is that single sensing technique is not enough to enable comprehensive remote monitor for the elder. As we have seen the fine-grained information that EMI sensing can extract, it is yet not the total solution in activity recognition. The fundamental limitation of using EMI sensing in activity recognition is that some activities are by nature easier to capture by other sensing approaches. For example, water-based activities (e.g., flashing a toilet) can be easily solved by another single sensor installed with the house water pipes [33]. To identify the room-level movement, it might be easier to install a motion sensor in each room instead of identifying appliances in each room. That being said, the work presented in this thesis is not to completely replace other existing sensing approaches. Instead, I presented an alternative, low-overhead approach (*i.e.*, a single set sensing device) to minimize the requirement of sensors deployed in the home while providing sufficient details for activity reference research. By combing different sensors with my work, it is possible to infer complex activities with minimal overhead in the sensor deployment. The event sequence ''fridge door open, use the kitchen faucet, turn on the electrical stove'' most likely implies the resident is *preparing a meal*. Identify such complex activities is critical in ADL (Activity of Daily Living) analysis and could be potentially achieved by combining the results presented in this thesis and other existing sensing approaches.

8.2.2 Locations of the Appliances

One missing piece in EMI-based sensing approach is to identify *where* an appliance is being used (*i.e.*, the location of the appliance). The ability to localize an appliance could be helpful; the elder might forget where he/she left the phone charger and knowing the location of the charger – at least at a room level – could reduce their effort in searching it. Kong *et al.* utilized current sensors in-lined with each individual appliances to location the electronic appliance, given the known floor plan and powerline infrastructure [53]. The fundamental physics behind this work is based upon the varying impedance when the relative distance between the appliance and the sensing device changes. When an appliance is located at a

further distance from the sensor, the current measure attenuates accordingly.

Based on similar phenomenon, we could infer *where* an appliance is being used. According to my observations on EMI signals, I found that the magnitude of EMI signal varies with the distance between the appliance and the sensing device. Without the prior knowledge of the house floor plan and powerline structure, it is possible to achieve appliance localization at a room-level accuracy by a finger-print based machining learning algorithm. Although, it can not achieve per-outlet accuracy as presented in [53], room-level accuracy could still provide useful information for rehab researchers as the mobility pattern studies in clinical trials mainly focuses on room-level movements in the house.

8.2.3 Higher Frequency

EMI sensing so far focuses on the spectrum below 500 kHz, where most modern appliances generate its electrical noise. The other interesting area that EMI sensing has not yet been fully explored is above 1 MHz (and might be up to 30 MHz or higher). For example, in our experiments, we observed that the Apple Macbook Pro produces strong EMI noise, which also varies with the CPU usage, at around 11 MHz. Our assumption on this strong EMI signal is that the microcontroller on either the power supply or on the motherboard functions as part of the voltage regulation circuitry and yields this varying EMI signal. Taking another commercial product called *Wally*[1] as an example, it leverages the powerline infrastructure as the media to transmit sensor data at 13 MHz. The spectrum in this relatively higher frequency is usually ''cleaner'' so it could yield better SNR for analysis.

I hope findings in the dissertation enlighten some new research areas to explore and look forward to someone in this field to continue and explore these unknowns.

[1]Wally: http://www.wallyhome.com

BIBLIOGRAPHY

[1] Adi Abileah and Patrick Green. Optical sensors embedded within amlcd panel: Design and applications. In *ACM SIGGRAPH 2007 Emerging Technologies*, SIGGRAPH '07, New York, NY, USA, 2007. ACM.

[2] Joana M Abreu, Francisco Camara Pereira, and Paulo Ferrao. Using pattern recognition to identify habitual behavior in residential electricity consumption, June 2012.

[3] Eli Y Adashi, H Jack Geiger, and Michael D Fine. Health Care Reform and Primary Care — The Growing Importance of the Community Health Center. *New England Journal of Medicine*, 362(22):2047–2050, June 2010.

[4] Oliver Amft, Clemens Lombriser, Thomas Stiefmeier, and Gerhard Tröster. Recognition of User Activity Sequences Using Distributed Event Detection. In *link.springer.com*, pages 126–141. EuroSSC'07, Berlin, Heidelberg, January 2007.

[5] Delena I Amsters, Kiley J Pershouse, Glenda L Price, and Melissa B Kendall. Long duration spinal cord injury: Perceptions of functional change over time. *Disability & Rehabilitation*, 27(9):489–497, January 2005.

[6] Ling Bao and Stephen S Intille. Activity Recognition from User-Annotated Acceleration Data. In *link.springer.com*, pages 1–17. Springer Berlin Heidelberg, Berlin, Heidelberg, 2004.

[7] Tracy S Barger and Donald E Brown. Health-status monitoring through analysis of behavioral patterns, January 2005.

[8] Christian Beckel, Leyna Sadamori, and Silvia Santini. Automatic socio-economic classification of households using electricity consumption data. In *the the fourth international conference*, pages 75–86, New York, New York, USA, 2013. ACM Press.

[9] R M Bertrand and S L Willis. Everyday problem solving in Alzheimer's patients: A comparison of subjective and objective assessments. *Aging & Mental Health*, 3(4):281–293, November 1999.

[10] Bernard Boulay, Francois Bremond, and Monique Thonnat. Applying 3D human model in a posture recognition system. *Pattern Recognition Letters*, 27(15):1788–1796, November 2006.

[11] Michael Buettner, Richa Prasad, Matthai Phillpose, and David Wetheral. Recognizing daily activities with RFID-based sensors, 2009.

[12] Susan Charlifue, Daniel P Lammertse, and Rodney H Adkins. Aging with spinal cord injury: Changes in selected health indices and life satisfaction. *Archives of Physical Medicine and Rehabilitation*, 85(11):1848–1853, November 2004.

[13] Ke-Yu Chen, Gabe A Cohn, Sidhant Gupta, and Shwetak N Patel. uTouch: sensing touch gestures on unmodified LCDs. In *CHI '13: Proceedings of the SIGCHI Conference on Human Factors in Computing Systems*. ACM Request Permissions, April 2013.

[14] Ke-Yu Chen, Mark Harniss, Justin Lim, Youngjun Han, Kurt Johnson, and Shwetak Patel. uLocate: A Ubiquitous Location Tracking System for People Aging with Disabilities. In *8th International Conference on Body Area Networks*. ACM, October 2013.

[15] Ke-Yu Chen, Mark Harniss, Shwetak Patel, and Kurt Johnson. Implementing technology-based embedded assessment in the home and community life of individuals aging with disabilities: a participatory research and development study. *Disability and Rehabilitation: Assistive Technology*, pages 1–9, June 2013.

[16] KONG Y CHEN, KATHLEEN F JANZ, WEIMO ZHU, and ROBERT J BRYCHTA. Redefining the Roles of Sensors in Objective Physical Activity Monitoring. *Medicine & Science in Sports & Exercise*, 44:S13–S23, January 2012.

[17] Gabe Cohn, Sidhant Gupta, Jon Froehlich, Eric Larson, and Shwetak N Patel. GasSense: Appliance-Level, Single-Point Sensing of Gas Activity in the Home. In *dl.acm.org*, pages 265–282. Pervasive'10, Berlin, Heidelberg, 2010.

[18] Gabe Cohn, Daniel Morris, Shwetak Patel, and Desney Tan. Humantenna: Using the Body as an Antenna for Real-Time Whole-Body Interaction. In *the 2012 ACM annual conference*, pages 1901–1910, New York, New York, USA, 2012. ACM Press.

[19] Sunny Consolvo, David W McDonald, Tammy Toscos, Mike Y Chen, Jon E Froehlich, Beverly Harrison, Predrag Klasnja, Anthony LaMarca, Louis LeGrand, Ryan Libby, Ian Smith, and James A Landay. Activity sensing in the wild: a field trial of ubifit garden, 2014.

[20] Diane J Cook and Narayanan Krishnan. Mining the home environment. *Journal of Intelligent Information Systems*, pages 1–17, October 2014.

[21] Amtmann D, Borson S, Salem R, Johnson KL, and Verral A. Aging with disabilities: Comparing symptoms and quality of life indicators of individuals aging with disabilities to U.S. general population norms. — Rehabilitation Research and Training Center on Aging With Physical Disabilities, 2012.

[22] K B Dassel and F A Schmitt. The Impact of Caregiver Executive Skills on Reports of Patient Functioning. *The Gerontologist*, 48(6):781–792, December 2008.

[23] George Demiris and B K Hensel. Technologies for an aging society: a system... [Yearb Med Inform. 2008] - PubMed - NCBI. *Yearb Med Inform*, pages 33–40, December 2008.

[24] George Demiris and H J Thompson. Mobilizing Older Adults: Harnessing the Pot... [Yearb Med Inform. 2012] - PubMed - NCBI. *Yearb Med Inform*, December 2012.

[25] B H Dobkin and A Dorsch. The Promise of mHealth: Daily Activity Monitoring and Outcome Assessments by Wearable Sensors. *Neurorehabilitation and Neural Repair*, 25(9):788–798, October 2011.

[26] Florian Echtler, Thomas Pototschnig, and Gudrun Klinker. An led-based multitouch sensor for lcd screens. In *Proceedings of the Fourth International Conference on Tangible, Embedded, and Embodied Interaction*, TEI '10, pages 227–230, New York, NY, USA, 2010. ACM.

[27] Miro Enev, Sidhant Gupta, Tadayoshi Kohno, and Shwetak N Patel. Televisions, video privacy, and powerline electromagnetic interference. In *the 18th ACM conference*, pages 537–550, New York, New York, USA, 2011. ACM Press.

[28] Linda Farinaccio and Radu Zmeureanu. Using a pattern recognition approach to disaggregate the total electricity consumption in a house into the major end-uses. *Energy and Buildings*, 30(3):245–259, August 1999.

[29] Marcia L Finlayson, Elizabeth W Peterson, and Chi C Cho. Risk Factors for Falling Among People Aged 45 to 90 Years With Multiple Sclerosis. *Archives of Physical Medicine and Rehabilitation*, 87(9):1274–1279, September 2006.

[30] Kenneth P Fishkin, Henry Kautz, Donald Patterson, Mike Perkowitz, and Matthai Philipose. Guide: Towards Understanding Daily Life via Auto-Identification and Statistical Analysis. *UbiHealth'03*, 2003.

[31] Kenneth P Fishkin, Henry Kautz, Donald Patterson, Mike Perkowitz, and Matthai Philipose. Guide: Towards Understanding Daily Life via Auto-Identification and Statistical Analysis. *UbiHealth'03*, 2003.

[32] Jon Froehlich, Eric Larson, Sidhant Gupta, Gabe Cohn, Matthew Reynolds, and Shwetak Patel. Disaggregated End-Use Energy Sensing for the Smart Grid. *IEEE Pervasive Computing*, 10(1):28–39, 2011.

[33] Jon E Froehlich, Eric Larson, Tim Campbell, Conor Haggerty, James Fogarty, and Shwetak N Patel. HydroSense: Infrastructure-mediated Single-point Sensing of Whole-home Water Activity. In *UbiComp '09*, page 235, New York, New York, USA, 2009. ACM Press.

[34] Sidhant Gupta, Matthew S Reynolds, and Shwetak N Patel. ElectriSense: Single-Point Sensing Using EMI for Electrical Event Detection and Classification in the Home. In *the 12th ACM international conference*, pages 139–148, New York, New York, USA, 2010. ACM Press.

[35] Raffay Hamid, Siddhartha Maddi, Aaron Bobick, and Irfan Essa. Unsupervised analysis of activity sequences using event-motifs. In *the 4th ACM international workshop*, page 71, New York, New York, USA, 2006. ACM Press.

[36] Derek Hao Hu, Sinno Jialin Pan, Vincent Wenchen Zheng, Nathan Nan Liu, and Qiang Yang. Real world activity recognition with multiple goals. In *the 10th international conference*, pages 30–39, New York, New York, USA, 2008. ACM Press.

[37] G W Hart. Nonintrusive appliance load monitoring. *Proceedings of the IEEE*, 80(12):1870–1891, 1992.

[38] David Hartley. Rural Health Disparities, Population Health, and Rural Culture, October 2004.

[39] Zhenyu He and Lianwen Jin. Activity recognition from acceleration data based on discrete consine transform and SVM. In *2009 IEEE International Conference on Systems, Man and Cybernetics - SMC*, pages 5041–5044. IEEE.

[40] Peter Hevesi, Sebastian Wille, Gerald Pirkl, Norbert Wehn, and Paul Lukowicz. Monitoring household activities and user location with a cheap, unobtrusive thermal sensor array. In *the 2014 ACM International Joint Conference*, pages 141–145, New York, New York, USA, 2014. ACM Press.

[41] Steve Hodges, Shahram Izadi, Alex Butler, Alban Rrustemi, and Bill Buxton. Thinsight: Versatile multi-touch sensing for thin form-factor displays. In *Proceedings of the 20th Annual ACM Symposium on User Interface Software and Technology*, UIST '07, pages 259–268, New York, NY, USA, 2007. ACM.

[42] Ramon Hofer, Daniel Naeff, and Andreas Kunz. Flatir: Ftir multi-touch detection on a discrete distributed sensor array. In *Proceedings of the 3rd International Conference on Tangible and Embedded Interaction*, TEI '09, pages 317–322, New York, NY, USA, 2009. ACM.

[43] Enamul Hoque and John Stankovic. AALO: Activity recognition in smart homes using Active Learning in the presence of Overlapped activities, May 2012.

[44] Tâm Huynh, Mario Fritz, and Bernt Schiele. Discovery of activity patterns using topic models. In *the 10th international conference*, page 10, New York, New York, USA, 2008. ACM Press.

[45] Stephen S Intille, John Rondoni, Charles Kukla, Isabel Ancona, and Ling Bao. A context-aware experience sampling tool, 2003.

[46] Stephen S Intille, Emmanuel Munguia Tapia, John Rondoni, Jennifer Beaudin, Chuck Kukla, Sitij Agarwal, Ling Bao, and Kent Larson. Tools for Studying Behavior and Technology in Natural Settings. In *link.springer.com*, pages 157–174. UbiComp'03, Berlin, Heidelberg, 2003.

[47] D Kahneman. A Survey Method for Characterizing Daily Life Experience: The Day Reconstruction Method. *Science*, 306(5702):1776–1780, December 2004.

[48] H Kikuchi, K Yoshiuchi, N Miyasaka, K Ohashi, Y Yamamoto, H Kumano, T Kuboki, and A Akabayashi. Reliability of recalled self-report on headache intensity: investigation using ecological momentary assessment technique. *Cephalalgia*, 26(11):1335–1343, November 2006.

[49] Hyungsul Kim, Manish Marwah, Martin Arlitt, Geoff Lyon, and Jiawei Han. Unsupervised Disaggregation of Low Frequency Power Measurements, 2010.

[50] Younghun Kim, Thomas Schmid, Zainul M Charbiwala, and Mani B Srivastava. ViridiScope: design and implementation of a fine grained power monitoring system for homes. In *UbiComp '09*, pages 245–254, New York, New York, USA, 2009. ACM Press.

[51] Wihelm Kleiminger, Thorsten Staake, and Silvia Santini. Occupancy Detection from Electricity Consumption Data, 2013.

[52] Anil Kokaram. An Algorithm for Total Variation Minimization and Applications. *Journal of Mathematical Imaging and Vision*, 20(1/2):163–177, January 2004.

[53] Quan Kong and Takuya Maekawa. Identifying outlets at which electrical appliances are used by electrical wire sensing to gain positional information about appliance use. In *the 2014 ACM International Joint Conference*, pages 349–360, New York, New York, USA, 2014. ACM Press.

[54] Narayanan C Krishnan and Diane J Cook. Activity recognition on streaming sensor data. *Pervasive and Mobile Computing*, 10:138–154, February 2014.

[55] Jonathan Lester, Tanzeem Choudhury, and Gaetano Borriello. A Practical Approach to Recognizing Physical Activities. In *link.springer.com*, pages 1–16. Springer Berlin Heidelberg, Berlin, Heidelberg, 2006.

[56] L Liao, D Fox, and H Kautz. Extracting Places and Activities from GPS Traces Using Hierarchical Conditional Random Fields. *The International Journal of Robotics Research*, 26(1):119–134, January 2007.

[57] Beth Logan, Jennifer Healey, Matthai Philipose, Emmanuel Munguia Tapia, and Stephen Intille. *A long-term evaluation of sensing modalities for activity recognition.* UbiComp'07, September 2007.

[58] Ralph Maddison and Cliona Ni Mhurchu. Global positioning system: a new opportunity in physical activity measurement. *International Journal of Behavioral Nutrition and Physical Activity*, 6(1):73, 2009.

[59] J Maitland, S Sherwood, L Barkhuus, I Anderson, M Hall, B Brown, M Chalmers, and H Muller. Increasing the Awareness of Daily Activity Levels with Pervasive Computing. In *2006 Pervasive Health Conference and Workshops*, pages 1–9. IEEE, 2006.

[60] David May, U S L Nayak, and Bernard Isaacs. The life-space diary: A measure of mobility in old people at home. 1985.

[61] Alex Mihailidis, Brent Carmichael, Jennifer Boger, and Geoff Fernie. An intelligent environment to support aging-in-place, safety, and independence of older adults with dementia. *citeseerxistpsuedu*, 2003.

[62] Andrés Molina-Markham, Prashant Shenoy, Kevin Fu, Emmanuel Cecchet, and David Irwin. Private memoirs of a smart meter. In *the 2nd ACM Workshop*, pages 61–66, New York, New York, USA, 2010. ACM Press.

[63] Margaret Morris, Stephen S Intille, and Jennifer S Beaudin. Embedded Assessment: Overcoming Barriers to Early Detection with Pervasive Computing. In *dl.acm.org*, pages 333–346. Springer Berlin Heidelberg, Berlin, Heidelberg, 2005.

[64] Meg E Morris, Brooke Adair, Kimberly Miller, Elizabeth Ozanne, Ralph Hansen, Alan J Pearce, Nick Santamaria, Luan Viega, Maureen Long, and Catherine M Said. Smart-home technologies to assist older people to live well at home. *Journal of aging science*, 1(1):1–9, January 2013.

[65] Nima Motamedi. Hd touch: Multi-touch and object sensing on a high definition lcd tv. In *CHI '08 Extended Abstracts on Human Factors in Computing Systems*, CHI EA '08, pages 3069–3074, New York, NY, USA, 2008. ACM.

[66] Usman Naeem, John Bigham, and Jinfu Wang. Recognising activities of daily life using hierarchical plans. *dl.acm.org*, pages 175–189, October 2007.

[67] Shwetak N Patel, Matthew S Reynolds, and Gregory D Abowd. Detecting Human Movement by Differential Air Pressure Sensing in HVAC System Ductwork: An Exploration in Infrastructure Mediated Sensing. In *dl.acm.org*, pages 1–18. Pervasive'08, Berlin, Heidelberg, 2008.

[68] Shwetak N Patel, Thomas Robertson, Julie A Kientz, Matthew S Reynolds, and Gregory D Abowd. *At the flick of a switch: detecting and classifying unique electrical events on the residential power line*. UbiComp'07, September 2007.

[69] Shwetak N Patel, Khai N Truong, and Gregory D Abowd. PowerLine Positioning: A Practical Sub-Room-Level Indoor Location System for Domestic Use. In *link.springer.com*, pages 441–458. UbiComp'06, Berlin, Heidelberg, 2006.

[70] Shyamal Patel, Hyung Park, Paolo Bonato, Leighton Chan, and Mary Rodgers. A review of wearable sensors and systems with application in rehabilitation. *Journal of NeuroEngineering and Rehabilitation*, 9(1):21, 2012.

[71] D J Patterson, D Fox, H Kautz, and M Philipose. Fine-Grained Activity Recognition by Aggregating Abstract Object Usage. In *Ninth IEEE International Symposium on Wearable Computers (ISWC'05)*, pages 44–51. IEEE, 2005.

[72] France Pavlovcic. Commutator motors as EMI sources. In *2010 International Symposium on Power Electronics, Electrical Drives, Automation and Motion (SPEEDAM 2010)*, pages 1789–1793. IEEE, 2010.

[73] Claire Peel, Patricia Sawyer Baker, David L Roth, Cynthia J Brown, Eric V Bodner, and Richard M Allman. Assessing Mobility in Older Adults: The UAB Study of Aging Life-Space Assessment. *Journal of American Physical Therapy Association*.

[74] Maria Noemi Valero Perez. A non-intrusive appliance load monitoring system for identifying kitchen activities. *Master Thesis*, 2011.

[75] Elizabeth W Perterson, Chi C Cho, Lena von Koch, and Marcia L Finlayson. Injurious Falls Among Middle Aged and Older Adults With Multiple Sclerosis, December 2008.

[76] Parisa Rashidi and Diane J Cook. COM: A method for mining and monitoring human activity patterns in home-based health monitoring systems. *ACM Transactions on Intelligent Systems and Technology*, 4(4):1–20, September 2013.

[77] Emily D Richardson, Jodi D Nadler, and Paul F Malloy. Neuropsychologic prediction of performance measures of daily living skills in geriatric patients, 1995.

[78] W A Rogers, B Meyer, and A D Fisk. Functional limitations to daily living tasks in the aged: a focus group analysis. *Human Factors*, 1998.

[79] Mario Romero, Alice Vialard, John Peponis, John Stasko, and Gregory Abowd. Evaluating video visualizations of human behavior. In *the 2011 annual conference*, page 1441, New York, New York, USA, 2011. ACM Press.

[80] N Roy, A Misra, and D Cook. *Infrastructure-assisted smartphone-based ADL recognition in multi-inhabitant smart environments*. IEEE International Conference on Pervasive Computing and Communication, 2013.

[81] Leonid I Rudin, Stanley Osher, and Emad Fatemi. Nonlinear total variation based noise removal algorithms. *Physica D*, 60(1-4):259–268, 1992.

[82] A Sadilek and H Kautz. Location-Based Reasoning about Complex Multi-Agent Behavior. *Journal of Artificial Intelligence Research*, pages 87–133, 2012.

[83] James Scott, A J Bernheim Brush, John Krumm, Brian Meyers, Michael Hazas, Stephen Hodges, and Nicolas Villar. PreHeat: Controlling Home Heating Using Occupancy Prediction. In *the 13th international conference*, pages 281–290, New York, New York, USA, 2011. ACM Press.

[84] Burr Settles. *Active Learning*, volume 6. Morgan & Claypool Publishers, June 2012.

[85] Aderiano M da Silva. Induction Motor Fault Diagnostic and Monitoring Methods, 2006.

[86] Erin M Snook and Robert W Motl. Physical Activity Behaviors in Individuals with Multiple Sclerosis: Roles of Overall and Specific Symptoms, and Self-Efficacy. *Journal of Pain and Symptom Management*, 36(1):46–53, July 2008.

[87] Timothy Sohn, Alex Varshavsky, Anthony LaMarca, Mike Y Chen, Tanzeem Choudhury, Ian Smith, Sunny Consolvo, Jeffrey Hightower, William G Griswold, and Eyal Lara. Mobility Detection Using Everyday GSM Traces. In *link.springer.com*, pages 212–224. Springer Berlin Heidelberg, Berlin, Heidelberg, 2006.

[88] B T Stalvey, C Owsley, M E Sloane, and K Ball. The Life Space Questionnaire: A Measure of the Extent of Mobility of Older Adults. *Journal of Applied Gerontology*, 18(4):460–478, December 1999.

[89] Maja Stikic, Tâm Huynh, Kristof Van Laerhoven, and Bernt Schiele. ADL recognition based on the combination of RFID and accelerometer sensing. In *2008 Second International Conference on Pervasive Computing Technologies for Healthcare (PervasiveHealth)*, pages 258–263. IEEE, 2008.

[90] Amarnag Subramanya, Alvin Raj, Jeff A Bilmes, and Dieter Fox. Recognizing Activities and Spatial Context Using Wearable Sensors. June 2012.

[91] Emmanuel Munguia Tapia, Stephen S Intille, and Kent Larson. Activity Recognition in the Home Using Simple and Ubiquitous Sensors. In *link.springer.com*, pages 158–175. Springer Berlin Heidelberg, Berlin, Heidelberg, 2004.

[92] Edison Thomaz, Vinay Bettadapura, Gabriel Rayes, Megha Sandesh, Grant Schindler, Thomas Plotz, and Gregory Abowd. Recognizing water-based activities in the home through infrastructure-mediated sensing, 2012.

[93] Lilli Thompson. Functional Changes in Persons Aging with Spinal Cord Injury. *Assistive Technology*, 11(2):123–129, December 1999.

[94] Tim van Kasteren, Athanasios Noulas, Gwenn Englebienne, and Ben Kröse. Accurate activity recognition in a home setting. In *the 10th international conference*, pages 1–9, New York, New York, USA, 2008. ACM Press.

[95] W Fred Van Raaij and Theo M M Verhallen. A behavioral model of residential energy use. *Journal of Economic Psychology*, 3(1):39–63, January 1983.

[96] Michael Zeifman and Kurt Roth. Nonintrusive appliance load monitoring: Review and outlook. *IEEE Transactions on Consumer Electronics*, 57(1):76–84, 2011.

[97] Z. Zhang and Y. Shan. System and method for transforming an ordinary computer monitor screen into a touch screen, August 10 2004. US Patent 6,774,889.

[98] Ahmed Zoha, Alexander Gluhak, Muhammad Imran, and Sutharshan Rajasegarar. Non-Intrusive Load Monitoring Approaches for Disaggregated Energy Sensing: A Survey. *Sensors*, 12(12):16838–16866, December 2012.

[99] Nadia Zouba, Bernard Boulay, Francois Bremond, and Monique Thonnat. Monitoring Activities of Daily Living (ADLs) of Elderly Based on 3D Key Human Postures. In *link.springer.com*, pages 37–50. Springer Berlin Heidelberg, Berlin, Heidelberg, 2008.